Investigation of the Impact of Mixing Intensity on Dissolved Oxygen Half Velocity Constants in a Sidestream Deammonification Environment

by

Biao Xie

A thesis

presented to the University of Waterloo

in fulfillment of the

thesis requirement for the degree of

Master of Applied Science

in

Civil Engineering

Waterloo, Ontario, Canada, 2017

Author's Declaration

I hereby declare that I am the sole author of this thesis. This is a true copy of the thesis, including any required final revisions, as accepted by my examiners.

I understand that my thesis may be made electronically available to the public.

Abstract

The liquid waste (centrate) from the dewatering stage in the solids treatment stream (sidestream) of a wastewater treatment plant is typically rich in ammonium. If this centrate is recycled to the wastewater treatment stream (mainstream), the aeration requirements in the mainstream bioreactor will increase. A new technology, sidestream deammonification, has been developed to reduce the loading of ammonium from the sidestream to the mainstream. However, this and similar technologies require delicate control of the dissolved oxygen (DO) in the bulk liquid. Therefore, improved knowledge of factors influencing the DO half-velocity constants (K_{O2}) of the functional organisms in the sidestream treatment will enhance the control of the growth of these organisms and ultimately nitrogen removal efficiency.

The impact of mixing conditions on K_{O2} values was investigated in this study. Experiments were conducted in a quasi-sequencing batch reactor (SBR) to reproduce a sidestream deammonification environment treating dewatering centrate. Once steady-state conditions were established, the mixer speed was changed from the initial setting of an average velocity gradient of 15/s at 8.0 L to 5.3/s at 8.0 L (from 150 rpm to 75 rpm) while maintaining other parameters constant. The objective of this study was to demonstrate the impact of mixing intensity on the estimated K_{O2} values of ammonium oxidizing bacteria (AOB) and anaerobic ammonium oxidizing (Anammox) bacteria.

The effect of mixing intensity was assessed in terms of overall nitrogen removal efficiency in the SBR and by examining the magnitude of K_{O2} values of AOB (K_{O2}^{AOB}) and Anammox bacteria ($K_{O2}^{Anammox}$) that were determined in activity tests. Nitrogen removal efficiency during steady-state conditions increased from 62% to 84%; and the value of estimated $K_{O2}^{Anammox}$ increased statistically significantly for the lower mixing intensity condition. However, the value of the estimated K_{O2}^{AOB} remained statistically the same. In conclusion, this research showed that mixing intensity had an impact on the estimated $K_{O2}^{Anammox}$ value and nitrogen removal in the SBR.

Acknowledgements

I am grateful to everyone who has helped and supported me during the period of my study. I would especially like to express my gratitude to the following people:

To my supervisor Prof. Wayne Parker and Dr. Chao Jin for their dedication to my project. I am very appreciative of having their guidance, patience, professional advice, and great diligence in my work.

To the members of my reading committee for revising my thesis and giving constructive suggestions.

To Mark Merlau, Tom Sullivan, Mark Sobon, Terry Ridgway, and Anne Allen for their technical support of the laboratory work. They are the reason why I could successfully operate my reactor and finish my experiments; To Dr. Weiwei Du for her technical support of BioWin™.

To Richard Liang for his commitment to assembling my LabVIEW™ hardware, developing the operation code, and troubleshooting the code errors.

To my family for their understanding and endless patience with me.

Table of Contents

Author's Declaration ii

Abstract iii

Acknowledgements iv

List of Figures vii

List of Tables viii

List of Abbreviations ix

1 Introduction 1

1.1 Background 1

1.2 Objective 2

1.3 Scope 2

1.4 Thesis Structure 3

2 Literature Review 4

2.1 Implementation of Partial Nitritation and Anammox (PN/A) Processes for Centrate Treatment 4

2.1.1 Active Metabolism 4

2.1.2 PN/A Process Configurations and Operating Strategies for Establishing Desired Metabolisms 5

2.2 Process Simulation 10

2.2.1 Biokinetics of AOB NOB and Anammox Metabolisms and Half-velocity Constants 10

2.2.2 Factors Influencing Half-velocity Constants 12

2.3 Quantifying Anammox Performance by Activity Tests 14

2.4 Summary of Literature Review 16

3 Materials and Methods 17

3.1 Reactor Configuration and Operation 17

3.1.1 Reactor Configuration 18

3.1.2 Reactor Startup and Feed Composition 20

3.1.3 Operational Strategy 22

3.1.4 Sample Collection and Analysis 27
3.1.5 Quality Control 28
3.2 Activity Testing 28
3.2.1 Test Plan 29
4 Results and Discussion 30
4.1 Steady-state Operation 30
4.2 Activity Tests 33
4.3 Mathematical Model Simulation 41
4.3.1 Model Development 41
4.3.2 Estimated DO half-velocity constants of AOB and Anammox Bacteria 43
5 Conclusions 47
6 Recommendations 48
7 References 49
8 Appendix 54
8.1 Results 54
8.2 Calculation of the Average Velocity Gradient 57
8.3 Calculation of the Solids Retention Time (SRT) of the Flocs and the Aggregates 58
8.4 Calculation for the Sample Standard Deviation of the Quotient of Nitrogen Conversion Rate over VSS Concentration 59
8.5 Derivation of the Linear Regression Equation 61
8.5.1 $\boldsymbol{\beta 1 \rightarrow 9}$ Definition 62
8.5.2 $\boldsymbol{x1 \rightarrow 5}$ and $\boldsymbol{y1 \rightarrow 3}$ Definition 64
8.5.3 K1 K2 Estimation (Assuming $\alpha = 0.05$) 69
8.5.4 Standard Deviation Estimation 72
8.5.5 $\boldsymbol{K1}$ and $\boldsymbol{K2}$ Two-Sample t-Tests 74

List of Figures

Figure 2-1: An illustration of nitrogen species state changes by AOB NOB and Anammox bacteria 5
Figure 3-1: Photo of reactor with clean water 19
Figure 3-2: Example of air diffusion in clean water with Bubble Mist – Bendable Air Wall 19
Figure 3-3: Process flow diagram 20
Figure 3-4: Example of settled "Waste MLSS" in the separatory funnel 23
Figure 3-5: Algorithm flow charts of Feed pump, Mixer, Decant pump, and Waste MLSS pump 25
Figure 3-6: Algorithm flow chart for air pump 26
Figure 3-7: Real-time screenshot of pH and DO profiles from LabVIEW® User Interface 27
Figure 4-1: Effluent profile from the beginning of the automated operation 32
Figure 4-2: Total suspended solids (TSS) volatile suspended solids (VSS) and VSS/TSS ratio in mixed liquor 33
Figure 4-3: Activity test results for ammonium at 150 rpm under (a) anoxic, (b) aerobic conditions 34
Figure 4-4: Activity test results at 150 rpm for nitrite under (a) anoxic , (b) aerobic conditions; for nitrate under (c) anoxic, (d) aerobic conditions 35
Figure 4-5: Anoxic activity test results referenced from 15 minutes for NH4+ at (a) 75 rpm (b) 150 rpm; for NO2- at (c) 75 rpm (d) 150 rpm; and for NO3- at (e) 75 rpm and (f) 150 rpm 36
Figure 4-6: Aerobic activity test results referenced from 15 minutes for NH4+ at (a) 75 rpm (b) 150 rpm; for NO2- at (c) 75 rpm (d) 150 rpm; and for NO3- at (e) 75 rpm and (f) 150 rpm 38
Figure 4-7: Activity test results at (a) 75 rpm and (b) 150 rpm 40
Figure 4-8: Estimated vs. actual activity test results at (a) 75 rpm and (b) 150 rpm 44
Figure 4-9: Plot of residuals vs. estimated nitrogen species conversion rates (Equation 4-1 – 4-3) for (a) 75 rpm and (b) 150 rpm 45
Figure 4-10: An illustration of the bacteria aggregate 46

List of Tables

Table 2-1: Relationships between the responses of Free Ammonia (FA) or Free Nitrous Acid (FNA) and temperature, pH, and ammonium or nitrite concentrations 9
Table 2-2: List of different Anammox activity test initial conditions 15
Table 2-3: AOB and Anammox half-velocity constants of ammonia, nitrite, and dissolved oxygen 16
Table 3-1: Reactor details and measument results 18
Table 3-2: Composition of synthetic centrate for this study 21
Table 3-3: Composition of trace element solution 21
Table 3-4: Details of operation parameters 22
Table 3-5: Operation sequence details 24
Table 3-6: Example of the beginning of time sequence 24
Table 3-7: Sample test methods for influent, effluent, and MLSS 27
Table 3-8: Substrate addition for activity testing 28
Table 3-9: Experiment plan to investigate the effect of mixing intensity using activity testing 29
Table 4-1: Estimated DO half-velocity constant values and sample standard deviations 44
Table 4-2: Student t-test results of DO half-velocity constants at two mixing intensities 44

List of Abbreviations

Anammox	Anaerobic Ammonium Oxidation
AOB	Ammonium-Oxidizing Bacteria
CANON	Completely Autotrophic Nitrogen-Removal Over Nitrite
CAS	Conventional Activated Sludge
CSV	Comma-Separated Values
DEMON®	Deammonification
DO	Dissolved Oxygen
FA	Free Ammonia
FNA	Free Nitrous Acid
IC	Ion Chromatograph
ISE	Ion Selective Electrode
LDO	Luminescent DO
MLSS	Mixed Liquor Suspended Solids
MLVSS	Mixed Liquor Volatile Suspended Solids
NOB	Nitrite-Oxidizing Bacteria
PN/A	Partial Nitritation and Anammox
SBR	Sequencing Batch Reactor
SRT	Solid Retention Time
TKN	Total Kjeldahl Nitrogen
TNRE	Total Nitrogen Removal Efficiency
TSS	Total Suspended Solids
VFBT	Vertical Flat Blade Turbine
VSS	Volatile Suspended Solids
WWTP	Wastewater Treatment Plant
YRTP	York River Treatment Plant

1 Introduction

1.1 Background

The centrates which are generated from dewatering anaerobically digested sludge in wastewater treatment plants (WWTP's) are known to be rich in ammonium. When recycled to the liquid train the centrate can substantially increase ammonium loadings to biological treatment processes. Even though the centrate flow typically represents a small fraction of the plant total influent flow rate, the additional total Kjeldahl nitrogen (TKN) from the centrate can contribute up to 25% of the daily influent TKN load to a wastewater treatment plant (Nifong et al., 2013; Musabyimana, 2008; Jung et al., 2007). Depending on the efficiency of sludge treatment, ammonium (NH_4^+) concentrations in the centrate can range from 500 mg N/L to 2000 mg N/L (Lackner et al., 2014; Jardin and Hennerkes, 2012). It has been argued that it is inefficient to treat centrate in the mainstream process train by conventional nitrogen treatment processes (Gilbert et al., 2015). This is due to the additional aeration required in mainstream to treat additional ammonium loadings for a complete nitrification. With as much as 100-fold concentration differences between raw wastewater and centrate, aeration costs can be substantial.

Anaerobic ammonium oxidation (Anammox) bacteria have attracted attention due to their ability to convert ammonium to nitrogen gas ($N_2(g)$) without either dissolved oxygen (DO) or external organic carbon sources. Anammox bacteria utilize nitrite to oxidize ammonium to produce nitrogen gas for nitrogen removal (Kartal et al., 2010). Since the first full-scale application of this new technology (Wett, 2007), over 100 implementations have been installed worldwide in 2014 with partial nitritation as the first step and Anammox as the second step (partial nitritation and Anammox, PN/A) (Lackner et al., 2014). With the growth of new installations, the need to model PN/A becomes paramount for better prediction and control of the process performance.

The switching functions in the classic activated sludge models (ASM), such as ASM1, are critical to accurately represent the substrate utilization by bacteria. In those models, the half-velocity constants of substrates are often treated as constant with only consideration of temperature differences. However, recent studies have shown that the values of the substrate half-velocity constants should be considered as variables in all conditions, not just in terms of temperature. Inadequate understanding of half-velocity constants has led to discrepancies in the reported values of half-velocity constants in the literature, namely DO half-velocity constants (K_{O2}) (Arnaldos et al., 2015; Ma et al., 2016). In some cases, the reported value have ranged greatly, e.g. 33 folds for the reported K_{O2} of ammonium-oxidizing bacteria (AOB). In the context of PN/A models, the DO half-velocity constants have been hypothesized to be impacted by

advection and diffusion limitations, in particular, K_{O2}'s of AOB and nitrite-oxidizing bacteria (NOB) in PN/A applications (Arnaldos et al., 2015). However, previous tests have most often been performed with the presence of just AOB and NOB to prove the hypothesis. These results provide little insight into the effects of advection and diffusion limitations on the K_{O2}'s in the context of PN/A processes. Thus, it is unknown whether mixing intensity has a statistically significant impact on the observed K_{O2} values in a PN/A process.

The availability of accurate values of K_{O2}'s is critical for modeling wastewater treatment processes, especially PN/A processes. For example, conventional wastewater treatment processes, e.g. nitrification, allow a large variation on the K_{O2} values since wastewater treatment plants (WWTP) typically operate at a DO concentration higher than the K_{O2} values. This fact makes conventional processes insensitive to the variation of K_{O2} values in the related models. On the other hand, PN/A processes often operate at a DO concentration near the K_{O2} values. This fact makes PN/A processes susceptible to the variation of K_{O2} values under different operating conditions if K_{O2} values vary. One of the factors that influence K_{O2} values is mixing intensity (Chu et al., 2003), which is the focus of this study.

1.2 Objective

The goal of this study was to determine whether mixing intensity changed the observed values of K_{O2} in a PN/A process. The confirmation of the results could provide evidence for considering the need to model treatment processes with additional factors in the switching functions, such as mixing intensity, especially in PN/A processes. The availability of accurate model simulations can assist wastewater treatment process practitioners to make informed decisions on daily tasks or during pressing situations. The detailed objectives of this study were to:

- Achieve steady-state conditions of a PN/A process at two different mixing intensities to identify whether the mixing intensity had an impact on the process performance;
- Develop and conduct a series of tests that generated data which could be employed in a simplified model for estimating K_{O2} values;
- Based on the test results, formulate a simplified model to describe the tests, and;
- Determine whether different mixing intensity statistically affected estimated K_{O2} values.

1.3 Scope

This study was carried out using a bench-scale quasi-sequencing batch reactor (SBR) with automation to execute control orders for a PN/A operation. A bench-scale SBR was selected due to the ease of use and versatility in operation. The SBR reactor configuration is the most common configuration employed in practice. Synthetic centrate was used in this study. Real centrate was not used as variations in ammonium

concentration that is typical of full scale operations. The variation in ammonium concentration may have caused upsets in the experiment. Hence, a widely referenced synthetic centrate composition was used in this study. Once steady state was determined, a series of activity tests were conducted to estimate the observed DO half-velocity constants. Using these results, a mathematical model was developed to describe the activity tests. Then, statistical tools were used to determine whether the K_{O2}'s of AOB and Anammox bacteria were impacted by reactor mixing conditions with a type I error of α=0.05.

1.4 Thesis Structure

This thesis has six chapters, one appendix, and references. Chapter 1 introduces the problem and the plan of investigation. Chapter 2 further provides more background and discussion of the properties of half-velocity constants as well as factors influencing the values of half-velocity constants. Chapter 3 presents the details of the experimental devices, configuration, and methods of conducting specific tests to evaluate in-situ K_{O2} readings. In Chapter 4, the effect of mixing intensity on K_{O2}'s as determined though application of a mathematical model and subsequent statistical significance testing is presented. Chapter 5 concludes the study and recommendations follow in Chapter 6.

2 Literature Review

The goal of this chapter is to introduce the information needed to understand why the improvement of half-velocity constant estimation is important when simulating partial-nitritation and anammox (PN/A) processes.

2.1 Implementation of Partial Nitritation and Anammox (PN/A) Processes for Centrate Treatment

2.1.1 Active Metabolism

Three dominant types of metabolism exist simultaneously inside a PN/A process, i.e. ammonium oxidation by Ammonium-Oxidizing Bacteria (AOB) to nitrite using dissolved oxygen (DO); nitrite oxidation by Nitrite-Oxidizing Bacteria (NOB) to nitrate using DO; and ammonium oxidation by nitrite using Anammox without the presence of DO. The fact that three bacteria groups coexist means that an equilibrium amongst three bacteria groups needs to be established for an ideal PN/A process. When DO is present in the reactor during aeration periods, AOBs compete with NOBs for space and DO for growth. When DO is diminished in the reactor during anoxic periods, Anammox bacteria compete with NOB for space and nitrite for growth; and meanwhile Anammox bacteria also compete against AOB for space and ammonium for growth. When DO ultimately drops to zero, Anammox bacteria grow in the presence of ammonium and nitrite. An ideal PN/A process depends on the balance amongst these three metabolisms.

Both AOB and NOB are autotrophic where inorganic carbon sources such as bicarbonate ions (HCO_3^-) are utilized for cell growth (Water Environment Federation Nutrient Removal,Task Force, 2011). Under aerobic conditions, nitrite is produced by AOB first and then subsequently consumed by NOB with excess DO in the environment. However, this pathway does not remove nitrogen species from the wastewater. Introduced in the late 1990's, PN/A is a process to remove nitrogen species completely from the wastewater through the production of nitrogen gas. As shown in Figure 2-1, the nitrogen removal path is shortened under PN/A processes compared to nitrification and denitrification. The Anammox bacteria group is also autotrophic and utilizes inorganic carbon, ammonium, and nitrite for cell growth. In general, the PN/A process requires no organic carbon addition and 62% less DO supply compared with nitrification and denitrification (Van Hulle et al., 2010).

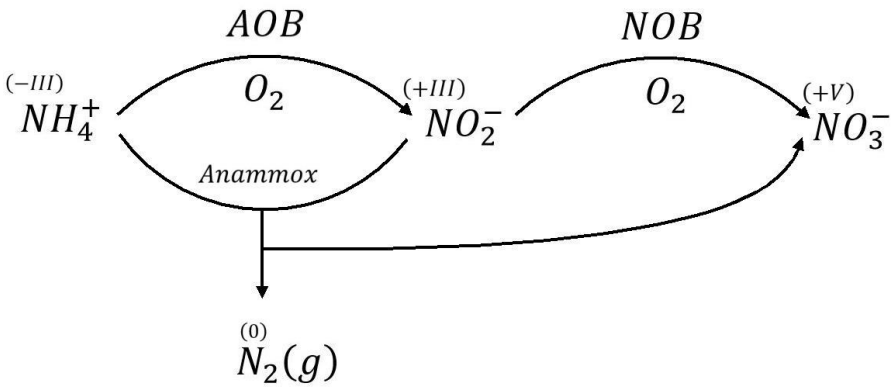

Figure 2-1: An illustration of nitrogen species state changes by AOB NOB and Anammox bacteria

As more and more applications of PN/A processes are used in wastewater treatment, the need to understand the competing mechanisms for substrates amongst AOB, NOB, and Anammox bacteria becomes paramount. Particularly, the conditions for NOB suppression in PN/A systems should be determined so that AOB and Anammox bacteria can establish a stable syntrophic relationship.

2.1.2 PN/A Process Configurations and Operating Strategies for Establishing Desired Metabolisms

Applications to incorporate Anammox in sidestream treatment processes come in many configurations. However, there are three fundamental elements which all treatment processes need to have in the process design, i.e. (1) either Anammox only or an AOB and Anammox mixture; (2) either single reactor or two reactors; and (3) either bacteria in suspension or attached in carrier media. There are many combinations of elements in the industry, for example, CANON (Completely Autotrophic Nitrogen-removal Over Nitrite) (Third et al., 2005; Third et al., 2001); and ANITA^{TM}Mox (Veuillet et al., 2014). The DEMON® (Deammonification) configuration that is the focus of this study includes (1) AOB and Anammox mixture, (2) one reactor, and (3) AOB-Anammox aggregates in suspension (Gonzalez-Martinez et al., 2015).

DEMON applications typically consist of a quasi-sequencing batch reactor (SBR). A typical SBR consists of steps of filling, reacting, settling, drawing and idling (Tchobanoglous et al., 2003). Every step starts only when the previous step finishes. In contrast with a conventional SBR, the actions of filling and reacting in a DEMON application are always simultaneous. After the filling and reacting step finishes, the DEMON reactor stops mixing and the entire reactor acts as a settler for solids to settle. After settling finishes, supernatant is discharged to mainstream wastewater treatment processes. Finally, another cycle of operation starts again. In the whole process, the changing nature of concentrations of biomass and

ammonium in the DEMON reactor makes an ideal operation difficult to maintain during filling and reacting. As a result, many control strategies are employed in DEMON applications to maintain satisfactory nitrogen species removal results as well as achieve steady state, i.e. intermittent DO profile with a maximum of 0.5 mg O_2/L; differential solid retention time (SRT) for AOB-NOB flocs and AOB-Anammox aggregates; reactor temperature at 35 °C; and inhibition of NOB growth for maximal NOB suppression.

2.1.2.1 pH Controlling Dissolved Oxygen (DO) Profile

In the DEMON process intermittent aeration is used to provide an aerobic condition for AOB growth as well as anoxic conditions for Anammox bacteria growth. Therefore, the details of intermittent aeration need to be determined in terms of both percentage of aeration time over total reaction time and DO concentration during the aeration time.

In terms of the strategy of executing intermittent aeration, for example, DEMON uses upper and lower pH boundaries to regulate the DO concentration profile (Wett et al., 2007). Aeration is turned on to achieve the target DO concentration when pH is higher than the upper pH limit. As AOB consumes ammonia and alkalinity this causes a decrease of pH and aeration is stopped when the pH reaches the lower pH limit. After aeration is stopped, the reactor undergoes anoxic conditions. This environment allows pH to be restored and reach the upper limit as centrate keeps flowing into the reactor and meanwhile Anammox reaction is taking place. As soon as the pH reaches the upper limit, another round of aeration will start. The typical pH boundary for the DEMON process has progressed over the years as measurement devices evolved, initially from a pH interval of 0.4 (Wett et al., 1998) to a pH interval of 0.01 (Wett, 2007). During the period of aeration, the target DO concentration is maintained in the range of 0.3 mg O_2/L for this technology (Wett et al., 2007). The DO is set at this value as AOB are considered having a high affinity to DO than NOB (Arnaldos et al., 2015; Picioreanu et al., 2016; Wu et al., 2017). Since there is insufficient DO for NOB to grow, the required SRT for NOB becomes longer than those of AOB. With the help of differential SRT between flocs and aggregates, as described in section 2.1.2.2, NOB cannot only be suppressed but also washed out of the system. The duration of aeration depends on the rate of pH decrease by alkalinity consumption from AOB. As a result, over-aeration needs to be prevented with the help of other parameters, such as time sequence or oxidation-reduction potential profiles.

Continuous aeration, an alternative to intermittent aeration, has been employed without nitrite accumulation. The nature of Anammox bacteria favors a syntrophic relationship with AOB, where AOB surrounds Anammox bacteria as a protective layer from DO penetration and at the meantime provides nitrite for Anammox reactions. Hence, AOB and Anammox bacteria tend to coexist either in a suspended

aggregate or in carrier media. In one study, the highest total nitrogen removal was achieved under continuous aeration regime that maintained 0.25 mg O_2/L (Corbalá-Robles et al., 2016). It was shown in the same study that, under the same average DO concentration, a higher percentage of aeration time over total reaction time resulted in a higher total nitrogen removal rate. In another study (Jaroszynski and Oleszkiewicz, 2011), the rate of partial nitritation by AOB was believed to be the rate limiting reaction in a PN/A reactor. These results suggest that when Anammox bacteria are protected by an AOB outer layer, a higher percentage of aeration time produces a higher total nitrogen removal since the rate of partial nitritation was higher.

2.1.2.2 Solid Retention Time (SRT) Control

Solids retention time (SRT) is defined as the average duration of solids retained in a reactor (Tchobanoglous et al., 2003) and is a key operating strategy that can be employed to control the growth rates of microbial population in bioreactors. Active biomass is usually suspended in a DEMON reactor. However, different groups of biomass are not distributed evenly. For example, since AOB and NOB consume DO for growth, they both grow in floc where there is a larger surface area than those in dense aggregates. On the other hand, since Anammox bacteria require an anoxic condition for growth, Anammox bacteria grow inside dense aggregate where AOB and NOB locate at the outer layer of the aggregate. As a result, Anammox bacteria can be protected from the exposure of DO by AOB and NOB when aerating during the filling and reacting step.

The most important goal to achieve effective operation in DEMON reactors is to suppress the growth of NOB. With proper surrounding conditions as listed in section 2.1.2, NOB growth rates can be suppressed. Furthermore, the fact that AOB-NOB-rich flocs and AOB-Anammox dense aggregates have different settling characteristics makes it possible to selectively waste flocs and retain aggregates (Hubaux et al., 2015). Hence, there exists a condition where not only NOB inside both floc and dense aggregates grows slowly but also NOB in flocs can be wasted faster than dense aggregates. As a result, the SRT's of AOB and Anammox bacteria can be maintained at desired levels. Eventually, a syntrophic relationship between AOB and Anammox bacteria in the form of dense aggregates can be established for DEMON processes. The consequences of selective wasting further favor the formation of AOB-Anammox aggregates in DEMON processes which have good settling properties.

In terms of the selective wasting method, DEMON® processes utilize hydrocyclones to control the SRT of low density AOB-NOB flocs and the SRT of high density AOB-Anammox aggregates in the system. This is accomplished by wasting both communities at different rates from the reactor (Lackner et al., 2014). On the one hand, the purpose of using the hydrocyclone is to maintain a sufficient floc SRT just

for AOB growth while NOB's growth is not only suppressed but also eliminated by being washed-out due to insufficient SRT. On the other hand, AOB-Anammox aggregates are retained efficiently by having a sufficient SRT (Wett et al., 2010a). Many pilot- and full-scale applications in USA have been using hydrocyclones as the selecting wasting apparatus (Nifong et al., 2013; Wett et al., 2010b; Klein et al., 2013).

2.1.2.3 Temperature

Temperature is one of the key physiological parameters that is controlled to induce maximum Anammox performance. The ideal range of temperature has been reported to be between 20 °C and 43 °C (Strous et al., 1999). The optimal temperature was found to be above 25 °C to favor the AOB growth rather than NOB growth (Guo et al., 2010). In a full-scale PN/A plant treating dewatering centrate, it was observed that a more stable operation was achieved at a reactor temperature of 35 °C than those of 37 °C (Bowden et al., 2007). When temperature further increased to 40 °C, AOB were deactivated (Van Hulle et al., 2010) where nitrite production was hindered. When temperature was above 45 °C, the Anammox bacteria population decreased irreversibly due to bacterial lysis. In contrast, when the temperature was below 15 °C, Anammox performance decreased (Dosta et al., 2008). In the same study, Anammox under low temperature triggered off a vicious circle where low temperature caused low Anammox performance; and then nitrite accumulated due to low Anammox performance; and then high nitrite concentration further inhibited Anammox performance.

In both pilot-scale and full-scale applications, it is critical to maintain a constant temperature inside the reactor. With this intention, many preventative measures have been employed in full scale scenarios. For example, one plant utilized not only heaters to offset heat loss due to pumping centrate through uninsulated pipes; but also a floating ball blanket to insulate centrate from heat loss to open-air in the centrate holding tank (Nifong et al., 2013).

2.1.2.4 Inhibitory Mechanisms – pH, Free Ammonia (FA), and Free Nitrous Acid (FNA)

The level of pH in the reactor is another key physiological parameter for successful operation by controlling the acid-base equilibria of inhibitory compounds. Both free ammonia (FA, NH_3) and free nitrous acid (FNA, HNO_2) have inhibitory effects on AOB, NOB, and Anammox bacteria. Once NOB growth is successfully inhibited with proper conditions, NOB can be washed out with the help of selective wasting. In order to control FA and FNA inhibition, their concentrations can be calculated from measured values of ammonium and nitrite ions respectively (Anthonisen et al., 1976). Three factors contribute to the calculated FA and FNA concentrations (i.e. temperature, pH, and the concentration of ammonia or nitrite ions respectively). The responses of FA and FNA are listed in Table 2-1 with respect to the

increase of each factor only. The concentration of FA increases when temperature, pH, or ammonium concentration increases. The concentration of FNA increases when temperature and pH decrease or nitrite concentration increases.

Table 2-1: Relationships between the responses of Free Ammonia (FA) or Free Nitrous Acid (FNA) and temperature, pH, and ammonium or nitrite concentrations

Factor	Free Ammonia (FA)	Free Nitrous Acid
Temperature Only	Positive Correlation	Negative Correlation
pH Only	Positive Correlation	Negative Correlation
Ammonium Only	Positive Correlation	No Effect
Nitrite Only	No Effect	Positive Correlation

In terms of nitrifying bacteria groups, AOB starts to exhibit the effect of being inhibited when FA concentrations range from 8.2 mg N/L to 124 mg N/L, while NOB inhibition starts when FA concentrations range from 0.08 mg N/L to 0.8 mg N/L. On the other hand, both AOB and NOB exhibit inhibition at the same FNA concentration range from 0.066 mg N/L to 0.83 mg N/L (Anthonisen et al., 1976). The fact that AOB and NOB have different tolerances to FA makes it possible to suppress NOB growth and to favor AOB growth. For example, FA was expected to be 1.57 mg N/L in a normal PN/A operation where the in-situ readings had an average ammonia of 150 mg N/L, an average pH of 7.3; and an average temperature of 24 °C in the reactor (Wett et al., 1998). NOB was successfully suppressed by FA so that all nitrite produced by AOB could be utilized by Anammox bacteria to achieve total nitrogen removal.

Anammox bacteria have been found to grow in an environment where the FA concentration is less than 25 mg N/L and FNA is less than 0.5 μg N/L (Fernández et al., 2012). However, different ranges of Anammox inhibition by nitrite have been reported, e.g. inhibition by nitrite from 30 mg N/L to 50 mg N/L for a six-day period (Fux et al., 2004); or complete inhibition by nitrite for more than 100 mg N/L (Strous et al., 1999). In one case where Anammox was inside carrier media, the Anammox bacteria inside the biofilm were not inhibited by NO_2^- at concentrations from 170 mg N/L to 250 mg N/L for a two-day period (Jaroszynski et al., 2011). Despite the inconsistency in the nitrite concentration thresholds under different Anammox configurations, it can be concluded that nitrite inhibits Anammox activity and hence excessive nitrite accumulation should be avoided.

2.2 Process Simulation

As previously described, the PN/A process can remove high concentrations of ammonium without organic carbon addition and with less oxygen supply than those under conventional nitrogen removal methods. Despite the advantages of PN/A's efficiency, PN/A process involves many control challenges that are detrimental to achieving stable total nitrogen removal (Lackner et al., 2014). As a result, process simulation can be a useful approach to improve the understanding of the PN/A processes and to assist with maintaining stable operation.

2.2.1 Biokinetics of AOB NOB and Anammox Metabolisms and Half-velocity Constants

One of the goals of model simulation is to simulate biomass growth rates according to measurable operation data. Although there are many assumptions about the biomass composition, e.g. models of floc-only (Ni et al., 2014), floc-aggregate mixture (Hubaux et al., 2015), and aggregate-only basis (Ni et al., 2009), biomass growth rates are calculated based on maximum biomass growth rates (μ_m), substrate switching functions, biomass concentrations (X), substrate concentrations (S), half-velocity constants (K), and biomass decay coefficients (b). An example of an expression to estimate the AOB growth rate in the context of floc-only biomass composition is presented for aerobic conditions in Equation 2-1 and anoxic conditions in Equation 2-2 (Ni et al., 2014):

Aerobic condition:

$$\frac{dX_{AOB}}{dt} = \mu_m^{AOB} \cdot X_{COD}^{AOB} \cdot \frac{S_{O2}}{K_{O2}^{AOB} + S_{O2}} \cdot \frac{S_{NH_4^+}}{K_{NH_4^+}^{AOB} + S_{NH_4^+}} - b_{AOB} \cdot X_{COD}^{AOB} \cdot \frac{S_{O2}}{K_{O2}^{AOB} + S_{O2}}$$

Equation 2-1

Anoxic condition:

$$\frac{dX_{AOB}}{dt} = \mu_m^{AOB} \cdot X_{COD}^{AOB} \cdot \frac{S_{O2}}{K_{O2}^{AOB} + S_{O2}} \cdot \frac{S_{NH_4^+}}{K_{NH_4^+}^{AOB} + S_{NH_4^+}} - b_{AOB} \cdot \eta_{AOB} \cdot X_{COD}^{AOB} \cdot \frac{K_{O2}^{AOB}}{K_{O2}^{AOB} + S_{O2}} \cdot \frac{S_{NO_2^-} + S_{NO_3^-}}{K_{NO_3^-}^{AOB} + S_{NO_2^-} + S_{NO_3^-}}$$

Equation 2-2

Where,

- μ_m^{AOB} = AOB maximum specific growth rates (1/hr)
- b_{AOB} = AOB decay rate coefficient (1/hr)
- X_{COD}^{AOB} = AOB biomass concentration (g COD/L)
- K_{O2}^{AOB} = AOB's DO half-velocity constant (mg O_2/L)

- S_{O2} = DO concentration (mg O_2/L)
- $K_{NH_4^+}^{AOB}$ = AOB's ammonium half-velocity constant (g N/L)
- $S_{NH_4^+}, S_{NO_2^-}, S_{NO_3^-}$ = Ammonium, nitrite, nitrate concentrations (g N/L)
- $K_{NO_3^-}^{AOB}$ = AOB's nitrate half-velocity constant (g N/L)
- η_{AOB} = anoxic reduction factor for b_{AOB} (dimensionless)

In the growth rate equations shown in Equation 2-1 and Equation 2-2, the theoretical kinetic values of different maximum biomass growth rates (μ_m) are around ten times larger than those biomass decay coefficients (b) (Corbalá-Robles et al., 2016; Ni et al., 2014; Vangsgaard et al., 2013). In the context of a PN/A operation, the ammonium concentration is often much larger than the AOB's ammonium half-velocity constant ($K_{NH_4^+}^{AOB}$) (Lackner et al., 2014). As a result, the DO concentration (S_{O2}) is a key and easy parameter to control AOB growth at any desired rate for operational needs. Meanwhile, NOB have similar growth rate equations as AOB's. Thus, an understanding of the DO switching functions of AOB, NOB, and Anammox bacteria is warranted to better simulate the growth of AOB, NOB, and Anammox bacteria in the PN/A reactions.

As shown in Equation 2-1 and Equation 2-2, the switching functions of AOB, NOB, and Anammox bacteria for DO can be expressed in Equation 2-3 as:

$$SF_{O2}^{AOB} = \frac{S_{O2}}{K_{O2}^{AOB} + S_{O2}}$$

$$SF_{O2}^{NOB} = \frac{S_{O2}}{K_{O2}^{NOB} + S_{O2}}$$

$$SF_{O2}^{Anammox} = \frac{K_{O2}^{Anammox}}{K_{O2}^{Anammox} + S_{O2}}$$

Equation 2-3

Where,

- K_{O2}^{AOB} = AOB's DO half-velocity constant (mg O_2/L)
- K_{O2}^{NOB} = NOB's DO half-velocity constant (mg O_2/L)
- $K_{O2}^{Anammox}$ = Anammox's DO half-velocity constant (mg O_2/L)
- S_{O2} = DO concentration (mg O_2/L)

The literature half-velocity constants of AOB, NOB, and Anammox bacteria are reported to have values of 0.6 mg O_2/L, 2.2 mg O_2/L, and 0.01 mg O_2/L, respectively (Corbalá-Robles et al., 2016; Ni et al., 2014; Vangsgaard et al., 2013). Hence, NOB growth could be suppressed with low DO concentration in PN/A reactors during aeration and meanwhile AOB growth could still be supported based on their literature values. However, a review of the experimentally determined values revealed discrepancies between the observed half-velocity constants of AOB and NOB and theoretical ones, especially. The half-velocity constant of AOB is often believed to be less than that of NOB (Arnaldos et al., 2015; Picioreanu et al., 2016; Wu et al., 2017). Even though the biomass origins and types of systems were different, the observed AOB half-velocity constant ranged from 0.18 mg O_2/L to 1.16 mg O_2/L and the observed NOB one ranged from 0.13 mg O_2/L to 3.00 mg O_2/L (Arnaldos et al., 2015; Ma et al., 2016). Additionally, there exist some occurrences where the AOB half-velocity constant was found to have a higher value than the NOB values. The wide range of half-velocity constants of AOB and NOB challenge the notion whether half-velocity constants are "constant" at all.

Half-velocity "constants" have been found to be more constant in conventional activated sludge (CAS) systems since the DO concentration is often maintained at 2.0 mg O_2/L to sustain conditions for complete nitrification (Tchobanoglous et al., 2003). Comparing to classic values of AOB and NOB at 0.3 mg O_2/L and 1.1 mg O_2/L, respectively (Wiesmann, 1994), the conditions in CAS are less sensitive to the variation of AOB's and NOB's half-velocity values. In contrast, PN/A reactors often maintain 0.5 mg O_2/L of DO when aerating. For this reason, PN/A simulations require high confidence in the accuracy of half-velocity constants of AOB, NOB, and Anammox bacteria, or essentially the values of substrate switching functions. This prompts the need to investigate the factors that change the magnitude of half-velocity constants.

2.2.2 Factors Influencing Half-velocity Constants

In the context of PN/A reactors, there are a few studies that have examined the reasons why observed half-velocity constants varied amongst different studies. The two main factors that were proposed to explain the discrepancy in the half-velocity constants were advection and diffusion limitations (Arnaldos et al., 2015). These two factors are not mutually exclusive from each other. For example with a change to mixing intensity, advection limitation, can change the availability of substrate and subsequently change the substrate gradient, diffusion limitation, which affects the diffusion driving force through boundary layers or bacterial cell membranes.

Mixing intensity affects half-velocity constants in many aspects. On the one hand, high mixing intensity causes high hydrodynamic forces that keep floc size from increasing. On the other hand, suboptimal

mixing intensity causes a non-ideal distribution of substrates in the reactor (Arnaldos et al., 2015). For those half-velocity constants that are measured in reactors, the values reflect the mixing conditions in the system. If the system is at suboptimal mixing conditions, the half-velocity constants become larger than those under optimal conditions, e.g. respirometers. One study looked into the impact of mixing intensity on the floc sizes and observed DO half-velocity constants of the activated sludge in a respirometer (Chu et al., 2003). It was found that floc size increased when mixing intensity decreased in a respirometer, which resulted an increase in observed DO half-velocity constants (K_{O2}). The reason why K_{O2} increased was believed that mass transfer limitations existed in large flocs under low mixing intensity. Another study found that the observed K_{O2} increased due to increased floc size and nitrifier density inside flocs (Wu et al., 2017). At a high floc diameter, e.g. 200 μm, a high DO concentration gradient was found. Additionally, the oxygen gradient for measuring K_{O2}^{AOB} was higher than that for measuring K_{O2}^{NOB}. Besides these results, the same study also found that K_{O2}^{AOB} increased faster than K_{O2}^{NOB} did when flocs' density increased. In the context of PN/A reactors, where NOB are less dense than AOB in the flocs, the observed K_{O2}^{NOB} is often close to its literature value while the observed K_{O2}^{AOB} is often much higher than its literature value. As one can see, mixing intensity does affect observed K_{O2} measurements.

In addition to mixing intensity, diffusion also affects the observed K_{O2} inside flocs. One study has found that substrate half-velocity constants (K_S) increased when diffusivity increased if advection was zero inside flocs (Shaw et al., 2015). Although diffusivity was dependent on substrate and temperature, the cell radius was considered as indicative of diffusion distance. An in-depth understanding of factors influencing K_S is needed, i.e. competition of organisms for the same substrate (e.g. AOB and NOB for DO and NOB and Anammox for nitrite), and the presence of transitional species (e.g. NO_2 in models of N_2O emissions). The same study suggested that more attention should be paid to modeling floc size and diffusion effects.

Another study also investigated the effect of distribution of microcolonies inside floc on observed K_{O2} variation (Picioreanu et al., 2016). It has been found that observed K_{O2} increased as colony size or floc size increased. Furthermore, the change of colony size had a larger influence on K_{O2} than the change of floc size. The study also found that large colony sizes in conventional activated sludge could explain why observed K_{O2}^{AOB} were greater than K_{O2}^{NOB} in some other study results. However, the effect could be only explained properly with a 3-dimentional diffusion-reaction model.

On the topic of K_S variation investigation, the need to model advection and diffusion limitations is shown in multiple studies. It has been shown that bulk-mixing conditions inside either laboratory reactors or full-scale reactors should be modeled first before calibrating K_S. After bulk-mixing has been properly

considered, diffusion should be modeled from bulk solution to floc and from floc to microcolonies inside flocs. The results from different studies warrant the need to model K_S in a resistance-in-series approach mentioned in a previous study (Arnaldos et al., 2015).

2.3 Quantifying Anammox Performance by Activity Tests

The quasi- chemical equation of Anammox bacteria growth utilizing ammonia and nitrite for cell growth has been theorized (Strous et al., 1998) in Equation 2-4:

$$\mathbf{1}NH_4^+ + \mathbf{1.32}NO_2^- + \mathbf{0.066}HCO_3^- + \mathbf{0.13}H^+ \rightarrow \mathbf{1.02}N_2 + \mathbf{0.26}NO_3^- + \mathbf{0.066}CH_2O_{0.5}N_{0.15} + \mathbf{2.03}H_2O$$

Equation 2-4

where ammonium (electron donor, ED) donates its electron to nitrite (electron acceptor, EA) to complete the oxidation-reduction reaction. Without considering the cell growth, the chemical reaction is expressed in Equation 2-5:

$$NH_4^+ + NO_2^- \rightarrow N_2 + 2H_2O$$

Equation 2-5

Therefore, the performance of Anammox can be measured by at least one of the following three terms: (1) the production rate of nitrogen gas per Anammox bacteria (g nitrogen gas/g Anammox – hour); (2) the consumption rate of ammonia per Anammox bacteria (g ammonia/g Anammox – hour); or (3) the consumption rate of nitrite per Anammox bacteria (g nitrite/g Anammox – hour). The higher the production or the consumption rates, the better the Anammox performance is.

Activity tests are typically conducted in batch with known initial conditions. Different initial conditions are listed in Table 2-2 from different studies. As observed in Table 2-2, although activity tests have been widely used, no consensus has been reached on standardized activity test procedures yet (Nifong et al., 2013; Sabine Marie et al., 2015; Williams et al., 2012; Tsushima et al., 2007). Nevertheless, these studies all aimed at high initial concentrations of ammonium (NH_4^+) or nitrite (NO_2^-) throughout the testing period to maintain constant consumption rates of NH_4^+ and NO_2^-. This was achieved by ensuring that NH_4^+ and NO_2^- concentrations were much greater than their corresponding half-velocity constants as listed in Table 2-3 (Corbalá-Robles et al., 2016; Ni et al., 2014; Vangsgaard et al., 2013). As a result, the rates were constant for ammonium and nitrite consumptions as substrates for Anammox bacteria during the entire period of testing. Therefore, DO could then be maintained at any concentration during activity tests for AOB activity testing.

Table 2-2: List of different Anammox activity test initial conditions

Measurement	Subject	Initial $[NH_4^+]$ (mg N/L)	Initial $[NO_2^-]$ (mg N/L)	Duration (hour)	Reference
N_2 production rate	Anammox in suspension	42, 56, or 70	42, 56, or 70	N/A	Dapena-Mora et al., 2007
N_2 production rate	AOB and Anammox in carrier media	5 (Constant value)	7 (Constant value)	N/A	Gilbert et al., 2014
NH_4^+, NO_2^- consumption rates	Anammox from biofilm	30 ~ 84	30 ~ 84	N/A	Tsushima et al., 2007
NH_4^+, NO_2^- consumption rates	Anammox from biofilm	70	70	N/A	Tang et al., 2009
NH_4^+, NO_2^- consumption rates	Anammox in suspension	100	70	4	Sabine Marie et al., 2015
NH_4^+, NO_2^- consumption rates	Anammox in suspension	100	100	N/A	Chen et al., 2014
NH_4^+, NO_2^- consumption rates	Anammox in suspension	≥15	≥15	0.25 ~ 1	Laureni et al., 2015
NH_4^+, NO_2^- consumption rates	AOB and Anammox in suspension	N/A	50	3 or 4	Nifong et al., 2013
NH_4^+, NO_2^- consumption rates	AOB and Anammox in suspension	Concentration level in MLSS	>50	1	Figdore et al., 2011
NH_4^+, NO_2^- consumption rates	AOB and Anammox in suspension	Concentration level in MLSS	>50	1	Wett et al., 2007
NH_4^+, NO_2^- consumption rates	AOB and Anammox in suspension	~ 130	~ 70	~ 2.5	Williams et al., 2012
NH_4^+, NO_2^- consumption rates	AOB and Anammox in suspension	Concentration level in MLSS	>50	1	Wett et al., 2010b
NH_4^+, NO_2^- consumption rates	AOB and Anammox in suspension	Concentration level in MLSS	~ 50	1	Bowden et al., 2007
NH_4^+, NO_2^- consumption rates	AOB and Anammox in suspension	~ 28 (2 mM)	~ 28 (2 mM)	4	Third et al., 2001

Table 2-3: AOB and Anammox half-velocity constants of ammonia, nitrite, and dissolved oxygen

Bacteria	K_{NH4+} (mg N/L)	K_{NO2-} (mg N/L)	K_{O2} (mg O_2/L)
AOB	2.4	No Effect	0.6
Anammox	0.07	0.05	0.01

2.4 Summary of Literature Review

PN/A technologies are increasingly being employed in both the EU and USA with multiple pilot- and full-scale operations. With more reports on the challenges of daily operation, it is apparent that the interactions amongst AOB, NOB, Anammox bacteria, and other groups of bacteria need to be better understood. By using mathematical models, more knowledge of the complex bacterial structures of PN/A can be gained. Having been demonstrated in the literature review, the importance of having accurate model inputs becomes paramount. The following section presents the methodology employed to investigate the effect of mixing intensity on the observed DO "half-velocity constants".

3 Materials and Methods

In this study a semi-continuously operated bench scale bioreactor was operated to generate data that could be employed to assess the impact of mixing intensity on the rates of substrate utilization in a Partial Nitritation and Anammox (PN/A) system. As was identified in Chapter 2, steady-state operation of the PN/A reactor was needed to investigate the effect of mixing intensities on DO half-velocity constants. This chapter details the apparatus that was employed and the operating strategies employed to achieve consistent effluent quality.

It was initially expected that biomass from a pilot-scale DEMON® process operating in southern Ontario would be employed in the project. However, satisfactory arrangements could not be established in this regard and hence DEMON® biomass from the York River Treatment Plant (YRTP), Virginia, USA, was used as the inoculum to initiate the PN/A process. The process was operated with a synthetic centrate (described in section 3.1.2.2) to ensure a constant influent composition. Regular sampling was performed on nitrogen species to evaluate the consistency of effluent quality. When steady-state operation was determined by consistent effluent quality, activity tests were conducted under a range of DO concentrations with one mixing intensity and when completed the mixing intensity was changed. After steady-state was achieved, under the new mixing condition activity tests under the same range of DO concentrations were repeated at this mixing intensity. The results from the two testing conditions were compared to identify the effect of mixing intensity on DO half-velocity constants.

The activity tests consisted of batch tests that were conducted with known initial conditions and lasted for a one-hour period. Nitrogen species concentrations and mixed liquor volatile suspended solids (MLVSS) concentrations were measured when the activity tests were finished. The conversion rates of nitrogen species concentrations were then calculated and normalized by MLVSS so that activity tests conducted on different days could be compared against each other. Since DO was the only variable in different activity tests, the trend of each nitrogen species conversion rates normalized by MLVSS against DO concentrations was able to be compared under two mixing intensities.

3.1 Reactor Configuration and Operation

The following sections describe the details of the reactor configuration and operation strategies employed in this study. In order to implement the process control strategies, input and output devices were all connected and controlled through a data acquisition module. The input devices measured pH, DO, and temperature sensors while the controller actuated three peristaltic pumps, an aquarium air pump, and a mechanical mixer. The control strategy logic was designed to provide favorable conditions for AOB-

Anammox aggregate growth. Regular influent and effluent tests were conducted to confirm whether or not favorable conditions were established.

3.1.1 Reactor Configuration

The reactor employed in this study was made of acrylic plastic. Some details of the reactor are listed in Table 3-1.

Table 3-1: Reactor details and measument results

Reactor Detail	**Measurement Value**
Inner Diameter	203 mm (8 inch)
Outer Diameter	216 mm (8.5 inch)
Maximum Height	406 mm (16 inch)
Maximum Volume	13.1 L
Operating Volume	8.0 L
Influent Feed Point	Top of the reactor
Decant Level	To 50% of the operating volume (i.e. 4.0 L)
Vertical Flat Blade Turbine (VFBT) radial flow Impeller Length	120 mm

As shown in Figure 3-1, the reactor was equipped with a VFBT for mixing, two luminescent DO probes equipped with temperature sensors (Hach LDO® probe, Product #5790000, Hach Company, Loveland, CO, USA), one pH sensor (Orion™ pH probe, Catalog #9107BN, Thermo Fisher Scientific, Sunnyvale, CA, USA) and one commercial air diffuser. Three stainless steel tubes entered the reactor through the lid to provide feed and air to the reactor, and to facilitate withdrawal of mixed liquor suspended solids (MLSS) from the reactor. A commercial product, *Bubble Mist – Bendable Air Wall* (Big Al's® Canada, Woodbridge, ON, Canada), was used to diffuse air along the perimeter of the bottom of the reactor, as shown in Figure 3-2.

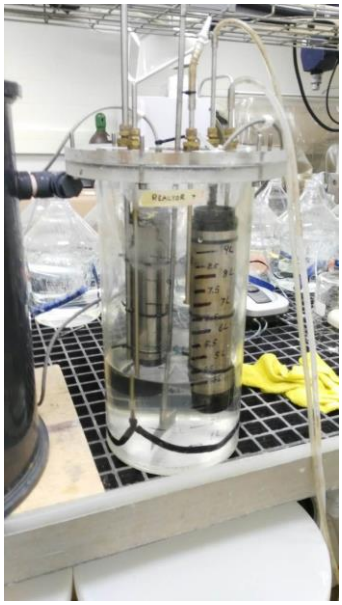

Figure 3-1: Photo of reactor with clean water

Figure 3-2: Example of air diffusion in clean water with Bubble Mist – Bendable Air Wall

Three peristaltic pumps (MASTERFLEX® Console Pump Drives, Model #77521-40 and Model #77521-50, Cole-Parmer Instrument Company, Vernon Hills, IL, USA) were used to move liquids in and out of the reactor as shown in Figure 3-3. A commercial aquarium air pump (Elite Optima Pump w/Rheostat, Model #A-807, Rolf C. Hagen Inc., Baie d'Urfé, QC, Canada) was used to pump air into the reactor. The pH, DO, and temperature were measured with the probes and the signals were transmitted to a data

acquisition module (National Instrument DAQ USB Device, NI USB-6001, National Instruments Corporation, Austin, TX, USA).

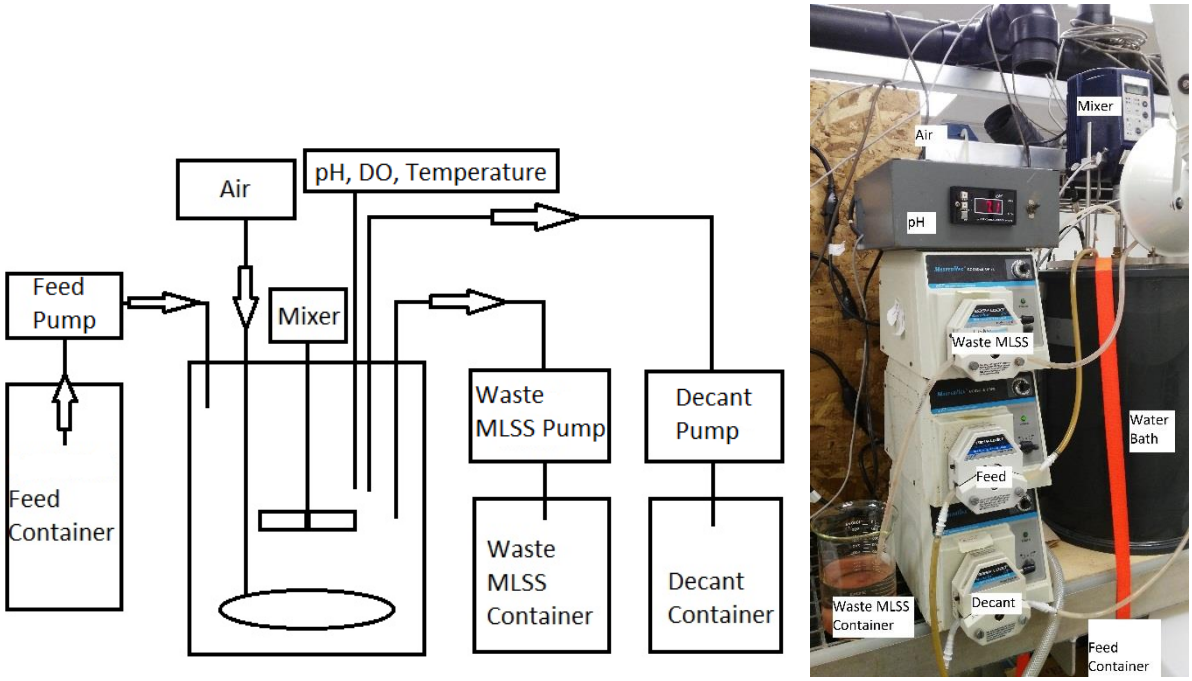

Figure 3-3: Process flow diagram

3.1.2 Reactor Startup and Feed Composition

The steady-state operation of the partial nitritation and anammox reactor was the foundation for further investigations. In order to quickly establish and maintain steady-state operation, an external inoculum and synthetic centrate were used. The following sections describe the details of the inoculum and synthetic centrate.

3.1.2.1 Inoculum

DEMON® biomass from the YRTP was employed as inoculum to reduce the time needed to generate AOB-Anammox aggregate. The YRTP was designed to treat an average flow of 71,500 gpd (271 m^3/day) of centrifuge centrate with the TKN concentration from 600 mg/L to 1,000 mg/L under DEMON® process (Nifong et al., 2013). The DEMON® biomass was transported from Virginia, USA, overnight through courier services in a cooler with ice packs. Upon receiving, the inoculum was stored in refrigerator at 4 °C.

3.1.2.2 Synthetic Centrate

A synthetic centrate was used to maintain a constant influent composition throughout the study. The centrate included ammonium (nitrogen source), bicarbonate (inorganic carbon source), trace elements (Van De Graaf et al., 1996), and other compounds as described in previous studies (Jung et al., 2007; Ni et al., 2009; Vangsgaard et al., 2013; Strous et al., 1998; Tsushima et al., 2007; Yu et al., 2014; Li et al., 2011; Strous et al., 1997). The composition of the major components in the synthetic centrate is shown in Table 3-2, and the composition of the trace element solution is shown in Table 3-3. Both solutions were dissolved in de-ionized water.

Table 3-2: Composition of synthetic centrate for this study

Component	**Concentration**
NH_4HCO_3	2820 mg/L (500 mg N/L)
$NaHCO_3$	420 mg/L
KH_2PO_4	27.2 mg/L
$MgSO_4$	147 mg/L
$CaCl_2 \cdot 2H_2O$	180 mg/L
Trace Element I	1 mL/L of synthetic centrate
Trace Element II	1 mL/L of synthetic centrate

Table 3-3: Composition of trace element solution

Component	**Concentration**
Trace Element I	
EDTA	5.0 g/L
$FeSO_4 \cdot 7H_2O$	9.15 g/L
Trace Element II	
EDTA	15.0 g/L
$ZnSO_4 \cdot 7H_2O$	0.430 g/L
$Co(NO_3) \cdot 6H_2O$	0.294 g/L
$MnCl_4 \cdot 4H_2O$	0.990 g/L
$CuSO_4 \cdot 5H_2O$	0.250 g/L
$(NH_4)_6Mo_7O_{24} \cdot 4H_2O$	0.177 g/L
$NiCl_2 \cdot 6H_2O$	0.190 g/L
Na_2SeO_3	0.105 g/L
H_3BO_3	0.0111 g/L

3.1.3 Operational Strategy

The operational strategy was adopted from previous articles (Jardin and Hennerkes, 2012; Wett et al., 2007; Strous et al., 1998; Yu et al., 2013; Wett, 2006). The key operating parameters are listed in Table 3-4. A mixing intensity of 150 rpm (the equivalent of average velocity gradient of 15/s at 8.0L) was employed in the first phase of study while an rpm of 75 rpm (the equivalent of average velocity gradient of 5.3/s at 8.0L) was employed in the second phase. The average velocity gradient (see Appendix 8.2) was calculated on the basis of a VFBT impeller diameter, the power number for the impeller, revolution speed, reactor volume, and other properties related to water properties (Tchobanoglous et al., 2003).

Table 3-4: Details of operation parameters

Operation Parameter	**Value**
HRT	12 hour
Cycle per HRT	2
SRT	$Floc \in (6.7, 22.5)\ day$ $Aggregate \in (22.5, +\infty)\ day$
Mixing Intensity	150rpm, and 75rpm
Reactor Temperature maintained by water bath	35 °C

The operating strategy sought to establish different SRT's for the aggregates and floc by using a selective wasting method to increase the SRT of aggregates, and meanwhile, decrease the SRT of the floc (Lackner et al., 2014). The goal of the selection was to favor the growth of AOB-Anammox aggregates in the MLSS. A separatory funnel was used to achieve selective wasting and the details of the selective wasting procedure are listed here:

1. Transferred 300 mL of "Waste MLSS" to a separatory funnel;
2. Swirled the funnel for 15 seconds, and then let the solids settle;
3. As the supernatant became clear, the stopcock was opened and biomass was collected from the stem at the bottom;
4. The stopcock was closed when the solids surface level reached $\frac{2}{3}H$ (see Figure 3-4);
5. Recycled the collected biomass from step 3 to the reactor;
6. Wasted the rest of the biomass left in the separatory funnel.

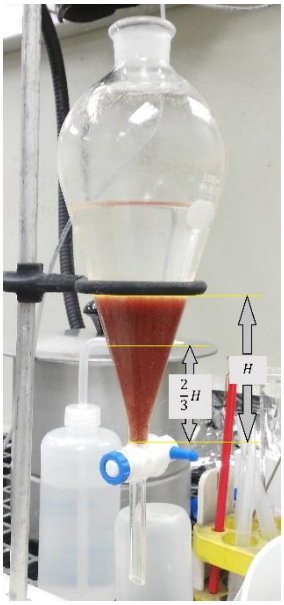

Figure 3-4: Example of settled "Waste MLSS" in the separatory funnel

The ranges of SRT's for the flocs and aggregates were estimated on the basis of two different assumptions regarding the concentrations of the floc and aggregate in the separatory funnel. One scenario assumed that the selective wasting method achieved no biomass separation. Thus, the reactor was wasting MLSS at a rate of 88.8 mL of MLSS per cycle (29.6% × 300 mL). As a result, the SRT's for the floc and aggregate were the same, with a value of 22.5 day. The alternate scenario assumed that the selective wasting method achieved perfect separation where all aggregates were recycled and at the same time all floc were wasted. In that case, floc were wasted at a rate of 300 mL of MLSS per cycle and aggregate was not wasted at all. Hence, floc SRT was 6.7 days and aggregate SRT approached infinite. It is believed that the actual SRT values were between the extremes. Detailed calculations are presented in Appendix 8.3.

The reactor was operated in a sequencing batch mode and this was achieved by implementing a time sequence for each action, i.e. feeding of centrate, mixing reactor, aerating MLSS, wasting MLSS, and decanting effluent. The details of the operating sequence are listed in Table 3-5. The reactor was operated to achieve partial nitritation and anammox via the activity of two different groups of bacteria, i.e. AOB that required oxygen for growth and Anammox that required oxygen depletion. Hence, a 6-minute aerated and 3-minute unaerated sequence was employed for aeration frequency (Jardin and Hennerkes, 2012; Wett et al., 1998; Jaroszynski and Oleszkiewicz, 2011). The aeration was further controlled during the aeration period to achieve target ranges of pH and DO using LabVIEW® (National Instruments, Austin, TX, USA).

Table 3-5: Operation sequence details

Action in 1 cycle	Duration (min)	Flow Rate	Volume (mL)
Feed and Mix	1 ~ 330	Liquid: 13.03 mL/min	4300
Aerate	1 ~ 6, 10 ~ 15, 19 ~ 24, …… 316 ~ 321	Air: 5.5 ~ 6.5 L/min	N/A
No Aeration	7 ~ 9, 16 ~ 18, 25 ~ 27 …… 322 ~ 330	Air: 0 L/min	N/A
Waste MLSS	320 ~ 325	Liquid: 50 mL/min	300
Settle	331 ~ 350	Liquid: 0 mL/min	0
Decant	351 ~ 360	Liquid: 400 mL/min	4000

LabVIEW® utilized a "comma-separated values" (csv) file to execute all sequences in Table 3-5. After transforming the actions presented in Table 3-5 into computer code a value of 1 was assigned in the csv for power on and a value of 0 was assigned for power off, as shown in Table 3-6. An unassigned control spot, "USER DEFINED", was implemented in the "time sequence.csv" to incorporate unforeseeable control needs for the time sequence.

Table 3-6: Example of the beginning of time sequence

TIME ELAPSED (MIN)	FEED PUMP	MIXER	AIR PUMP	DECANT PUMP	Waste MLSS PUMP	USER DEFINED
1	1	1	1	0	0	0
2	1	1	1	0	0	0
3	1	1	1	0	0	0
4	1	1	1	0	0	0
5	1	1	1	0	0	0
6	1	1	1	0	0	0
7	1	1	0	0	0	0
8	1	1	0	0	0	0
9	1	1	0	0	0	0
10	1	1	1	0	0	0
11	1	1	1	0	0	0

The algorithms employed to power the Feed Pump, Mixer, Decant Pump, and Waste MLSS Pump followed the logic at each time step of "time sequence.csv", as shown in Figure 3-5. When the time sequence.csv was launched in LabVIEW®, LabVIEW® started to track time in its internal clock. For example, when the operation cycle was just started to execute time sequence.csv, the Feed Pump, Mixer, Air Pump, would be powered on; the Decant Pump, and Waste MLSS pump would be powered off, during the time between 00:00:01 (hh:mm:ss) to 00:07:00. Later, Feed Pump and Mixer would remain on and the Air Pump, Decant Pump, and Waste MLSS Pump would be powered off, during the time between 00:07:01 to 00:10:00. The entire operation would be restarted all over again when time passed 06:00:00.

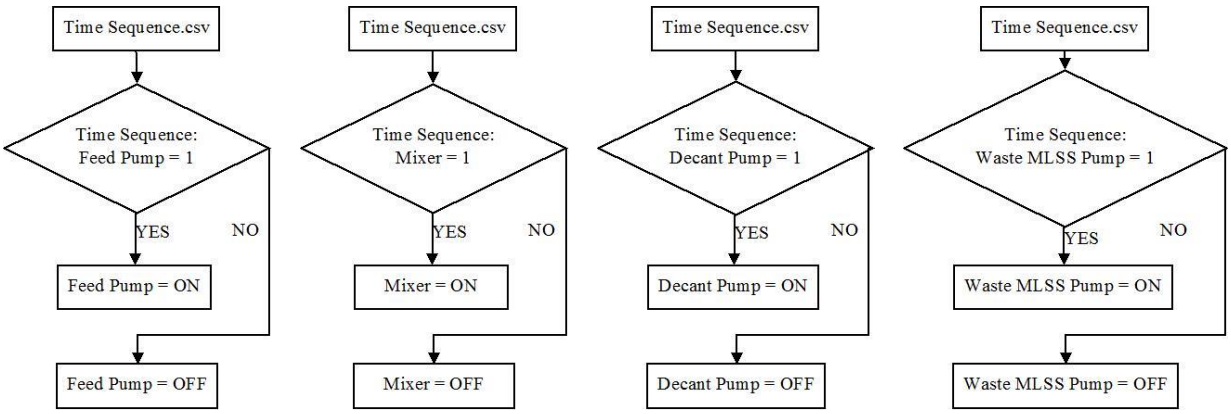

Figure 3-5: Algorithm flow charts of Feed pump, Mixer, Decant pump, and Waste MLSS pump

The algorithm that controlled the air pump integrated an additional level of control that built upon the time sequence.csv. The algorithm initially checked the values in the time sequence.csv; then checked the pH value; and finally the DO concentrations in the MLSS. The air pump was powered on if the (1) Time Sequence Air pump was equal to 1; (2) the pH in the MLSS was greater than or equal to 7.00; and (3) the DO in the MLSS was less than or equal to 0.8 mg O_2/L. Additional operating scenarios are illustrated in Figure 3-6. If the DO was greater than 0.8 mg O_2/L, the Air Pump would be powered off, and then the algorithm would be executed again. If the pH was less than 7.00, the air pump would only be powered on until the time when Time Sequence AIR PUMP changed from 0 to 1. As a result, the actual duration of aeration depended on real-time data and therefore the duration of aeration was not always equal to 6 minutes and the duration of no aeration was not always equal to 3 minutes.

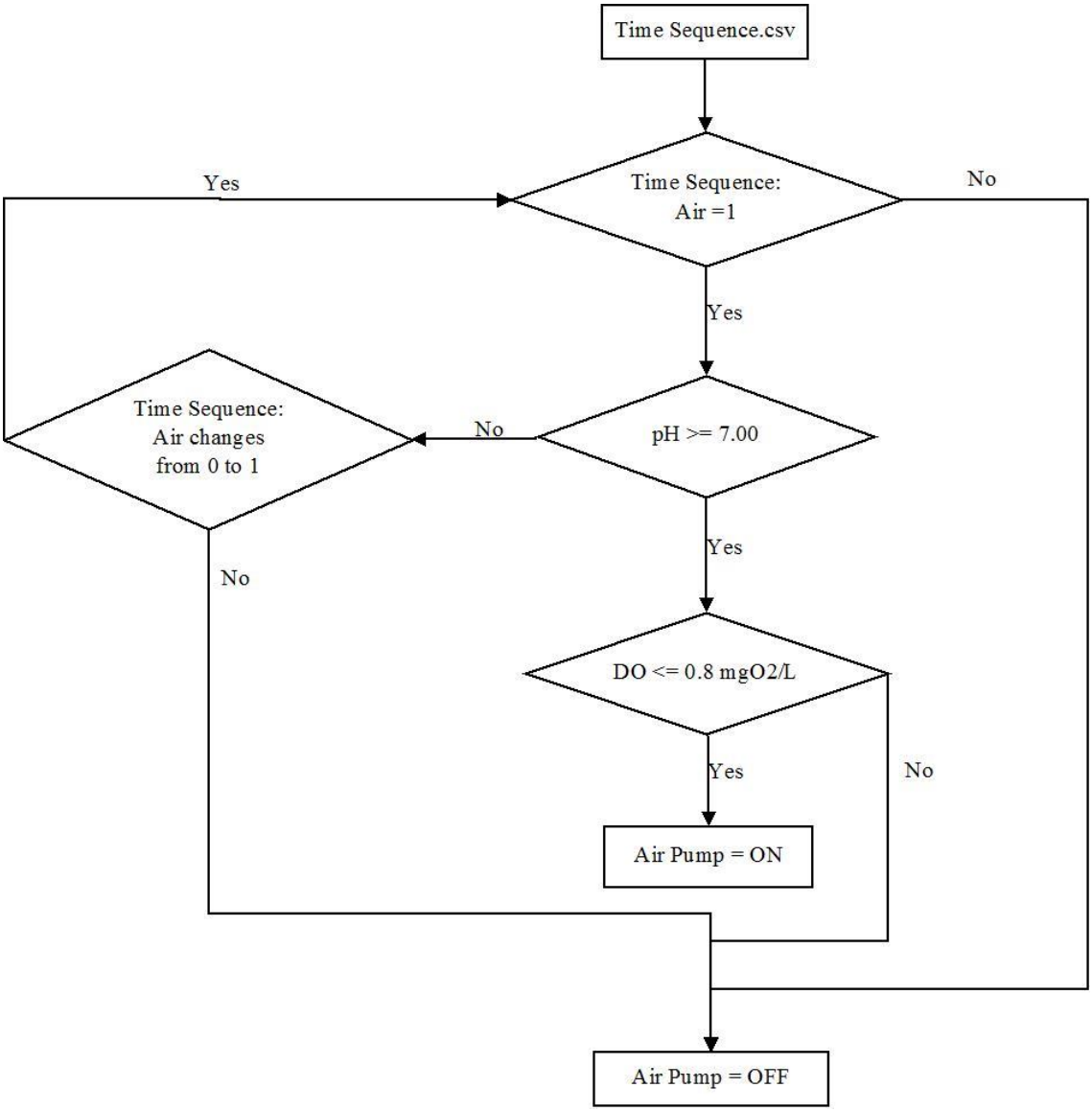

Figure 3-6: Algorithm flow chart for air pump

Under the control algorithm, the real-time DO profile behaved in a way that, within the duration of the aeration, maintained an average of 0.5 mg O_2/L and a minimum pH of 7.0 (Figure 3-7). In the period of no aeration, the DO was effectively maintained at 0 mg O_2/L.

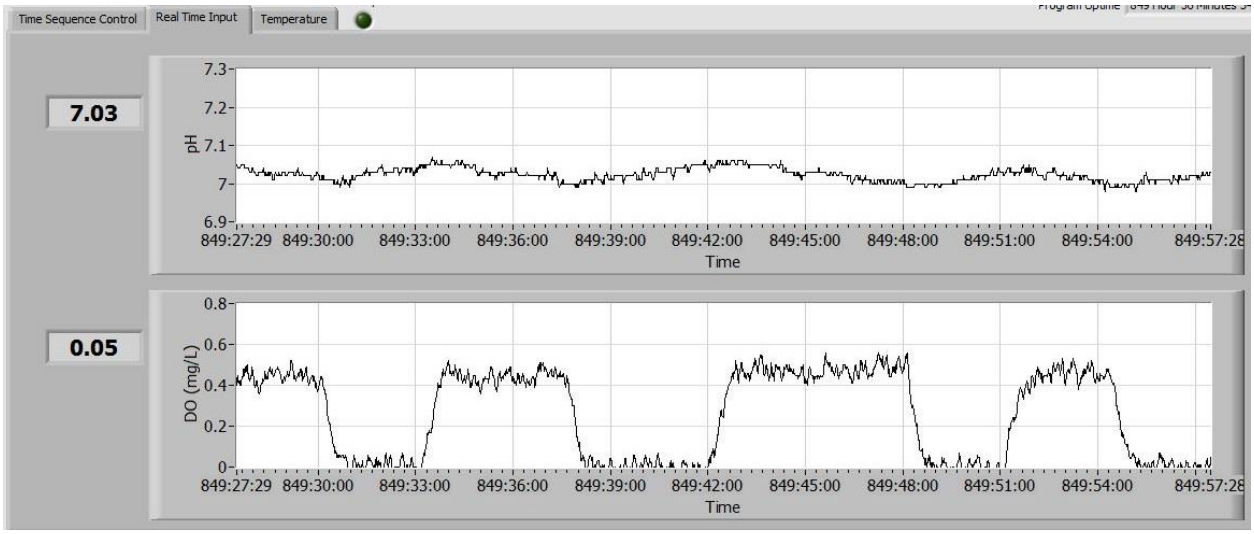

Figure 3-7: Real-time screenshot of pH and DO profiles from LabVIEW® User Interface

3.1.4 Sample Collection and Analysis

Influent, effluent, and MLSS samples were tested twice per week at the beginning of the study and then reduced to once per week as effluent quality became consistent. The analyses were performed according to the Standard Methods (APHA, 2005). The method detection limits (MDLs) were identified to indicate the minimum values for measuring ammonium, nitrite, and nitrate ions for selecting valid data results for the activity testing (described in section 3.2). The testing methods are detailed in Table 3-7.

Table 3-7: Sample test methods for influent, effluent, and MLSS

Test	Method	Influent	Effluent	MLSS	MDLs
NH_4^+	4500-NH_4^+-F	Triplicate	Triplicate	Not applicable	0.01 mg N/L
NO_2^-	4500-NO_2^--C	Not applicable	Duplicate	Not applicable	0.03 mg N/L
NO_3^-	4500-NO_3^--C	Not applicable	Duplicate	Not applicable	0.02 mg N/L
TSS	2540 D	Not applicable	Not applicable	Triplicate	Not applicable
VSS	2540 E	Not applicable	Not applicable	Triplicate	Not applicable
pH	4500-H^+-B	Triplicate	Not applicable	Continuous recording	Not applicable
DO	Hach LDO	Not applicable	Not applicable	Continuous recording	Not applicable

3.1.5 Quality Control

In terms of NO_2^- and NO_3^- measurements, both a raw sample and a diluted sample were analyzed so that both NO_2^- and NO_3^- were in the calibration range of the Ion Chromatograph (IC) (Dionex IonPac™ AS4A-SC, Thermo Fisher Scientific, Sunnyvale, CA, USA).

Multiple activity tests were conducted throughout the study to compare against different sets of activity tests on different days. Such results indicated whether the level of anammox performance changed over time or not.

Maintenance and calibration of pH and DO probes were performed periodically as specified by the user's manuals from the manufacturers.

3.2 Activity Testing

Activity tests were conducted with the previously described reactor operating in batch mode to allow characterization of the rates of change of nitrogen species during a one-hour period. High initial concentrations of ammonium (around 0.20 $gNH_4^+ - N/L$) or nitrite (around 0.075 $gNO_2^- - N/L$) were employed to maintain constant consumption rates of NH_4^+ or NO_2^- throughout the anoxic testing period. This was achieved by maintaining the NH_4^+ or NO_2^- concentrations greater than their corresponding half-velocity constants (Corbalá-Robles et al., 2016; Ni et al., 2014; Vangsgaard et al., 2013). Hence, the conversion rates of nitrogen species during the one-hour activity tests remained constant. In terms of the aerobic testing period, only ammonium was added to maintain an initial concentration of around 0.20 $gNH_4^+ - N/L$. The details of initial substrate addition concentrations are listed in Table 3-8.

A range of DO concentrations were employed to compare the nitrogen species rates at two different mixing intensities. A detailed plan of testing is described in section 3.2.1.

Table 3-8: Substrate addition for activity testing

Test	**Substrate**	**Addition at full operating volume, i.e. 8.0 L**
Anoxic	NH_4HCO_3 $NaNO_2$	2.26 g 2.96 g
Aerobic	NH_4HCO_3 DO	9.03 g 0.3 ~ 6.4 mg O_2/L

On the basis of previous studies (Nifong et al., 2013; Sabine Marie et al., 2015; Williams et al., 2012; Tsushima et al., 2007), the activity test procedures employed in this study are as follows:

1. Stop automation when sequence "Feed and Mix" finishes;
2. Elevate ammonium (NH_4^+) and nitrite (NO_2^-) concentrations by adding substrates according to Table 3-8;
3. Mix reactor for 6 minutes; then start one-hour anoxic activity test;
4. Filter and collect 5 samples (15 minutes apart) for NH_4^+, NO_2^-, and NO_3^- analyses;
5. The end of anoxic activity test;
6. Elevate ammonium (NH_4^+) concentration by adding substrates according to Table 3-8;
7. Elevate DO to target concentration;
8. Mix reactor for 6 minutes; then start one-hour aerobic activity test;
9. Filter and collect 5 samples (15 minutes apart) for NH_4^+, NO_2^-, and NO_3^- analyses;
10. The end of aerobic activity test;
11. Collect MLSS for total suspended solids (TSS) and volatile suspended solids (VSS) analyses;

The nitrogen species conversion rates were calculated and normalized by the VSS measured at the end of each activity test.

3.2.1 Test Plan

As determined in Chapter 2, mixing intensity was proposed to be a factor that can affect the values of half-velocity constants. This study investigated the effect of mixing intensities on DO half-saturation constants. The activity test was utilized since all initial conditions were known; all nitrogen species conversion rates could be calculated; and DO half-velocity constants could be estimated from mathematical model simulations. Therefore, a series of activity tests were conducted under a range of DO values at two different mixing intensities, as shown in Table 3-9. An ideal activity test result would show linear responses of nitrogen species concentrations over one-hour period.

Table 3-9: Experiment plan to investigate the effect of mixing intensity using activity testing

Target Activity Test DO Concentrations (mg O_2/L)	**Actual DO Values at 75 rpm (mg O_2/L)**	**Actual DO Values at 150 rpm (mg O_2/L)**
0.3	Not applicable	0.25
0.5	0.39	0.46
0.8	0.78	0.76
1.2	1.21	1.21
2.5	2.52	2.52
4.0	4.03	4.03, 4.18
6.0	5.84	6.36, 6.42

4 Results and Discussion

Three stages of the experiment are discussed in this section and they include the steady-state operation results, characterization of nitrogen species conversion during activity testing, and the investigation of the DO half-velocity constants of AOB and Anammox bacteria at two mixing speeds. Specifically, Section 4.1 presents the results of normal operation that were employed to establish steady-state operation. Section 4.2 summarizes the results from all activity tests under aerobic and anoxic conditions. Based on experimental observations from Section 4.2, a model was developed in Section 4.3 to estimate the DO half-velocity constants for AOB and Anammox bacteria at the different mixing conditions.

4.1 Steady-state Operation

Achieving steady-state operation was the first step for this study. Achieving stable concentrations of different groups of bacteria was expected to increase the accuracy of the activity testing and the confidence in the estimation of the DO half-velocity constants (K_{O2}'s). Steady-state conditions were assessed based upon the presence of stable effluent concentrations of ammonium (NH_4^+), nitrite (NO_2^-), and nitrate (NO_3^-) over time. The steady-state conditions were initially established with a mixer speed of 150 rpm in the quasi-sequencing batch reactor (SBR).

The experiment was divided into four phases namely:

- Phase I: Anammox bacteria growth at 150 rpm;
- Phase II: steady-state condition and conducting activity tests at 150 rpm according to the test plan;
- Phase III: transition from 150 rpm to 75 rpm;
- Phase IV: steady-state condition and conducting activity tests at 75 rpm according to the test plan.

The mixing speed of 150 rpm resulted in an average velocity gradient (G) of 15/s when the reactor volume was 8.0 L, while operation at 75 rpm resulted in a G value of 5.3/s when the reactor volume was 8.0 L. When steady-state conditions were achieved, the average Total Nitrogen Removal Efficiency (TNRE) was calculated for Phases II and IV, respectively. The TNRE values were used to assess whether the concentrations and activity of AOB, NOB, and Anammox bacteria changed due to the changing mixing speed.

As shown in Figure 4-1, Phase I of this study operated from day 1 to day 81. The influent NH_4^+ concentration was maintained around 0.50 g N/L. A trend towards a stable effluent NH_4^+ profile was seen around day 50 of operation in Phase I. Before day 50, the effluent NH_4^+ profile showed significant variability. After day 50, the effluent NH_4^+ gradually stabilized around 0.12 g N/L. Effluent NO_3^- showed

a steady decrease as time progressed towards day 20 and plateaued around 0.050 g N/L onwards. It should be noticed that the effluent NO_2^- concentration through this study was around 0.001 g N/L thus being considered as negligible throughout the operation. By maintaining a low NO_2^- concentration, an environment was created where Anammox bacteria could grow successfully. The fact that NO_2^- was relatively low as compared to NH_4^+ indicated that the implemented automated systems and associated operations were able to minimize NO_2^- accumulation in the DEMON® process.

Phase II was operated from day 81 to day 165 and as shown in Figure 4-1, the fluctuations of NH_4^+ concentrations were minimized. The steady-state condition in phase II had an average TNRE of 62% on the basis of an average influent NH_4^+ concentration of 0.47±0.036g N/L (sample mean±sample standard deviation), effluent NH_4^+ concentration of 0.11±0.020g N/L, effluent NO_2^- concentration of 0.00060±0.00023 g N/L, and effluent NO_3^- concentration of 0.069±0.0078 g N/L, respectively.

Phase III was initiated on day 165 when the mixing speed was decreased from 150 to 75 rpm. When the mixing intensity was changed, the effluent NH_4^+ fluctuated in the range from 0.092 to 0.14 g N/L. Phase IV was determined based upon the effluent measurements collected from day 199 to day 228. At steady state concentration of the influent NH_4^+ of 0.52±0.013 g N/L, effluent NH_4^+ of 0.037±0.0062 g N/L, effluent NO_2^- of 0.00081±0.00039 g N/L, and effluent NO_3^- 0.046±0.0030 g N/L, were observed respectively and hence the average TNRE of 84%.

Comparing Phase II with Phase IV, the average effluent NH_4^+ concentration in Phase IV decreased to approximately 33% of that observed in Phase II. The average effluent NO_2^- and NO_3^- concentrations were similar in both phases. The effluent concentration of NO_2^- remained negligible and the average effluent NO_3^- concentration decreased in Phase IV. This suggested that NOB were suppressed by the conditions associated with the reduced mixing speed. Hence, the increase of TNRE from Phase II to Phase IV in Figure 4-1 was attributed to the decrease of mixing intensity.

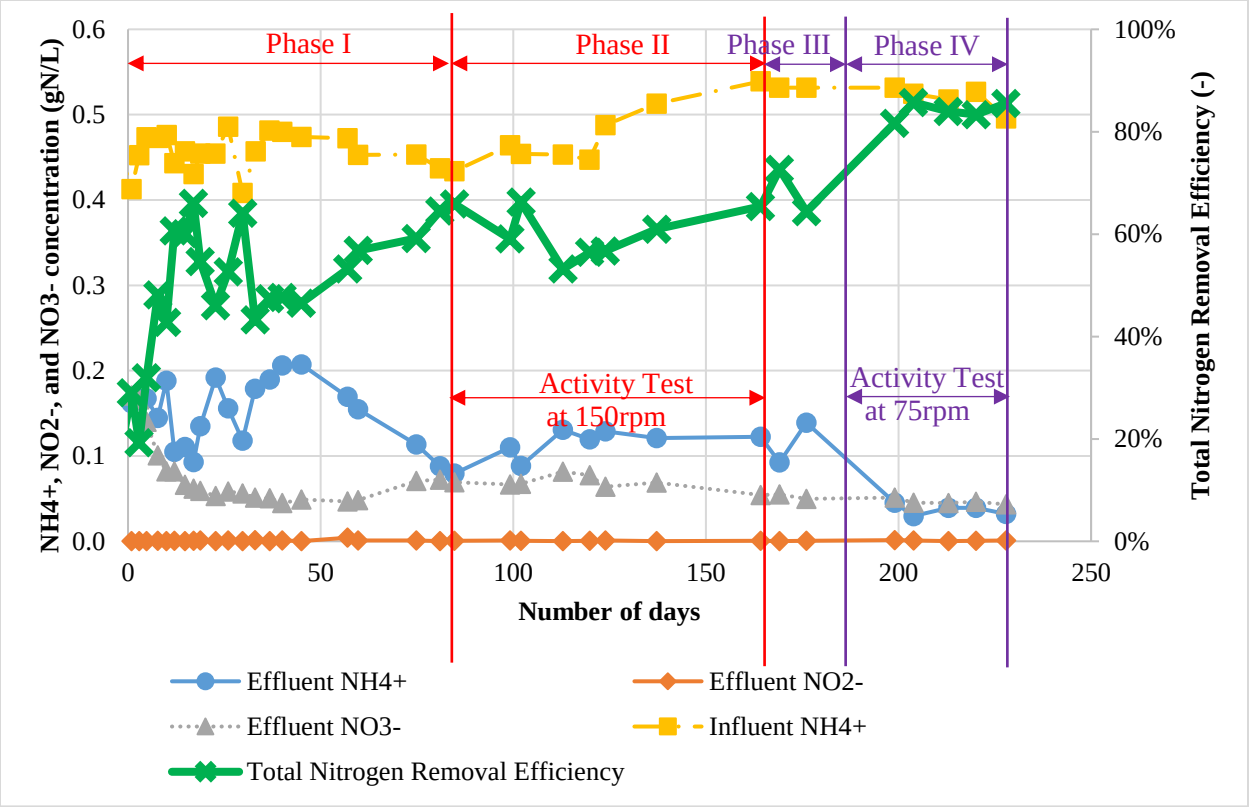

Figure 4-1: Effluent profile from the beginning of the automated operation

To better understand the bioreactor operation and the corresponding changes in the bacterial community in the reactor, the mixed liquor suspended solids (MLSS) concentration profile was evaluated. As can be seen in Figure 4-2, both TSS and VSS concentrations showed a decrease for approximately the first 20 days from the start of operation. Meanwhile, the ratio of VSS over TSS ($\frac{VSS}{TSS}$) steadily increased from 70% initially to a plateau of 90% at the end of the experiment despite the change in mixing speed. This was attributed to the influent characteristics that had very low inert solids concentration. When comparing the average VSS concentration during the steady-state periods of phase II and phase IV, it can be seen that the VSS concentration increased (from an average of 0.92 g VSS/L to an average of 1.7 g VSS/L) suggesting that the amount of viable biomass increased due to the decrease of mixing intensity.

It should be noted that since only suspended solids were measured, the TSS and VSS concentrations failed to capture the entire solids present in the reactor, particularly biofilm formation. It was not until day 84 when the attachment of the biofilm was identified and addressed by scraping the biofilms off the surfaces. The sudden TSS and VSS increases on day 84, 102, 137, 164, 169, 221 correspond to the scraping exercise as shown in Figure 4-2. Therefore, scraping the biofilms did have a significant impact

on the VSS concentration profile. However, the change in VSS concentration had negligible impact on nitrogen removal for those corresponding days of scraping.

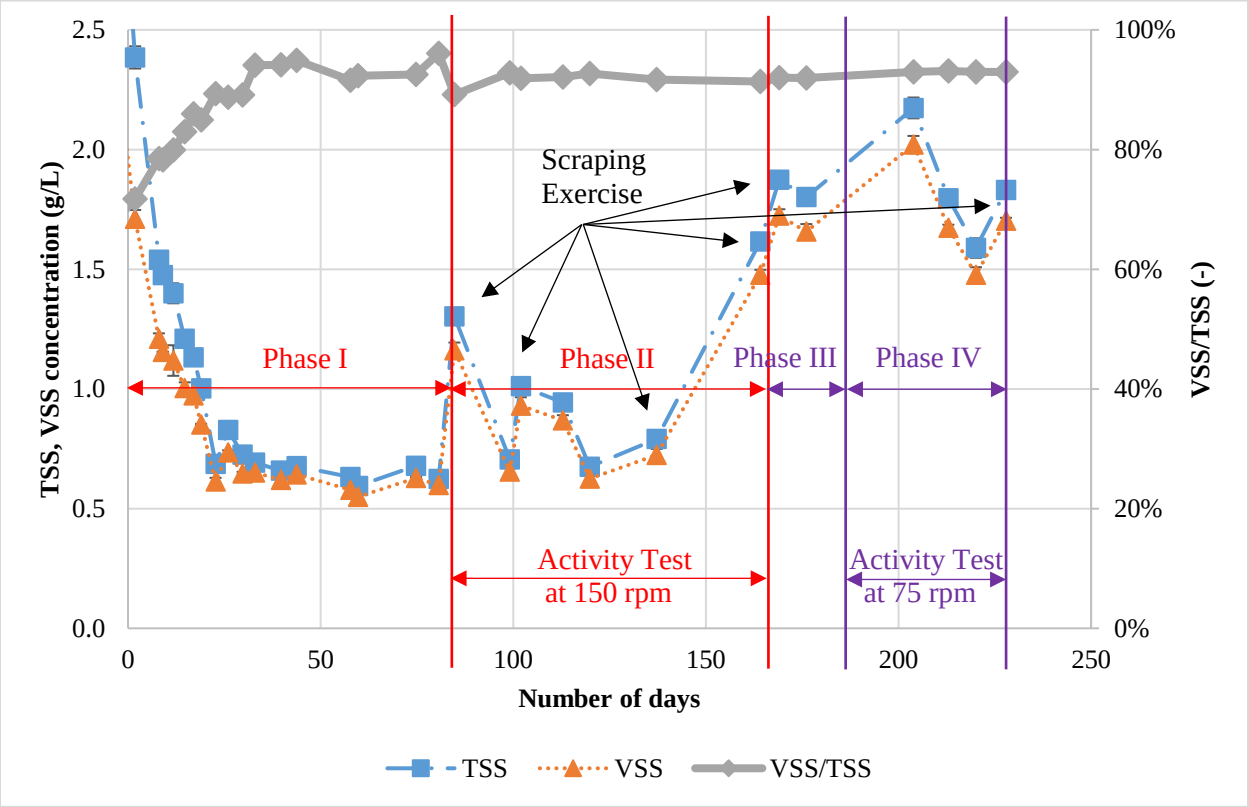

Figure 4-2: Total suspended solids (TSS) volatile suspended solids (VSS) and VSS/TSS ratio in mixed liquor

When the effluent profile in Figure 4-1 and the MLSS profile in Figure 4-2 are viewed collectively it was clear that the decrease of mixing speed led to an increase in TNRE and average VSS concentration. The results suggest that the decrease of mixing speed may have caused the biological composition to change for the bacteria in the process, especially the percentages of AOB, NOB, and Anammox bacteria in the composition. Therefore, it was deemed necessary to further investigate the underlying biological processes.

4.2 Activity Tests

In the present study, activity tests were designed in a batch reactor with known initial conditions of substrate concentrations of NH_4^+, NO_2^-, and NO_3^-. Operated in a controlled environment, the determined substrate utilization rates were used to evaluate the K_{O_2} for AOB, NOB, and Anammox bacteria. Representative results of the NH_4^+ concentration profiles at 150 rpm in Figure 4-3 are discussed here. It

can be seen that the concentration of NH_4^+ first increased and then decreased linearly at different DO conditions. This pattern was attributed to the test mixing conditions that required 10 to 15 minutes to achieve homogeneous concentrations within the reactor after NH_4^+ was added to the reactor. The insufficient mixing phenomenon was most apparent in the observed profiles of NH_4^+ results at different DO conditions. As the purpose of activity tests were to quantify the conversion rates of specific components in the batch reactor, only the concentration profiles of NH_4^+, NO_2^-, and NO_3^- shown in both Figure 4-3 and Figure 4-4 for the period after 15 min were used for further analysis throughout this work.

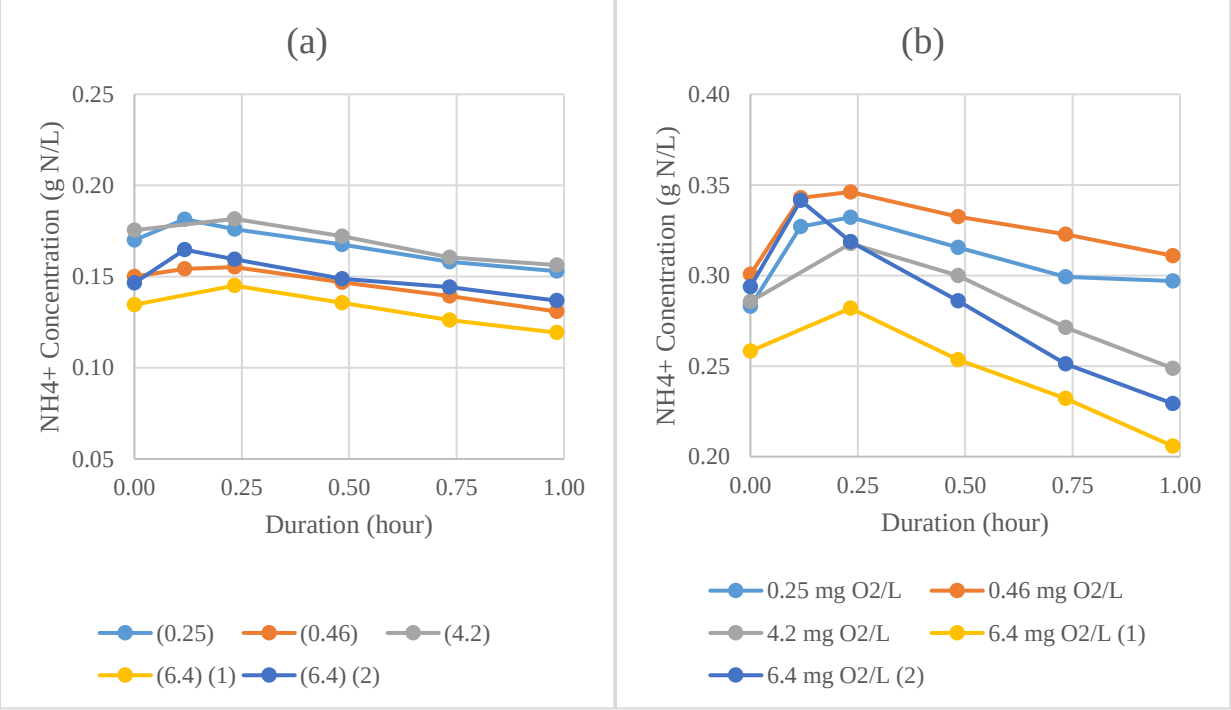

Figure 4-3: Activity test results for ammonium at 150 rpm under (a) anoxic, (b) aerobic conditions

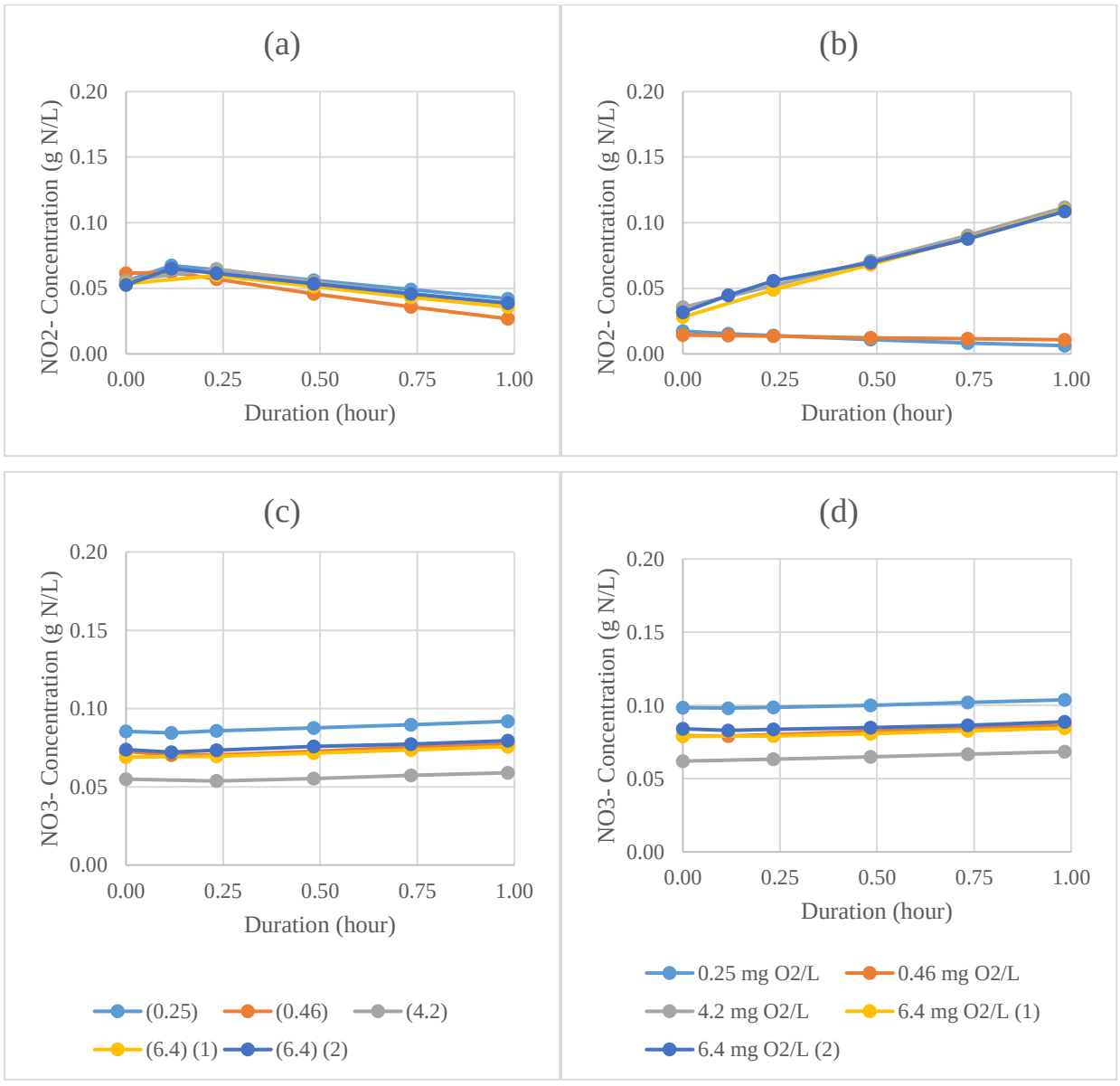

Figure 4-4: Activity test results at 150 rpm for nitrite under (a) anoxic , (b) aerobic conditions; for nitrate under (c) anoxic, (d) aerobic conditions

Figure 4-5 and Figure 4-6 present the concentration profiles of NH_4^+, NO_2^-, and NO_3^- at different DO conditions. The anoxic activity test results of NH_4^+, NO_2^-, and NO_3^- concentrations specifically are shown in Figure 4-5. Figure 4-5 (a), (c), and (e) show the tests results of NH_4^+, NO_2^-, and NO_3^- at a mixer speed of 75 rpm, respectively. Figure 4-5 (b), (d), and (f) show the tests at a mixer speed of 150 rpm, respectively. The aerobic activity test results are shown in Figure 4-6. Similarly, Figure 4-6 (a), (c), and (e) show the tests results of NH_4^+, NO_2^-, and NO_3^- at a mixer speed of 75 rpm, respectively, while Figure 4-6 (b), (d), and (f) show the tests at a mixer speed of 150 rpm, respectively.

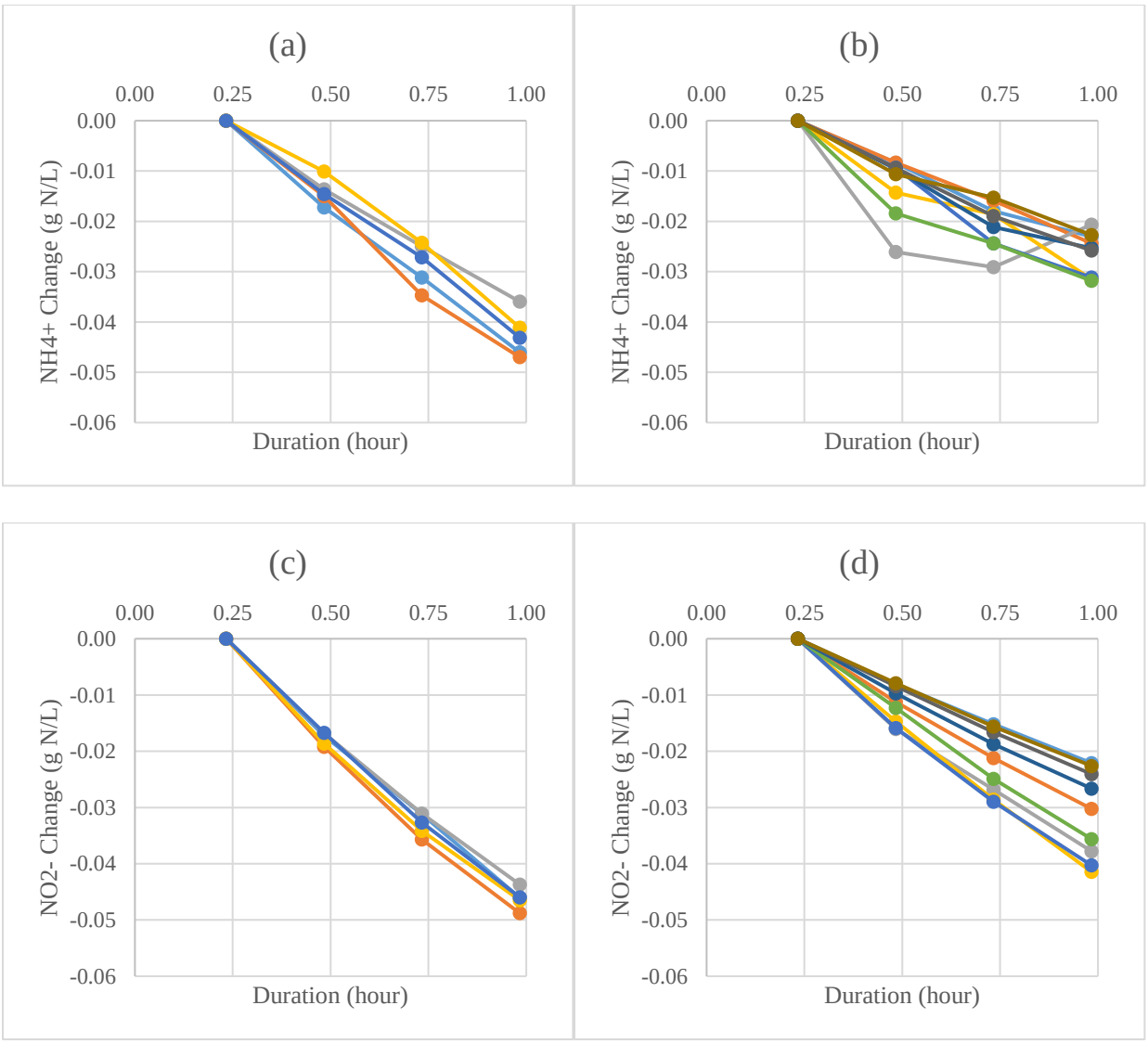

Figure 4-5: Anoxic activity test results referenced from 15 minutes for NH4+ at (a) 75 rpm (b) 150 rpm; for NO2- at (c) 75 rpm (d) 150 rpm; and for NO3- at (e) 75 rpm and (f) 150 rpm

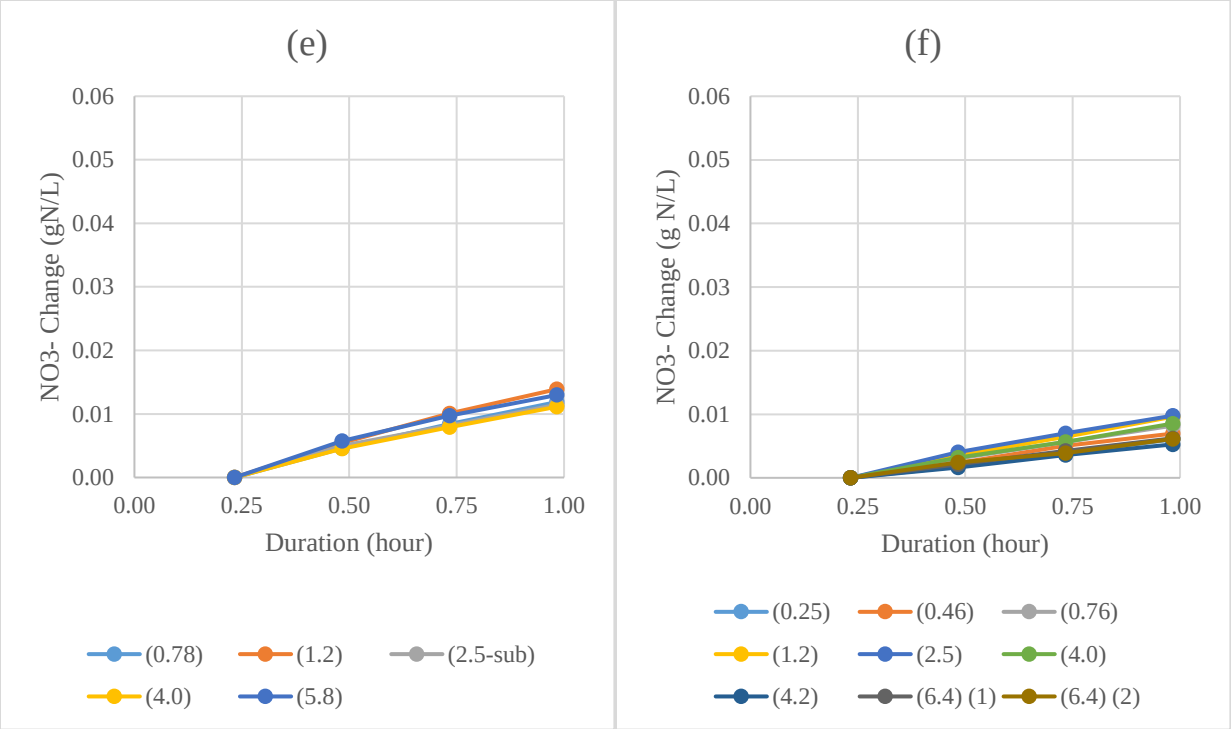

Figure 4-5 Continued: Anoxic activity test results referenced from 15 minutes for NH4+ at (a) 75 rpm (b) 150 rpm; for NO2- at (c) 75 rpm (d) 150 rpm; and for NO3- at (e) 75 rpm and (f) 150 rpm

While viewed collectively, the concentration profiles of NH_4^+, NO_2^-, and NO_3^- all had linear responses with respect to reaction time. To quantitatively describe these changes, the slope of each concentration profile (i.e. the rates of nitrogen conversion) were calculated. It should be noted that the measured results of NH_4^+ had larger variability due to the limitation of the analytical method than the results of NO_2^-, and NO_3^- (i.e. ion selective electrode (ISE) for measuring NH_4^+ and IC for measuring NO_2^-, and NO_3^-). However, the slopes and standard errors were deemed to be valid for estimating rates.

The anoxic activity tests aimed to characterize the performance of Anammox bacteria since AOB and NOB were assumed to be inactive due to the absence of DO. Under the anoxic condition for both mixing speed, the rates of NH_4^+ and NO_2^- were negative suggesting consumption during the tests, and the slope of the NO_3^- response was positive suggesting production during the tests. This phenomenon supported the activity of Anammox bacteria in the reactor.

The aerobic activity test results are shown in Figure 4-6. In contrast to the behavior under anoxic condition, the slopes of the NH_4^+ and NO_2^- responses had larger ranges of values at the different DO concentrations. Interestingly, the NO_2^- responses had a positive relationship to the DO concentration in the reactor as the NO_2^- rate increased as the DO concentration increased. When operating at 75 rpm, the

DO was 0.78 mg O_2/L and 0.46 mg O_2/L, the rates of NO_2^- generation were -0.0056 and -0.0044 gN/gVSS-hour respectively suggesting a net consumption of NO_2^-. The fact that NO_2^- was being consumed during these conditions indicated that Anammox bacteria were still active. When the DO concentration was increased, the rates of NO_2^- generation became positive indicating a net accumulation of NO_2^- in the system. As the DO concentration was above 4.0 mg O_2/L, the rates of NO_2^- started to plateau. At the high DO concentration range from 4.0 to 6.0 mg O_2/L, Anammox bacteria could be assumed to be inactive. In addition, Figure 4-6 (e) and (f) suggest that NOB concentrations were low since little NO_3^- was produced even when DO was in the high range. Hence, AOB and Anammox bacteria were considered as the dominant groups of bacteria during the entire DO concentration ranges at both 75 rpm and 150 rpm.

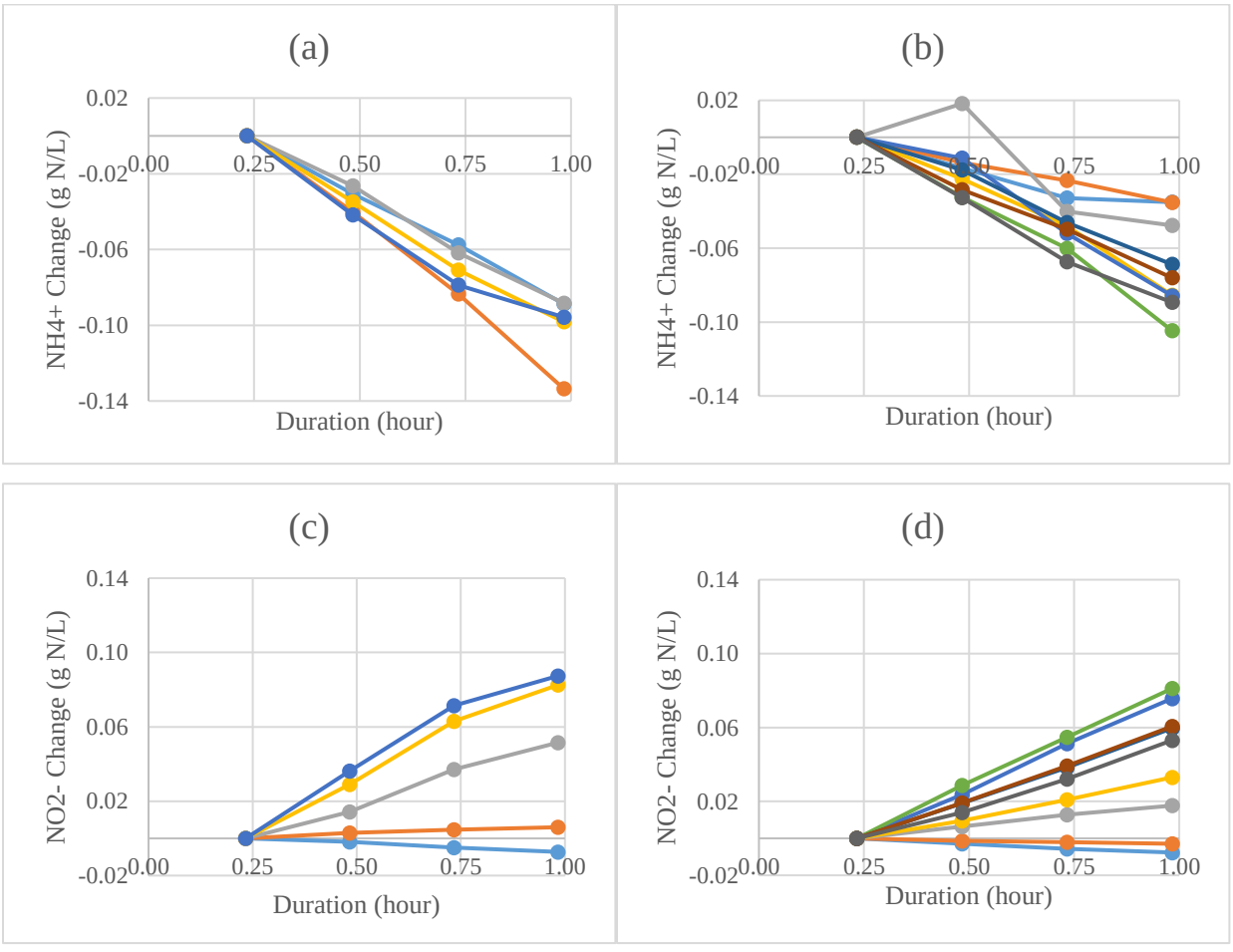

Figure 4-6: Aerobic activity test results referenced from 15 minutes for NH4+ at (a) 75 rpm (b) 150 rpm; for NO2- at (c) 75 rpm (d) 150 rpm; and for NO3- at (e) 75 rpm and (f) 150 rpm

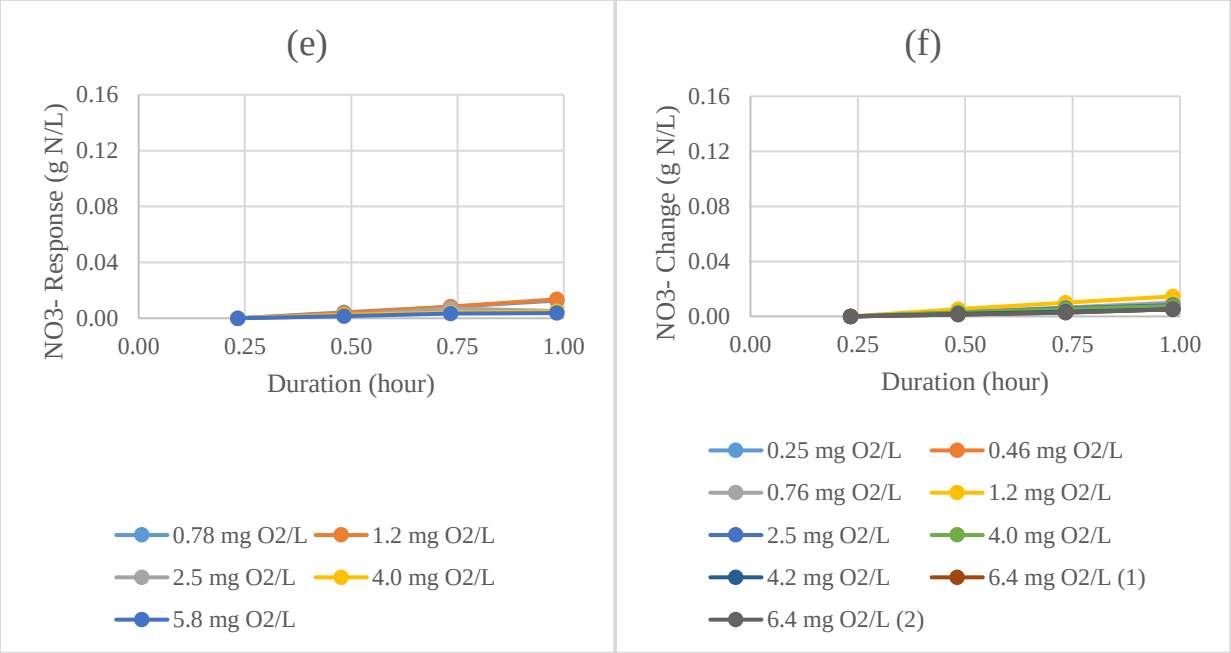

Figure 4-6 Continued: Aerobic activity test results zeroed from 15th minute for NH4+ at (a) 75 rpm (b) 150 rpm; for NO2- at (c) 75 rpm (d) 150 rpm; and for NO3- at (e) 75 rpm and (f) 150 rpm

As described in section 3.2, the results of the activity tests were expressed as the quotients of the rate of substrate change over the VSS concentration measured at the end of the activity test for normalization. An example of the quotient's sample standard deviation calculation is shown in the Appendix 8.4. As shown in Figure 4-7, a majority of the activity test responses were well fit by a linear model since the errors associated with the values were low. The error was calculated as the ratio of the sample standard deviation to the sample mean. With the exception of the activity test that was conducted at a DO of 0.76 mg O_2/L at 150 rpm (an error of 28%), the errors were all less than 11%. It was believed that the NH_4^+ measuring technique contributed to the error. Overall, the activity test results were deemed to be accurate enough to assess the impact of the experimental variables on the response rates.

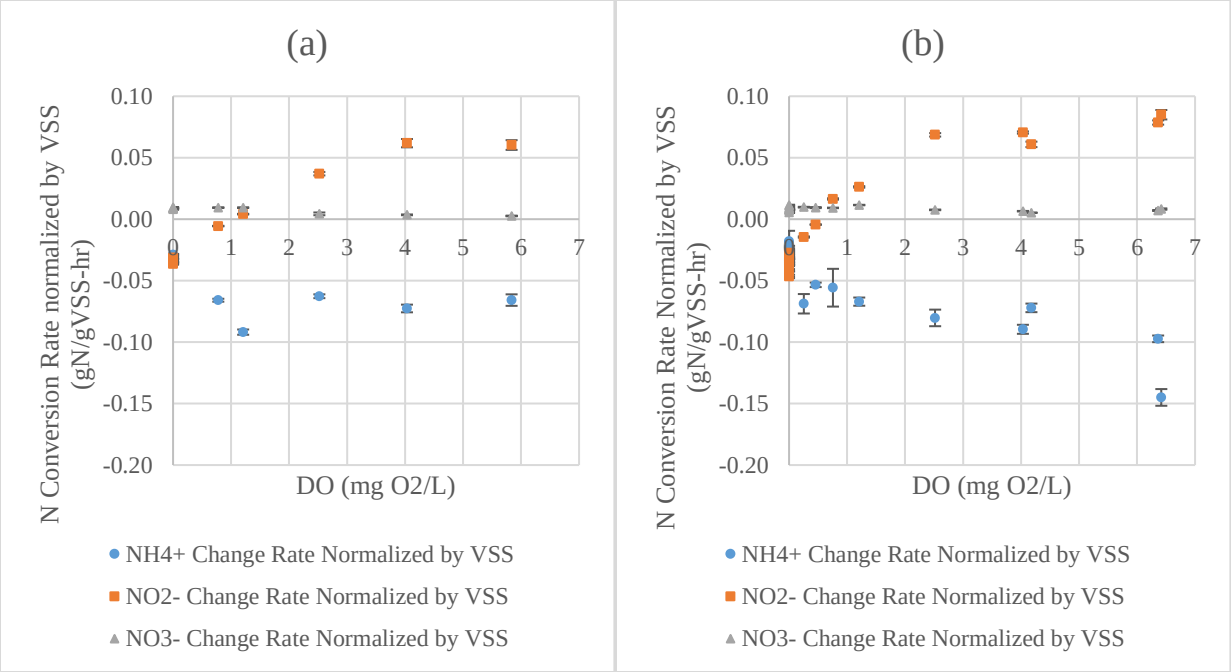

Figure 4-7: Activity test results at (a) 75 rpm and (b) 150 rpm

Figure 4-7 collectively describes the observed rates of NH_4^+, NO_2^-, and NO_3^- at both 75 and 150 rpm. In general, the trends of these curves were similar whereas DO concentration increased:

1) NH_4^+ conversion rates decreased and plateaued indicating that the rate of NH_4^+ consumption increased first and then plateaued;
2) NO_2^- conversion rates increased and plateaued indicating that
    a. When the DO concentration was less than or equal to 0.78 mg O_2/L at 75 rpm or 0.46 mg O_2/L at 150 rpm, NO_2^- was being consumed;
    b. When the DO concentrations were larger than or equal to 1.21 mg O_2/L at 75 rpm or 0.76 mg O_2/L at 150 rpm, NO_2^- was being produced;
    c. When the DO concentration increased from 1.21 mg O_2/L at 75 rpm or 0.76 mg O_2/L at 150 rpm, the rate of NO_2^- production increased and then plateaued;
3) NO_3^- conversion rates decreased slightly as compared to those of NH_4^+ and NO_2^- indicating that the rate of NO_3^- production decreased slightly.

In general, the variability of the data points was small, except a few cases of DO concentration at 6.0 mg O_2/L. Although the trends of NO_2^- conversion rates were similar at 75 rpm and 150 rpm, the DO concentrations at which the NO_2^- conversion rate equaled to zero were different. At 75 rpm the DO concentration that the NO_2^- conversion rate equaled zero was between 0.78 and 1.2 mg O_2/L; whereas at 150 rpm this DO concentration was between 0.25 to 0.76 mg O_2/L. In contrast, for DO concentrations at 0.0 and around 6.0 mg O_2/L the NO_2^- conversion rates were similar at 75 rpm and 150 rpm.

Activity testing was found to be a robust tool to investigate the conversion rates by different bacteria. By controlling the inputs to the reactor, the reactions could be manipulated to meet the objectives of the study while other parameters, (e.g. temperature, time, stable mixing conditions at each mixing speed) could remained unchanged. The concentrations of NH_4^+ and NO_2^- were deliberately elevated such that corresponding switching functions in the subsequent modeling would approach a value of 1.0 so that the model functions could be simplified. Therefore, the activity testing is a method of investigating the performance of different groups of bacteria in terms of different substrates in the system.

4.3 Mathematical Model Simulation

Mathematical modeling was employed to describe the dependence of the nitrogen species conversion rates on the DO half-velocity constants of AOB, NOB, and Anammox bacteria. As demonstrated in the previous section, the activity test results showed that the mixing intensity had a significant impact on the NO_2^- conversion rate. After the mixing speed was reduced the DO concentration where the NO_2^- conversion rate changed from consumption to production was different. In the following section, a model was developed aiming to estimate the K_{O2} values and the impact of changing mixing speed on K_{O2} values.

4.3.1 Model Development

Three groups of bacteria were assumed to be the dominant groups that might impact the nitrogen species conversion rates of NH_4^+, NO_2^-, and NO_3^- in the activity tests. These groups of bacteria were AOB, NOB and Anammox bacteria (Gilbert et al., 2012). The individual nitrogen conversion rates could be expressed as Equation 4-1, Equation 4-2, and Equation 4-3 based on the model of Ni et al., (2014).

$$\frac{dSNH_4^+}{dt} = -\left(i_{NBM} + \frac{1}{Y_{AOB}}\right) \cdot \mu_m^{AOB} \cdot \left(\frac{S_{NH4}}{K_{NH4}^{AOB} + S_{NH4}}\right) \cdot X_{COD}^{AOB} \cdot \left(\frac{S_{O2}}{K_{O2}^{AOB} + S_{O2}}\right) - i_{NBM} \cdot \mu_m^{NOB} \cdot \left(\frac{S_{NO2}}{K_{NO2}^{NOB} + S_{NO2}}\right) \cdot X_{COD}^{NOB} \cdot \left(\frac{S_{O2}}{0.5\ mg\ O_2/L + S_{O2}}\right) - \left(i_{NBM} + \frac{1}{Y_{Anam}}\right) \cdot \mu_m^{Anam} \cdot \left(\frac{S_{NH4}}{K_{NH4}^{Anammox} + S_{NH4}}\right) \cdot \left(\frac{S_{NO2}}{K_{NO2}^{Anammox} + S_{NO2}}\right) \cdot X_{COD}^{Anam} \cdot \left(\frac{K_{O2}^{Anammox}}{K_{O2}^{Anammox} + S_{O2}}\right)$$

Equation 4-1

$$\frac{dSNO_2^-}{dt} = \left(\frac{1}{Y_{AOB}}\right) \cdot \mu_m^{AOB} \cdot \left(\frac{S_{NH4}}{K_{NH4}^{AOB} + S_{NH4}}\right) \cdot X_{COD}^{AOB} \cdot \left(\frac{S_{O2}}{K_{O2}^{AOB} + S_{O2}}\right) - \left(\frac{1}{Y_{NOB}}\right) \cdot \mu_m^{NOB} \cdot \left(\frac{S_{NO2}}{K_{NO2}^{NOB} + S_{NO2}}\right) \cdot X_{COD}^{NOB} \cdot \left(\frac{S_{O2}}{0.5\ mg\ O_2/L + S_{O2}}\right) - \left(\frac{1}{Y_{Anam}} + \frac{1}{1.143\ gCOD/gNO2 - N}\right) \cdot \mu_m^{Anam} \cdot \left(\frac{S_{NH4}}{K_{NH4}^{Anammox} + S_{NH4}}\right) \cdot \left(\frac{S_{NO2}}{K_{NO2}^{Anammox} + S_{NO2}}\right) \cdot X_{COD}^{Anam} \cdot \left(\frac{K_{O2}^{Anammox}}{K_{O2}^{Anammox} + S_{O2}}\right)$$

Equation 4-2

$$\frac{dSNO_3^-}{dt} = \frac{1}{Y_{NOB}} \cdot \mu_m^{NOB} \cdot \left(\frac{S_{NO2}}{K_{NO2}^{NOB} + S_{NO2}}\right) \cdot X_{COD}^{NOB} \cdot \left(\frac{S_{O2}}{0.5\ mg\ O_2/L + S_{O2}}\right) + \left(\frac{1}{1.143\ gCOD/gNO2 - N}\right) \cdot \mu_m^{Anam} \cdot \left(\frac{S_{NH4}}{K_{NH4}^{Anammox} + S_{NH4}}\right) \cdot \left(\frac{S_{NO2}}{K_{NO2}^{Anammox} + S_{NO2}}\right) \cdot X_{COD}^{Anam} \cdot \left(\frac{K_{O2}^{Anammox}}{K_{O2}^{Anammox} + S_{O2}}\right)$$

Equation 4-3

Where,

- i_{NBM} = Nitrogen content of biomass (g N/g COD)
- Y_{AOB} = yield coefficient for AOB (g COD/g N)
- μ_m^{AOB} = maximum growth rate of AOB (1/hour)
- K_{NH4}^{AOB} = Ammonium half-velocity constant for AOB (g N/L)
- X_{COD}^{AOB} = AOB concentration (g COD/L)
- K_{O2}^{AOB} = DO half-velocity constant for AOB (mg O_2/L)
- Y_{NOB} = yield coefficient for NOB (g COD/g N)
- μ_m^{NOB} = maximum growth rate of NOB (1/hour)
- K_{NO2}^{NOB} = Nitrite half-velocity constant for NOB (g N/L)
- X_{COD}^{NOB} = NOB concentration (g COD/L)
- Y_{Anam} = yield coefficient for Anammox bacteria (g COD/g N)
- $K_{NH4}^{Anammox}$ = Ammonium half-velocity for Anammox bacteria (g N/L)
- $K_{NO2}^{Anammox}$ = Nitrite half-velocity for Anammox bacteria (g N/L)
- $K_{O2}^{Anammox}$ = DO half-velocity for Anammox bacteria (g N/L)
- S_{NH4} = Ammonium concentration (g N/L)
- S_{NO2} = Nitrite concentration (g N/L)
- S_{NO3} = Nitrate concentration (g N/L)
- S_{O2} = DO concentration (mg O_2/L)

By solving Equation 4-1 – 4-3 simultaneously, the DO half-velocity constants of AOB and Anammox bacteria, K_{O2}^{AOB} and $K_{O2}^{Anammox}$ respectively were estimated. The model was complex to solve, and thus, necessary simplification was made as follows:

1. Some products of terms in Equation 4-1 – 4-3 remained relative constant in terms of different DO concentrations. Therefore, those values were represented by a set of constant values for each mixing condition (details are discussed in Appendix 8.5);
2. Only AOB, NOB and Anammox bacteria were assumed to be active for all the activity tests;
3. The NOB concentration which was estimated by the activity tests with a DO at 6.0 mg O_2/L for each mixing condition was assumed to be constant throughout one mixing condition;
4. It was assumed that the AOB concentration/mixed liquor volatile suspended solids (MLVSS) concentration was constant and corresponded to that measured at the end of each aerobic activity test.

With these assumptions, Equation 4-1 – 4-3 was simplified to form a linear model. Therefore, the unknown parameters of K_{O2}^{AOB} and $K_{O2}^{Anammox}$ in Equation 4-1 – 4-3 were calculated using linear regression.

4.3.2 Estimated DO half-velocity constants of AOB and Anammox Bacteria

The estimated values and sample standard deviations of the K_{O2}^{AOB} and $K_{O2}^{Anammox}$ parameters as determined by regression of the simplified equations are listed in Table 4-1. The student t-test was employed to compare the results between the differing mixing intensities and the outcomes of this analysis are listed in Table 4-2. To better compare the estimated results and the observed values for nitrogen species conversion rates, Figure 4-8 was plotted with the abscissa as the observed values and the ordinate as the estimated values. The residuals for the best-fit model are plotted in Figure 4-9. From Figure 4-9 it can be seen that the residuals were randomly distributed and hence it was concluded that the model successfully described the K_{O2}^{AOB} and $K_{O2}^{Anammox}$ in the study system.

Based upon the results presented in Table 4-1, Table 4-2 and Figure 4-8 it was concluded that:

- The estimated results matched the experiment values well as shown in Figure 4-8;
- The estimated K_{O2}^{AOB} was within the range of reported literature K_{O2}^{AOB} values that vary from 0.18 to 1.16 mg O_2/L (Arnaldos et al., 2015; Ma et al., 2016);
- The estimated K_{O2}^{AOB} at 75 rpm was statistically the same as the estimated K_{O2}^{AOB} at 150 rpm;
- The estimated $K_{O2}^{Anammox}$ was higher than the literature $K_{O2}^{Anammox}$ value of 0.01 mg O_2/L (Corbalá-Robles et al., 2016; Ni et al., 2014; Vangsgaard et al., 2013).
- The estimated $K_{O2}^{Anammox}$ value at 75 rpm was statistically larger than the estimated $K_{O2}^{Anammox}$ value at 150 rpm;

Table 4-1: Estimated DO half-velocity constant values and sample standard deviations

	K_{O2}^{AOB}	Sample Standard Deviation	$K_{O2}^{Anammox}$	Sample Standard Deviation
Unit	**mg O_2/L**	**mg O_2/L**	**mg O_2/L**	**mg O_2/L**
75 rpm	0.54	0.56	0.55	0.40
150 rpm	0.68	0.34	0.13	0.09

Table 4-2: Student t-test results of DO half-velocity constants at two mixing intensities

Null hypothesis	**t-test p-value**
Estimated $K_{O2}^{AOB}\big\|_{75rpm} = K_{O2}^{AOB}\big\|_{150rpm}$	$0.19 > Type\ I\ error = 0.05$
Estimated $K_{O2}^{Anammox}\big\|_{75rpm} = K_{O2}^{Anammox}\big\|_{150rpm}$	$3.9 \times 10^{-10} < Type\ I\ error = 0.05$

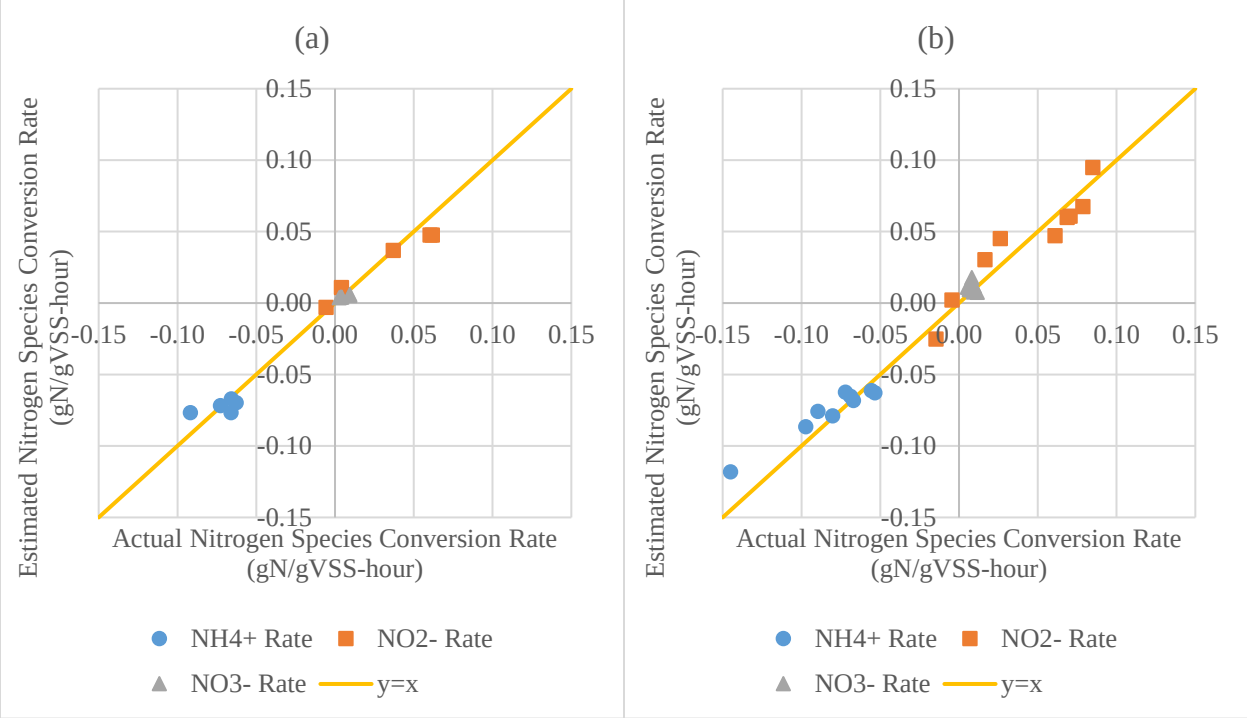

Figure 4-8: Estimated vs. actual activity test results at (a) 75 rpm and (b) 150 rpm

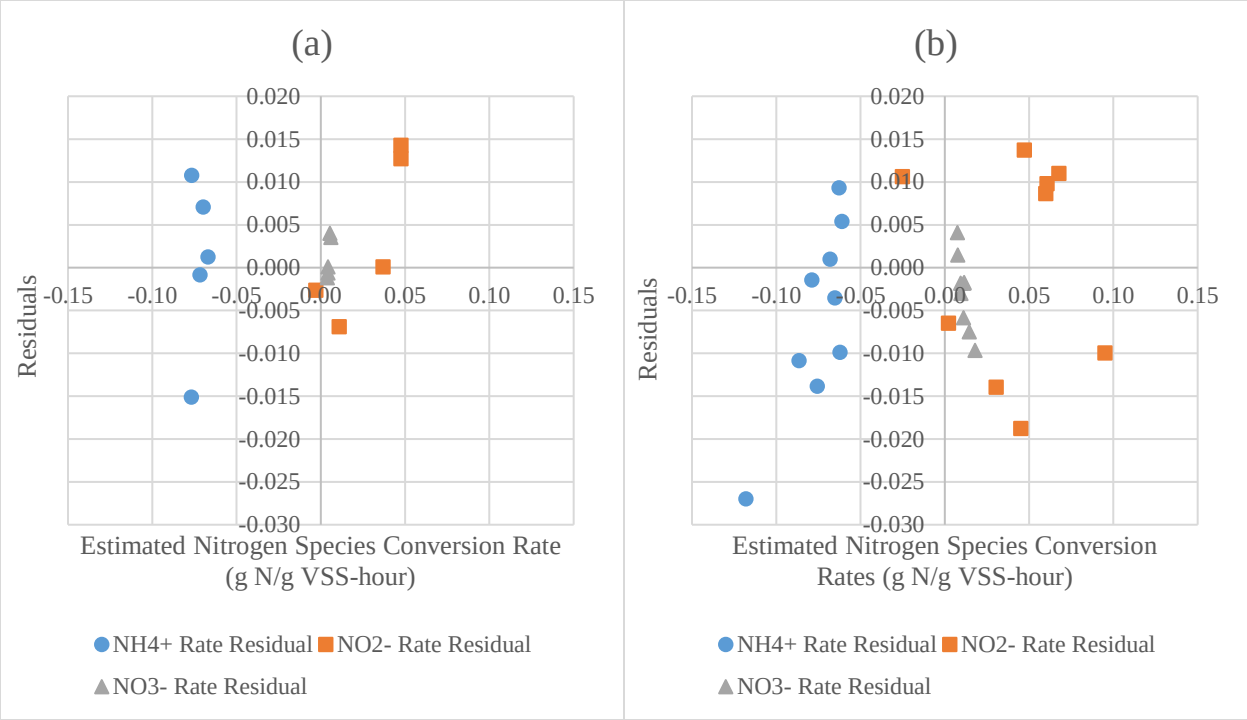

Figure 4-9: Plot of residuals vs. estimated nitrogen species conversion rates (Equation 4-1 – 4-3) for (a) 75 rpm and (b) 150 rpm

The developed model (Equation 4-1– 4-3) uses the DO concentration in the bulk liquid to describe the exposure of bacteria to dissolved oxygen. It is believed that this was the primary reason why the estimated $K_{O2}^{Anammox}$'s at both mixing conditions were higher than the literature value. In contrast, the literature values of K_{O2}^{AOB} and $K_{O2}^{Anammox}$ were based on the DO concentrations next to the bacteria in pure culture systems (Arnaldos et al., 2015; Picioreanu et al., 2016; Wu et al., 2017).

For a reactor with aggregates of different groups of bacteria, the DO concentration decreases along the direction from the bulk liquid to the core of an aggregate (IWA Task Group on Biofilm Modelling, 2006). As illustrated in Figure 4-10, the DO concentration is reduced after diffusion through the boundary layer (from point 1 to point 2 in Figure 4-10). The DO concentration is reduced again due to consumption by AOB's and NOB's as it diffuses through the outer layer of the aggregate (from point 2 to point 3 in Figure 4-10). Therefore, using the DO concentration values in the bulk liquid resulted in the estimated $K_{O2}^{Anammox}$ values being larger than the literature value because the estimated $K_{O2}^{Anammox}$ incorporated the effect of all the resistances to the DO penetration due to the two layers surrounding the Anammox bacteria core. Interestingly, the estimated K_{O2}^{AOB}'s were close to the literature value since the DO concentrations at point 2 in Figure 4-10 were close to the DO concentration in the bulk liquid (point 1 in Figure 4-10). Therefore, the two mixing conditions produced similar K_{O2}^{AOB} values.

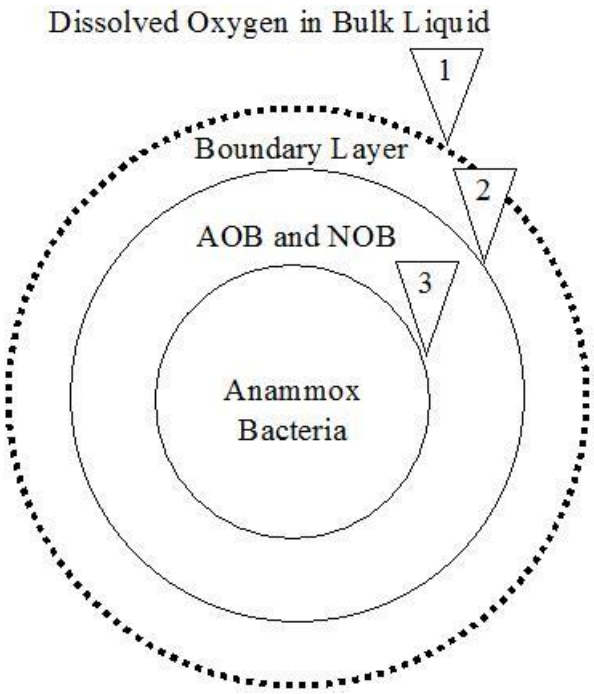

Figure 4-10: An illustration of the bacteria aggregate

The estimated K_{O2}^{AOB} and $K_{O2}^{Anammox}$ values give some insights into the functionality of the different bacterial communities and their abilities to consume nitrogen species substrates in the environments. The quantity of biomass for AOB, NOB and Anammox bacteria and their activities are the core operational principals for DEMON process. Ideally, the final production rates of NO_2^- from AOB and NOB layer should be equal to the consumptions rate of NO_2^- from Anammox bacteria in the core (Jaroszynski and Oleszkiewicz, 2011).

The TNRE observed in this study indicates that the performance was better at the mixing speed of 75 rpm than that at 150 rpm. In terms of the estimated K_{O2}^{AOB} and $K_{O2}^{Anammox}$ values, it was found that $K_{O2}^{Anammox}$ decreased as the mixing speed increased. Thus the Anammox bacteria experienced less DO inhibition at 75 rpm as compared to 150 rpm. Thus, the TNRE was higher at 75 rpm when other operating parameters remained the same. This result provides process engineers with guidance in establishing mixing conditions that could increase nitrogen removal performance.

5 Conclusions

In this study, the effects of mixing intensity on the half-velocity constants of DO for AOB (K_{O2}^{AOB}) and Anammox bacteria ($K_{O2}^{Anammox}$) in a PN/A process were characterized. A quasi-SBR test setup was used to simulate the DEMON® process with an automated process control. After steady-state operation was successfully achieved, activity tests at different DO concentrations were conducted at mixing intensities of 75 rpm (the equivalent of average velocity gradient 5.3/s with an 8.0 L reactor) and 150 rpm (the equivalent of average velocity gradient 15/s with an 8.0 L reactor). When the mixing intensity increased from 5.3/s to 15/s under normal operating conditions, the total nitrogen removal decreased. The conclusions from this study are summarized below:

- Steady-state operation was achieved after 83 days of operation at 15/s with an average total nitrogen removal of 62%; while after 22 days of operation at 5.3/s with an average of total nitrogen removal of 84%;
- Activity tests were conducted at mixing intensities of both 5.3/s and 15/s. The results showed that as DO increased at both G values, the VSS normalized rates of ammonium consumption increased and then plateaued; the VSS normalized rate of nitrite production increased and then plateaued; and the VSS normalized rate of nitrate production had no apparent change. The VSS normalized rates of ammonium and nitrite change plateaued at higher DO values for G values of 5.3/s when compared to 15/s;
- A mathematical model was used to estimate the values of K_{O2}^{AOB} and $K_{O2}^{Anammox}$: with a type I error of α=0.05,
    - It was found that the estimated DO half-velocity constant of AOB did not change statistically significantly. It ranged from 0.54 mg O_2/L at 5.3/s to 0.68 mg O_2/L at 15/s;
    - The estimated DO half-velocity constant of Anammox bacteria changed statistically significantly. It equaled 0.55 mg O_2/L at 5.3/s and 0.13 mg O_2/L at 15/s;
- Wastewater treatment process practitioners can benefit from the simplified calculations of using the DO concentration in the bulk liquid and the estimated values of K_{O2}^{AOB} and $K_{O2}^{Anammox}$. Without the calculations for diffusion equations, the effective switching function values of DO for AOB and Anammox bacteria can be utilized for predicting treatment performances, e.g. total nitrogen removal efficiency.

6 Recommendations

Automation in this study was demonstrated to be a successful method of operating the DEMON® system with little maintenance effort. With more signal inputs, more sophisticated control strategies can be developed so that the experiment could treat real centrate with a varying influent profile.

The DO half-velocity constants of AOB and Anammox bacteria were estimated with assumptions that the estimated values contained diffusions. Future work can focus on the comparison between the simplified estimation done in this study against detailed diffusion modelling. The purpose of the future work can provide knowledge on the limitations of the mathematical model with simplified estimation and detailed diffusion.

The activity tests produced satisfactory results in terms of providing conversion rates of ammonium, nitrite, and nitrate concentrations. The recommendations for conducting better activity tests include:

- All test runs at different DO concentrations should be finished as quickly as possible to eliminate the impact of changing viable biomass concentration on test results;
- Initial nitrite concentrations under anoxic activity tests could increase more than specified in chapter 3 for those periods where the total nitrogen removal rate was high (>80%). Since nitrite is not added in the aerobic activity tests, nitrite could be a limiting factor during those aerobic activity tests where DO is low ($0 < DO < 1$ mg O_2/L);
- The effluent quality should be tested frequently enough to reveal steady-state operation within a series of activity tests at different DO concentrations;
- Pre-mixing time should be extended to exceed the 6 minutes employed in this study to ensure complete mixing conditions at the beginning of the anoxic activity tests.

7 References

Anthonisen, A. C., Loehr, R. C., Prakasam, T. B. S., Srinath, E. G., 1976. Inhibition of Nitrification by Ammonia and Nitrous Acid. Journal (Water Pollution Control Federation). 48 (5), 835-852.

APHA, 2005 Standard methods for the examination of water and wastewater : including bottom sediments and sludges. American Public Health Association, New York, N.Y., .

Arnaldos, M., Amerlinck, Y., Rehman, U., Maere, T., Van Hoey, S., Naessens, W., Nopens, I., 2015. From the affinity constant to the half-saturation index: Understanding conventional modeling concepts in novel wastewater treatment processes. Water Research. 70, 458-470.

Bowden, G., Wett, B., Takacs, I., Murthy, S., Deur, A., Musabyimana, M., Love, N., 2007. Evaluation of the Single Sludge Deammonification Process for the Treatment of Plant Recycle Streams Containing a High Ammonium Concentration. Proceedings of the Water Environment Federation. 2007 (19), 321-343.

Chen, H., Yu, J., Jia, X., Jin, R., 2014. Enhancement of anammox performance by Cu(II), Ni(II) and Fe(III) supplementation. Chemosphere. 117, 610-616.

Chu, K. H., Van Veldhuizen, H. M., Van Loosdrecht, M. C. M. , 2003. Respirometric measurement of kinetic parameters: Effect of activated sludge floc size. Water Science and Technology 48 (8), 61-68.

Corbalá-Robles, L., Picioreanu, C., van Loosdrecht, M. C. M., Pérez, J., 2016. Analysing the effects of the aeration pattern and residual ammonium concentration in a partial nitritation-anammox process. Environmental Technology. 37 (6), 694-702.

Dapena-Mora, A., Fernandez, I., Campos, J. L., Mosquera-Corral, A., Mendez, R., Jetten, M. S. M., 2007. Evaluation of activity and inhibition effects on Anammox process by batch tests based on the nitrogen gas production. Enzyme and Microbial Technology. 40 (4), 859-865.

Dosta, J., Fernandez, I., Vazquez-Padin, J. R., Mosquera-Corral, A., Campos, J. L., Mata-Alvarez, J., Mendez, R., 2008. Short- and long-term effects of temperature on the Anammox process. Journal of Hazardous Materials. 154 (1-3), 688-693.

Fernández, I., Dosta, J., Fajardo, C., Campos, J. L., Mosquera-Corral, A., Méndez, R., 2012. Short- and long-term effects of ammonium and nitrite on the Anammox process. Journal of Environmental Management. 95 Suppl, S170-S174.

Figdore, B., Bowden, G., Stinson, B., Wett, B., Hell, M., Bailey, W., Carr, J., Der Minassian, R., Murthy, S., 2011. Treatment of Dewatering Sidestream from a Thermal Hydrolysis-Mesophilic Anaerobic Digestion Process with a Single-Sludge Deammonification Process. Proceedings of the Water Environment Federation. 2011 (18), 249-264.

Fux, C., Marchesi, V., Brunner, I., Siegrist, H. , 2004. Anaerobic ammonium oxidation of ammonium-rich waste streams in fixed-bed reactors. Water Science and Technology 49 (11-12), 77-82.

Gilbert, E. M., Agrawal, S., Schwartz, T., Horn, H., Lackner, S., 2015. Comparing different reactor configurations for Partial Nitritation/Anammox at low temperatures. Water Research. 81, 92-100.

Gilbert, E. M., Agrawal, S., Karst, S. M., Horn, H., Nielsen, P. H., Lackner, S., 2014. Low temperature partial nitritation/anammox in a moving bed biofilm reactor treating low strength wastewater. Environmental Science and Technology. 48 (15), 8784-8792.

Gilbert, E. M., Müller, E., Horn, H., Lackner, S., 2012. Microbial activity of suspended biomass from a nitritation-anammox SBR in dependence of operational condition and size fraction. Applied Microbiology and Biotechnology. 97 (19), 8795-8804.

Gonzalez-Martinez, A., Rodriguez-Sanchez, A., Munoz-Palazon, B., Garcia-Ruiz, M., Osorio, F., van Loosdrecht, M. C., Gonzalez-Lopez, J., 2015. Microbial community analysis of a full-scale DEMON bioreactor. Bioprocess and Biosystems Engineering. 38 (3), 499-508.

Guo, J., Peng, Y., Huang, H., Wang, S., Ge, S., Zhang, J., Wang, Z., 2010. Short- and long-term effects of temperature on partial nitrification in a sequencing batch reactor treating domestic wastewater. Journal of Hazardous Materials. 179 (1-3), 471-479.

Hubaux, N., Wells, G., Morgenroth, E., 2015. Impact of coexistence of flocs and biofilm on performance of combined nitritation-anammox granular sludge reactors. Water Research. 68 (Complete), 127-139.

IWA Task Group on Biofilm Modelling, 2006. Mathematical modeling of biofilms. IWA Pub, London, .

Jardin, N. and Hennerkes, J., 2012. Full-scale experience with the deammonification process to treat high strength sludge water -- a case study. Water Science and Technology. 65 (3), 447-455.

Jaroszynski, L. W., Cicek, N., Sparling, R., Oleszkiewicz, J. A., 2011. Importance of the operating pH in maintaining the stability of anoxic ammonium oxidation (anammox) activity in moving bed biofilm reactors. Bioresource Technology. 102 (14), 7051-7056.

Jaroszynski, L. W. and Oleszkiewicz, J. A., 2011. Autotrophic ammonium removal from reject water: Partial nitrification and anammox in one-reactor versus two-reactor systems. Environmental Technology. 32 (3), 289-294.

Jung, J. Y., Kang, S. H., Chung, Y. C., Ahn, D. H., 2007. Factors affecting the activity of anammox bacteria during start up in the continuous culture reactor. Water Science and Technology. 55 (1-2), 459-468.

Kartal, B., Kuenen, J. G., Van Loosdrecht, M. C. M., 2010. Sewage treatment with anammox. Science. 328 (5979), 702-703.

Klein, A., Williams, L., Summers, A., Johnson, C., Melcer, H., 2013. Application of lessons learned during a pilot investigation to the full scale design of a DEMON® system to remove nitrogen from dewatering centrate. Proceedings of the Water Environment Federation. 2013 (4), 350-364.

Lackner, S., Gilbert, E. M., Vlaeminck, S. E., Joss, A., Horn, H., van Loosdrecht, M. C. M., 2014. Full-scale partial nitritation/ anammox experiences – An application survey. Water Research. 55, 292-303.

Laureni, M., Weissbrodt, D. G., Szivák, I., Robin, O., Nielsen, J. L., Morgenroth, E., Joss, A., 2015. Activity and growth of anammox biomass on aerobically pre-treated municipal wastewater. Water Research. 80, 325-336.

Li, X., Xiao, Y., Liao, D., Zheng, W., Yi, T., Yang, Q., Zeng, G., 2011. Granulation of Simultaneous Partial Nitrification and Anammox Biomass in One Single SBR System. Applied Biochemistry and Biotechnology. 163 (8), 1053-1065.

Ma, B., Wang, S., Cao, S., Miao, Y., Jia, F., Du, R., Peng, Y., 2016. Biological nitrogen removal from sewage via anammox: Recent advances. Bioresource Technology. 200, 981-990.

Musabyimana, M.,2008. Deammonification Process Kinetics and Inhibition Evaluation. Ph.D., Virginia Polytechnic Institute and State University, United States -- Virginia,.

Ni, B., Chen, Y., Liu, S., Fang, F., Xie, W., Yu, H., 2009. Modeling a granule-based anaerobic ammonium oxidizing (ANAMMOX) process. Biotechnology and Bioengineering. 103 (3), 490-499.

Ni, B., Joss, A., Yuan, Z., 2014. Modeling nitrogen removal with partial nitritation and anammox in one floc-based sequencing batch reactor. Water Research. 67, 321-329.

Nifong, A., Nelson, A., Johnson, C., Bott Charles, B., 2013. Performance of a Full-Scale Sidestream DEMON® Deammonification Installation. Proceedings of the Water Environment Federation. 2013 (13), 3686-3709.

Picioreanu, C., Pérez, J., van Loosdrecht, M. C. M. , 2016. Impact of cell cluster size on apparent half-saturation coefficients for oxygen in nitrifying sludge and biofilms. Water Research 106, 371-382.

Sabine Marie, P., Pümpel, T., Markt, R., Murthy, S., Bott, C., Wett, B., 2015. Comparative evaluation of multiple methods to quantify and characterise granular anammox biomass. Water Research. 68, 194-205.

Shaw, A., Takacs, I., Pagilla, K., Riffat, R., Declippeleir, H., Wilson, C., Murthy, S., 2015. Toward Universal Half- Saturation Coefficients: Describing Extant K_S as a Function of Diffusion. Water Environment Research. 87 (5), 387.

Strous, M., Kuenen, J. G., Jetten, M. S. M., 1999. Key Physiology of Anaerobic Ammonium Oxidation. Applied and Environmental Microbiology. 65 (7), 3248-3250.

Strous, M., Heijnen, J. J., Kuenen, J. G., Jetten, M. S. M., 1998. The sequencing batch reactor as a powerful tool for the study of slowly growing anaerobic ammonium-oxidizing microorganisms. Applied Microbiology and Biotechnology. 50 (5), 589-596.

Strous, M., Van Gerven, E., Zheng, P., Kuenen, J. G., Jetten, M., 1997. Ammonium removal from concentrated waste streams with the anaerobic ammonium oxidation (Anammox) process in different reactor configurations. Water Research. 31 (8), 1955-1962.

Tang, C., Zheng, P., Mahmood, Q., Chen, J., 2009. Start-up and inhibition analysis of the Anammox process seeded with anaerobic granular sludge. Journal of Industrial Microbiology and Biotechnology. 36 (8), 1093-1100.

Tchobanoglous, G., Burton, F. L., Stensel, H. D., Metcalf & Eddy, (2003) Wastewater engineering : treatment and reuse. Boston : McGraw-Hill, Boston, MA, .

Third, K. A., Paxman, J., Schmid, M., Strous, M., Jetten, M., Cord-Ruwisch, R., 2005. Treatment of Nitrogen-Rich Wastewater Using Partial Nitrification and Anammox in the CANON process. Water Science & Technology. 52 (4), 47.

Third, K. A., Sliekers, A. O., Kuenen, J. G., Jetten, M. S. M., 2001. The CANON System (Completely Autotrophic Nitrogen-removal Over Nitrite) under Ammonium Limitation: Interaction and Competition between Three Groups of Bacteria. Systematic and Applied Microbiology. 24 (4), 588-596.

Tsushima, I., Ogasawara, Y., Kindaichi, T., Satoh, H., Okabe, S., 2007. Development of high-rate anaerobic ammonium-oxidizing (anammox) biofilm reactors. Water Research. 41 (8), 1623-1634.

Van De Graaf, A. A., De Bruijn, P., Robertson, L. A., Jetten, M. S. M., Kuenen, J. G., 1996. Autotrophic growth of anaerobic ammonium-oxidizing micro-organisms in a fluidized bed reactor. Microbiology. 142 (8), 2187-2196.

Van Hulle, S. W. H., Vandeweyer, H. J. P., Meesschaert, B. D., Vanrolleghem, P. A., Dejans, P., Dumoulin, A., 2010. Engineering aspects and practical application of autotrophic nitrogen removal from nitrogen rich streams. Chemical Engineering Journal. 162 (1), 1-20.

Vangsgaard, A. K., Mutlu, A. G., Gernaey, K. V., Smets, B. F., Sin, G., 2013. Calibration and validation of a model describing complete autotrophic nitrogen removal in a granular SBR system. Journal of Chemical Technology and Biotechnology. 88 (11), 2007-2015.

Veuillet, F., Lacroix, S., Bausseron, A., Gonidec, E., Ochoa, J., Christensson, M., Lemaire, R., 2014. Integrated fixed-film activated sludge ANITA™Mox process - A new perspective for advanced nitrogen removal. Water Science and Technology. 69 (5), 915-922.

Water Environment Federation Nutrient Removal,Task Force, 2011. Nutrient removal. WEF Press ; McGraw-Hill, Alexandria, Va.; New York, .

Wett, B., Hell, M., Nyhuis, G., Puempel, T., Takacs, I., Murthy, S., 2010a. Syntrophy of aerobic and anaerobic ammonia oxidisers. Water Science and Technology. 61 (8), 1915-1922.

Wett, B., Nyhuis, G., Takács, I., Murthy, S., 2010b. Development of enhanced deammonification selector. Proceedings of the Water Environment Federation. 2010 (10), 5917-5926.

Wett, B., 2007. Development and Implementation of a Robust Deammonification Process. Water Science & Technology. 56 (7), 81-88.

Wett, B., Murthy, S., Takács, I., Hell, M., Bowden, G., Deur, A., O'Shaughnessy, M., 2007. Key parameters for control of DEMON deammonification process. Water Practice. 1 (5), 1-11.

Wett, B., 2006. Solved Upscaling Problems for Implementing Deammonification of Rejection Water. Water Science & Technology. 53 (12), 121-128.

Wett, B., Rostek, R., Rauch, W., Ingerle, K., 1998. pH-controlled reject-water-treatment. Water Science and Technology. 37 (12), 165-172.

Wiesmann, U. (1994) Biological nitrogen removal from wastewater. In: Anonymous Biotechnics/Wastewater, Springer Berlin Heidelberg, 113-154.

Williams, L., Green, K., Newman, D., Klein, A., Melcer, H., Wan, J., Wett, B., 2012. Methods for monitoring Anammox reactor systems: lessons learned from piloting DEMON® sidestream treatment. Proceedings of the Water Environment Federation. 2012 (15), 1975-1991.

Wu, J., Zhang, Y., Zhang, M., Li, Y., 2017. Effect of nitrifiers enrichment and diffusion on their oxygen half-saturation value measurements. Biochemical Engineering Journal 123, 110-116.

Yu, Y., Tao, Y., Gao, D., 2014. Effects of HRT and nitrite/ammonia ratio on anammox discovered in a sequencing batch biofilm reactor. RSC Advances. 4 (97), 54798-54804.

Yu, Y., Gao, D., Tao, Y., 2013. Anammox start-up in sequencing batch biofilm reactors using different inoculating sludge. Applied Microbiology and Biotechnology. 97 (13), 6057-6064.

8 Appendix

8.1 Results

Influent Profile

Time (EDT)	# SRT	NH4+ (gN/L)	NH4+ Stdev	Alk (mgCaCO3/L)	Alk Stdev	pH	pH Stdev
7/7/2016 13:05	-3.12	0.469	0.005	1946	16.4	7.93	0.01
7/11/2016 13:40	0.90	0.413	0.011	1888	1.3	7.91	0.01
7/13/2016 13:05	2.88	0.453	0.005	1962	21.6	7.83	0.01
7/15/2016 10:30	4.77	0.474	0.008	1921	10.2	7.95	0.00
7/18/2016 10:35	7.78	0.473	0.003	1980	15.7	7.85	0.01
7/20/2016 16:30	10.02	0.476	0.005	1948	10.0	7.82	0.01
7/22/2016 16:20	12.02	0.443	0.005	1969	1.4	7.89	0.01
7/25/2016 10:10	14.76	0.457	0.005	1885	1.5	7.93	0.00
7/27/2016 16:30	17.02	0.430	0.017	1997	12.0	7.97	0.01
7/29/2016 10:20	18.77	0.454	0.004	1960	0.1	7.94	0.00
8/2/2016 09:00	22.71	0.454	0.007	1922	13.3	7.99	0.01
8/5/2016 15:30	25.98	0.486	0.000	1983	0.4	7.91	0.01
8/9/2016 09:30	29.73	0.408	0.022	1961	22.1	7.96	0.01
8/12/2016 18:30	33.11	0.457	0.001	1962	2.2	7.97	0.00
8/16/2016 09:50	36.75	0.481	0.003	1937	14.3	7.95	0.00
8/19/2016 17:35	40.07	0.480	0.002	1975	12.8	7.82	0.00
8/24/2016 15:50	45.00	0.474	0.008	1906	27.9	8.07	0.00
8/29/2016 16:45	50.03	0.462	0.010	1941	11.6	7.97	0.01
8/30/2016 16:00	51.00	0.455	0.001	#DIV/0!	#DIV/0!	0.00	#DIV/0!
9/2/2016 09:45	53.74	0.471	0.004	1979	4.6	7.91	0.01
9/5/2016 16:20	57.02	0.472	0.013	1935	12.2	8.10	0.00
9/8/2016 10:10	59.76	0.453	0.002	1883	4.5	8.13	0.00
9/23/2016 11:35	74.82	0.453	0.007	1903	12.8	8.07	0.00
9/29/2016 15:20	80.97	0.437	0.003	1865	0.8	7.83	0.01
10/3/2016 09:30	84.73	0.434	0.015	1892	18.0	7.94	0.01
10/17/2016 19:45	99.16	0.464	0.002	1777	46.2	7.92	0.01
10/20/2016 16:30	102.02	0.454	0.004	1810	21.5	8.05	0.01
10/31/2016 13:25	112.89	0.453	0.002	1811	1.4	7.97	0.01
11/7/2016 11:20	119.81	0.447	0.006	1864	14.4	7.98	0.00
11/11/2016 15:15	123.97	0.488	0.005	1867	9.1	8.02	0.01
11/24/2016 21:49	137.24	0.513	0.009	1881	6.2	7.83	0.01
12/21/2016 20:46	164.20	0.539	0.034	1814	28.0	8.02	0.00
12/26/2016 17:36	169.07	0.532	0.024	1860	5.9	8.06	0.00
1/2/2017 18:35	176.11	0.532	0.025	1810	25.0	8.10	0.00

Time (EDT)	# SRT	NH4+ (gN/L)	NH4+ Stdev	Alk (mgCaCO3/L)	Alk Stdev	pH	pH Stdev
1/25/2017 16:00	199.00	0.532	0.034	1832	45.0	8.01	0.00
1/30/2017 12:30	203.86	0.524	0.026	1772	38.8	8.21	0.01
2/8/2017 15:30	212.98	0.518	0.014	1816	70.4	7.94	0.01
2/15/2017 18:58	220.13	0.527	0.008	1887	8.5	7.92	0.00
2/23/2017 13:50	227.91	0.496	0.004	1871	12.0	7.93	0.01

Effluent Profile

Time (EDT)	# SRT	NO2- (mg/L)	NO3- (mg/L)	NH4+ (gN/L)	NH4+ Stdev	NO2- (gN/L)	NO3- (gN/L)	Alk (mgCaCO3/L)	N Removal Rate (%)
7/7/2016 13:00	-3.12	2.40	888	0.225	0.003	0.001	0.201	304	12%
7/11/2016 13:00	0.88	1.21	756	0.162	0.004	0.000	0.171	271	29%
7/13/2016 13:00	2.88	0.78	737	0.167	0.002	0.000	0.166	271	19%
7/15/2016 10:45	4.78	0.84	620	0.167	0.000	0.000	0.140	271	32%
7/18/2016 10:00	7.75	1.98	446	0.144	0.002	0.001	0.101	367	48%
7/20/2016 16:02	10.00	0.74	363	0.188	0.001	0.000	0.082	645	43%
7/22/2016 16:02	12.00	1.54	364	0.105	0.002	0.000	0.082	324	61%
7/25/2016 10:00	14.75	1.13	293	0.110	0.001	0.000	0.066	363	60%
7/27/2016 16:03	17.00	2.36	274	0.093	0.002	0.001	0.062	390	66%
7/29/2016 10:02	18.75	2.94	262	0.135	0.001	0.001	0.059	547	55%
8/2/2016 10:04	22.75	0.79	236	0.192	0.003	0.000	0.053	733	46%
8/5/2016 16:04	26.00	3.40	258	0.156	0.002	0.001	0.058	603	53%
8/9/2016 10:05	29.76	0.89	249	0.118	0.003	0.000	0.056	653	64%
8/12/2016 16:05	33.01	4.74	227	0.179	0.002	0.001	0.051	710	43%
8/16/2016 10:05	36.76	1.20	224	0.189	0.000	0.000	0.051	704	47%
8/19/2016 16:05	40.01	3.79	198	0.206	0.001	0.001	0.045	793	48%
8/24/2016 16:05	45.01	1.15	217	0.207	0.002	0.000	0.049	796	47%
8/29/2016 16:05	50.01	94.47	152	0.260	0.002	0.029	0.034	963	32%
8/30/2016 16:05	51.01	79.98	131	0.268	0.003	0.024	0.030	#DIV/0!	30%
9/2/2016 10:05	53.76	74.44	149	0.216	0.004	0.023	0.034	810	40%
9/5/2016 16:05	57.01	13.85	206	0.169	0.001	0.004	0.047	670	53%
9/8/2016 10:05	59.76	3.72	213	0.155	0.001	0.001	0.048	607	57%
9/23/2016 12:00	74.84	3.51	312	0.113	0.001	0.001	0.071	410	59%
9/29/2016 15:00	80.96	1.36	320	0.088	0.001	0.000	0.072	288	65%
10/3/2016 09:50	84.75	1.81	307	0.079	0.001	0.001	0.069	316	66%
10/17/2016 19:20	99.14	2.84	295	0.110	0.002	0.001	0.067	367	59%
10/20/2016 16:10	102.01	2.28	299	0.088	0.002	0.001	0.068	293	66%
10/31/2016 13:28	112.90	1.02	361	0.131	0.002	0.000	0.081	390	53%

Time (EDT)	# SRT	NO2- (mg/L)	NO3- (mg/L)	NH4+ (gN/L)	NH4+ Stdev	NO2- (gN/L)	NO3- (gN/L)	Alk (mgCaCO3/L)	N Removal Rate (%)
11/7/2016 12:12	119.84	1.99	343	0.119	0.002	0.001	0.078	436	56%
11/11/2016 13:50	123.91	3.28	283	0.129	0.002	0.001	0.064	438	57%
11/24/2016 21:35	137.23	1.06	305	0.121	0.001	0.000	0.069	402	61%
12/21/2016 20:35	164.19	1.98	240	0.123	0.008	0.001	0.054	358	65%
12/26/2016 18:25	169.10	0.71	243	0.092	0.002	0.000	0.055	274	73%
1/2/2017 18:20	176.10	1.41	221	0.139	0.007	0.000	0.050	343	64%
1/25/2017 16:10	199.01	4.22	226	0.045	0.000	0.001	0.051	155	82%
1/30/2017 13:40	203.90	3.30	201	0.030	0.003	0.001	0.045	158	86%
2/8/2017 15:20	212.97	0.76	198	0.039	0.001	0.000	0.045	169	84%
2/15/2017 18:56	220.12	2.22	205	0.039	0.001	0.001	0.046	165	83%
2/23/2017 14:10	227.93	2.75	191	0.032	0.000	0.001	0.043	170	86%

75 rpm data for model simulation

X1	X2	X3	X4	X5	Y1	Y2	Y3
X1 DO (mg O2/L)	X2 AOB (gCOD/L)	X3 Anam (gCOD/L)	X4 VSS total (gVSS/L)	X5 NOB (gCOD/L)	Y1 dSNH4/dt-VSS (gN/gVSS-hr)	Y2 dSNO2/dt-VSS (gN/gVSS-hr)	Y3 dSNO3/dt-VSS (gN/gVSS-hr)
0	0.169	0.554	1.781	0.009	-0.034	-0.036	0.009
0	0.184	0.650	1.934	0.009	-0.033	-0.034	0.010
0	0.182	0.527	1.631	0.009	-0.029	-0.036	0.009
0	0.180	0.517	1.822	0.009	-0.030	-0.034	0.008
0	0.180	0.603	1.972	0.009	-0.029	-0.031	0.009
0.780	0.169	0.554	1.781	0.009	-0.066	-0.006	0.009
1.209	0.184	0.650	1.934	0.009	-0.092	0.004	0.009
2.522	0.182	0.527	1.917	0.009	-0.063	0.037	0.004
4.033	0.180	0.517	1.822	0.009	-0.073	0.062	0.004
5.837	0.180	0.603	1.972	0.009	-0.066	0.060	0.003

150 rpm data for model simulation

X1	X2	X3	X4	X5	Y1	Y2	Y3
X1 DO (mg O2/L)	X2 AOB (gCOD/L)	X3 Anam (gCOD/L)	X4 VSS total (gVSS/L)	X5 NOB (gCOD/L)	Y1 dSNH4/dt-VSS (gN/gVSS-hr)	Y2 dSNO2/dt-VSS (gN/gVSS-hr)	Y3 dSNO3/dt-VSS (gN/gVSS-hr)
0	0.093	0.278	0.707	0.021	-0.044	-0.042	0.011
0	0.114	0.323	0.865	0.021	-0.037	-0.047	0.011
0	0.191	0.373	1.448	0.021	-0.018	-0.034	0.008
0	0.222	0.435	1.683	0.021	-0.023	-0.033	0.008
0	0.196	0.442	1.485	0.021	-0.029	-0.036	0.009
0	0.183	0.384	1.528	0.021	-0.027	-0.031	0.007
0	0.128	0.243	1.303	0.021	-0.027	-0.027	0.005
0	0.135	0.284	1.027	0.021	-0.034	-0.031	0.008
0	0.150	0.271	0.836	0.021	-0.035	-0.036	0.009
0.255	0.093	0.278	0.707	0.021	-0.069	-0.015	0.010
0.459	0.114	0.323	0.865	0.021	-0.053	-0.004	0.009
0.758	0.191	0.373	1.448	0.021	-0.056	0.016	0.009
1.210	0.222	0.435	1.683	0.021	-0.067	0.026	0.012
2.519	0.196	0.442	1.485	0.021	-0.080	0.069	0.008
4.032	0.183	0.384	1.528	0.021	-0.090	0.071	0.007
4.179	0.128	0.243	1.303	0.021	-0.072	0.061	0.005
6.363	0.135	0.284	1.027	0.021	-0.097	0.079	0.007
6.418	0.150	0.271	0.836	0.021	-0.145	0.085	0.008

8.2 Calculation of the Average Velocity Gradient

Power for Mixing, P: (Tchobanoglous et al., 2003, eq 5-9)

- N_P = power number for impeller, unitless = 3.5 (Tchobanoglous et al., 2003, table 5-12)
- ρ = density of water = 1000 kg/m^3
- n = revolutions per second = 75 and 150 r/s
- D = diameter of impeller = 0.12 m
- $P(75rpm) = N_P \rho n^3 D^5$ = 0.1701 W
- $P(150rpm) = N_P \rho n^3 D^5$ = 1.3608 W

Average velocity gradient, G: (Tchobanoglous et al., 2003, eq 5-3)

- $\mu(water, 35℃)$ = dynamic viscosity of water at 35 °C = 0.726 N s/m^2
- V = flocculator volume = 8×10^{-3} m^3

- $G(75rpm, 8.0L) = \sqrt{\frac{P}{\mu V}}$ = 5.28 /s
- $G(150rpm, 8.0L) = \sqrt{\frac{P}{\mu V}}$ =14.9 /s

8.3 Calculation of the Solids Retention Time (SRT) of the Flocs and the Aggregates

Based on the notation in Figure 3-4:

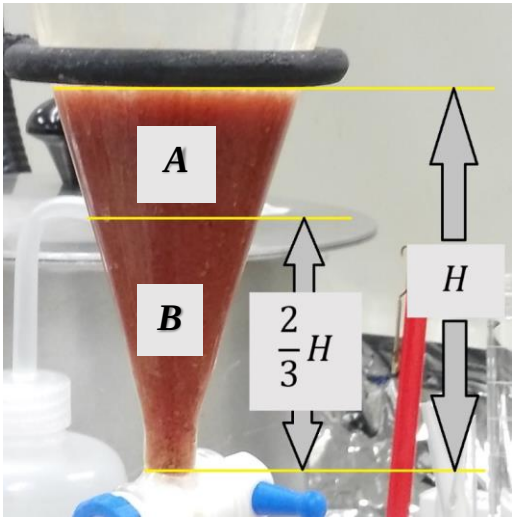

$$Volume(A+B) = \frac{1}{3}\pi R^2 H$$

$$Volume(B) = \frac{1}{3}\pi\left(\frac{2}{3}R\right)^2\left(\frac{2}{3}H\right) = \frac{8}{81}\pi R^2 H$$

Thus,

$$Volume(A) = Volume(A+B) - Volume(B) = \frac{19}{81}\pi R^2 H$$

Thus,

$$\frac{Volume(A)}{Volume(A+B)} = \frac{19}{27}$$

$$\frac{Volume(B)}{Volume(A+B)} = \frac{8}{27}$$

The volume which was wasted was calculated according to the following actions:

1. After every 6 hour, 300 mL of MLSS was transferred to the separatory funnel;
2. Once the supernatant became clear, the stopcock was turned on and the settled solids was collected. Then, the stopcock was turned off until the solids level reached $\frac{2}{3}H$;
3. The solids which left behind was wasted.
4. The volume which was wasted equaled to Volume B, $\frac{8}{27} \cdot 300mL = 88.9mL$

Scenario 1: the selective wasting method achieved no biomass separation

$$SRT(Flocs\ \&Aggregates) = \frac{8.0\ L}{\frac{\frac{8}{27} \cdot 0.3\ L}{\frac{6\ hour}{24\ hour/day}}} = 22.5\ day$$

Scenario 2: the selective wasting method achieved perfect separation where all aggregates were recycled and at the same time all floc were wasted

Therefore, the 300 mL of the flocs from the reactor was wasted and none of the aggregates from the reactor was wasted.

$$SRT(Aggregates) \rightarrow +\infty$$

$$SRT(Flocs) = \frac{8.0\ L}{\frac{0.3\ L}{\frac{6\ hour}{24\ hour/day}}} = 6.7\ day$$

8.4 Calculation for the Sample Standard Deviation of the Quotient of Nitrogen Conversion Rate over VSS Concentration

	Mean	Variance
N conversion rate (a)	μ_a	σ_a^2
VSS concentration (b)	μ_b	σ_b^2

Derive $Var\left(\frac{a}{b}\right)$

Suppose a and b are independent

$$Var\left(\frac{a}{b}\right) = E\left(\frac{a^2}{b^2}\right) - \left[E\left(\frac{a}{b}\right)\right]^2 = E(a^2) \cdot E\left(\frac{1}{b^2}\right) - \left[\frac{E(a)}{E(b)}\right]^2$$

$$E(a^2) = Var(a) + [E(a)]^2 = \sigma_a^2 + \mu_a^2$$

$$E(b^2) = \sigma_b^2 + \mu_b^2$$

Suppose

$$b \sim N(\mu_b, \sigma_b^2)$$

Then by delta method,

$$b - \mu_b \sim N(0, \sigma_b^2)$$

$$g(b) - g(\mu_b) \sim N(0, g'(\mu_b)^2 \cdot \sigma_b^2)$$

Where,

$$g(\mu_b) = \frac{1}{\mu_b}$$

$$g'(\mu_b)^2 = \mu_b^{-4}$$

$$\frac{1}{b} \sim N\left(\frac{1}{\mu_b}, \frac{\sigma_b^2}{\mu_b^4}\right)$$

$$E\left(\frac{1}{b^2}\right) = Var\left(\frac{1}{b}\right) + \left[E\left(\frac{1}{b}\right)\right]^2 = \frac{\sigma_b^2 + \mu_b^2}{\mu_b^4}$$

Therefore,

$$Var\left(\frac{a}{b}\right) = (\sigma_a^2 + \mu_a^2) \cdot \frac{\sigma_b^2 + \mu_b^2}{\mu_b^4} - \left(\frac{\mu_a}{\mu_b}\right)^2$$

A sample calculation of the sample standard deviation of the ammonium conversion rate normalized by VSS concentration of the aerobic activity test when DO was 0.78 mg O_2/L and mixing speed was 75 rpm:

	Mean	Variance
NH_4^+ conversion rate (a) (gN/L-hr)	$\mu_a = -0.117$	$\sigma_a^2 = 1.67 \times 10^{-6}$
VSS concentration (b) (gVSS/L)	$\mu_b = 1.78$	$\sigma_b^2 = 6.32 \times 10^{-4}$

$$Var\left(\frac{a}{b}\right) = 1.39 \times 10^{-6}$$

Therefore, this sample standard deviation was 1.18×10^{-3}.

8.5 Derivation of the Linear Regression Equation

Based on Equation 4-3, the concentrations of Anammox bacteria were estimated by the following equation:

$$\frac{dSNO_3^-}{dt} = \beta_{NO3}^{AOB} \cdot X_{COD}^{AOB} \cdot \frac{S_{O2}}{K_{O2}^{AOB} + S_{O2}} + \beta_{NO3}^{NOB} \cdot X_{COD}^{NOB} \cdot \frac{S_{O2}}{0.5 + S_{O2}} + \beta_{NO3}^{Anam} \cdot X_{COD}^{Anam} \cdot \frac{K_{O2}^{Anammox}}{K_{O2}^{Anammox} + S_{O2}}$$

For all anoxic activity tests where S_{O2} = 0, the equation changed to:

$$\frac{dSNO_3^-}{dt} = \beta_{NO3}^{Anam} \cdot X_{COD}^{Anam}$$

Thus, the concentrations of Anammox bacteria could be estimated by the nitrate conversion rate:

$$X_{COD}^{Anam} = \frac{\frac{dSNO_3^-}{dt}}{\beta_{NO3}^{Anam}}$$

Based on the Equation 4-1 and assumptions, the concentrations of NOB were estimated by:

$$\frac{dSNH_4^+}{dt} = \beta_{NH4}^{AOB} \cdot X_{COD}^{AOB} \cdot \frac{S_{O2}}{K_{O2}^{AOB} + S_{O2}} + \beta_{NH4}^{NOB} \cdot X_{COD}^{NOB} \cdot \frac{S_{O2}}{0.5 + S_{O2}} + \beta_{NH4}^{Anam} \cdot X_{COD}^{Anam} \cdot \frac{K_{O2}^{Anammox}}{K_{O2}^{Anammox} + S_{O2}}$$

$$\frac{dSNO_2^-}{dt} = \beta_{NO2}^{AOB} \cdot X_{COD}^{AOB} \cdot \frac{S_{O2}}{K_{O2}^{AOB} + S_{O2}} + \beta_{NO2}^{NOB} \cdot X_{COD}^{NOB} \cdot \frac{S_{O2}}{0.5 + S_{O2}} + \beta_{NO2}^{Anam} \cdot X_{COD}^{Anam} \cdot \frac{K_{O2}^{Anammox}}{K_{O2}^{Anammox} + S_{O2}}$$

Where S_{O2} around 6.0 mg O_2/L, the switching functions could be estimated with:

$$\frac{S_{O2}}{K_{O2}^{AOB} + S_{O2}} \to 1;\ \frac{S_{O2}}{0.5 + S_{O2}} \to 1;\ \frac{K_{O2}^{Anammox}}{K_{O2}^{Anammox} + S_{O2}} \to 0$$

Therefore,

$$\frac{dSNH_4^+}{dt} = \beta_{NH4}^{AOB} \cdot X_{COD}^{AOB} + \beta_{NH4}^{NOB} \cdot X_{COD}^{NOB}$$

$$\frac{dSNO_2^-}{dt} = \beta_{NO2}^{AOB} \cdot X_{COD}^{AOB} + \beta_{NO2}^{NOB} \cdot X_{COD}^{NOB}$$

Therefore, a pair of best fit solutions of AOB and NOB concentrations could be calculated in the DO concentrations around 6.0 mg O_2/L. The mean of the NOB concentrations were calculated and used for model simulation.

Based on assumptions, the ratio of AOB concentration to VSS concentration could be calculated. Therefore, the AOB concentrations were estimated in the DO concentration range from 0.1 to 4.5 mg O_2/L.

8.5.1 $\overrightarrow{\boldsymbol{\beta_{1\to 9}}}$ Definition

$$\beta_1 = \beta_{NH4}^{AOB} = -\left(i_{NBM} + \frac{1}{Y_{AOB}}\right) \cdot \mu_m^{AOB} \cdot (SF_{NH4}^{AOB})$$

$$\beta_2 = \beta_{NH4}^{NOB} = -i_{NBM} \cdot \mu_m^{NOB} \cdot (SF_{NO2}^{NOB})$$

$$\beta_3 = \beta_{NH4}^{Anammox} = -\left(i_{NBM} + \frac{1}{Y_{Anam}}\right) \cdot \mu_m^{Anam} \cdot (SF_{NH4}^{Anammox}) \cdot (SF_{NO2}^{Anammox})$$

$$\beta_4 = \beta_{NO2}^{AOB} = +\left(\frac{1}{Y_{AOB}}\right) \cdot \mu_m^{AOB} \cdot (SF_{NH4}^{AOB})$$

$$\beta_5 = \beta_{NO2}^{NOB} = -\frac{1}{Y_{NOB}} \cdot \mu_m^{NOB} \cdot (SF_{NO2}^{NOB})$$

$$\beta_6 = \beta_{NO2}^{Anammox} = -\left(\frac{1}{Y_{Anam}} + \frac{1}{1.143\ gCOD/gNO2-N}\right) \cdot \mu_m^{Anam} \cdot (SF_{NH4}^{Anammox}) \cdot (SF_{NO2}^{Anammox})$$

$$\beta_7 = \beta_{NO3}^{AOB} = 0$$

$$\beta_8 = \beta_{NO3}^{NOB} = +\frac{1}{Y_{NOB}} \cdot \mu_m^{NOB} \cdot (SF_{NO2}^{NOB})$$

$$\beta_9 = \beta_{NO3}^{Anammox} = +\left(\frac{1}{1.143\ gCOD/gNO2-N}\right) \cdot \mu_m^{Anam} \cdot (SF_{NH4}^{Anammox}) \cdot (SF_{NO2}^{Anammox})$$

Therefore, all β (gN/gCOD-hr) were known:

75rpm	Beta-1	Beta-2	Beta-3	Beta-4	Beta-5	Beta-6	Beta-7	Beta-8	Beta-9
ID	Beta-NH4-AOB (gN/gCOD-hr)	Beta-NH4-NOB (gN/gCOD-hr)	Beta-NH4-Anam (gN/gCOD-hr)	Beta-NO2-AOB (gN/gCOD-hr)	Beta-NO2-NOB (gN/gCOD-hr)	Beta-NO2-Anam (gN/gCOD-hr)	Beta-NO3-AOB (gN/gCOD-hr)	Beta-NO3-NOB (gN/gCOD-hr)	Beta-NO3-Anam (gN/gCOD-hr)
75rpm-0.78-2-Aer	-0.713	-0.005	-0.259	0.706	-0.763	-0.283	0.000	0.763	0.026
75rpm-1.21-2-Aer	-0.711	-0.005	-0.283	0.704	-0.772	-0.308	0.000	0.772	0.028
75rpm-2.52-3-Aer	-0.714	-0.005	-0.298	0.706	-0.775	-0.325	0.000	0.775	0.029
75rpm-4.03-1-Aer	-0.714	-0.005	-0.300	0.706	-0.776	-0.327	0.000	0.776	0.030
75rpm-5.84-1-Aer	-0.713	-0.005	-0.300	0.705	-0.776	-0.327	0.000	0.776	0.030
Average	-0.713	-0.005	-0.288	0.706	-0.772	-0.314	0.000	0.772	0.028
Stdev.s	0.001	0.000	0.018	0.001	0.005	0.019	0.000	0.005	0.002

150rpm	Beta-1	Beta-2	Beta-3	Beta-4	Beta-5	Beta-6	Beta-7	Beta-8	Beta-9
ID	Beta-NH4-AOB (gN/gCOD-hr)	Beta-NH4-NOB (gN/gCOD-hr)	Beta-NH4-Anam (gN/gCOD-hr)	Beta-NO2-AOB (gN/gCOD-hr)	Beta-NO2-NOB (gN/gCOD-hr)	Beta-NO2-Anam (gN/gCOD-hr)	Beta-NO3-AOB (gN/gCOD-hr)	Beta-NO3-NOB (gN/gCOD-hr)	Beta-NO3-Anam (gN/gCOD-hr)
150rpm-0.25-1-Aer	-0.715	-0.005	-0.275	0.708	-0.768	-0.300	0.000	0.768	0.027
150rpm-0.46-1-Aer	-0.715	-0.005	-0.282	0.708	-0.770	-0.308	0.000	0.770	0.028
150rpm-0.76-1-Aer	-0.715	-0.005	-0.296	0.708	-0.774	-0.323	0.000	0.774	0.029
150rpm-1.21-3-Aer	-0.714	-0.005	-0.299	0.707	-0.775	-0.326	0.000	0.775	0.030
150rpm-2.52-3-Aer	-0.714	-0.005	-0.301	0.707	-0.776	-0.328	0.000	0.776	0.030
150rpm-4.03-2-Aer	-0.715	-0.005	-0.301	0.708	-0.776	-0.329	0.000	0.776	0.030
150rpm-4.18-1-Aer	-0.715	-0.005	-0.302	0.708	-0.776	-0.329	0.000	0.776	0.030
150rpm-6.36-1-Aer	-0.715	-0.005	-0.301	0.707	-0.776	-0.328	0.000	0.776	0.030
150rpm-6.42-2-Aer	-0.715	-0.005	-0.301	0.707	-0.776	-0.329	0.000	0.776	0.030
Average	-0.715	-0.005	-0.295	0.708	-0.774	-0.322	0.000	0.774	0.029
Stdev.s	0.000	0.000	0.010	0.000	0.003	0.011	0.000	0.003	0.001

Since all β values had low sample standard deviations, all β's were assumed as constants and the values were the corresponding means throughout model simulation, expressed as:

$$\vec{\beta}_{(9\times1)} = \begin{bmatrix} \beta_1 \\ \beta_2 \\ \vdots \\ \beta_9 \end{bmatrix}$$ Unit: gN/gCOD-hr

8.5.2 $\overrightarrow{x_{1\to5}}$ and $\overrightarrow{y_{1\to3}}$ Definition

Let

$$\overrightarrow{x_1}_{(k\times1)} = S_{O2} = \begin{bmatrix} x_{11} \\ x_{12} \\ \vdots \\ x_{1k} \end{bmatrix}$$ Unit: mg O2/L

$$\overrightarrow{x_2}_{(k\times1)} = X_{COD}^{AOB} = \begin{bmatrix} x_{21} \\ x_{22} \\ \vdots \\ x_{2k} \end{bmatrix}$$ Unit: g COD/L

$$\overrightarrow{x_3}_{(k\times1)} = X_{COD}^{Anam} = \begin{bmatrix} x_{31} \\ x_{32} \\ \vdots \\ x_{3k} \end{bmatrix}$$ Unit: g COD/L

$$\overrightarrow{x_4}_{(k\times1)} = VSS_{Total} = \begin{bmatrix} x_{41} \\ x_{42} \\ \vdots \\ x_{4k} \end{bmatrix}$$ Unit: g VSS/L

$$\overrightarrow{x_5}_{(k\times1)} = X_{COD}^{NOB} = \begin{bmatrix} x_{51} \\ x_{52} \\ \vdots \\ x_{5k} \end{bmatrix}$$ Unit: g COD/L

$$\overrightarrow{y_1}_{(n_1\times1)} = \frac{\frac{dSNH_4}{dt}}{VSS_{Total}} = \begin{bmatrix} y_{11} \\ y_{12} \\ \vdots \\ y_{1n_1} \end{bmatrix}$$ Unit: gN/gVSS-hr

$$\overrightarrow{y_2}_{(n_2\times1)} = \frac{\frac{dSNO_2}{dt}}{VSS_{Total}} = \begin{bmatrix} y_{21} \\ y_{22} \\ \vdots \\ y_{2n_2} \end{bmatrix}$$ Unit: gN/gVSS-hr

$$\overrightarrow{y_3}_{(n_2\times1)} = \frac{\frac{dSNO_3}{dt}}{VSS_{Total}} = \begin{bmatrix} y_{31} \\ y_{32} \\ \vdots \\ y_{3n_1} \end{bmatrix}$$ Unit: gN/gVSS-hr

$K_1 = K_{O2}^{AOB}$ Unit: mg O2/L

$K_2 = K_{O2}^{Anam}$ Unit: mg O2/L

Thus, literature formulas could be expressed as:

$$\begin{cases} \dfrac{\frac{dSNH4}{dt}}{VSS_{Total}} = \left(\dfrac{\beta_{NH4}^{AOB} \cdot X_{COD}^{AOB} \cdot \frac{S_{O2}}{K_{O2}^{AOB} + S_{O2}} + \beta_{NH4}^{NOB} \cdot X_{COD}^{NOB} \cdot \frac{S_{O2}}{0.5 + S_{O2}} + \beta_{NH4}^{Anam} \cdot X_{COD}^{Anam} \cdot \frac{K_{O2}^{Anam}}{K_{O2}^{Anam} + S_{O2}}}{VSS_{Total}} \right) \\ \dfrac{\frac{dSNO2}{dt}}{VSS_{Total}} = \left(\dfrac{\beta_{NO2}^{AOB} \cdot X_{COD}^{AOB} \cdot \frac{S_{O2}}{K_{O2}^{AOB} + S_{O2}} + \beta_{NO2}^{NOB} \cdot X_{COD}^{NOB} \cdot \frac{S_{O2}}{0.5 + S_{O2}} + \beta_{NO2}^{Anam} \cdot X_{COD}^{Anam} \cdot \frac{K_{O2}^{Anam}}{K_{O2}^{Anam} + S_{O2}}}{VSS_{Total}} \right) \\ \dfrac{\frac{dSNO3}{dt}}{VSS_{Total}} = \left(\dfrac{\beta_{NO3}^{AOB} \cdot X_{COD}^{AOB} \cdot \frac{S_{O2}}{K_{O2}^{AOB} + S_{O2}} + \beta_{NO3}^{NOB} \cdot X_{COD}^{NOB} \cdot \frac{S_{O2}}{0.5 + S_{O2}} + \beta_{NO3}^{Anam} \cdot X_{COD}^{Anam} \cdot \frac{K_{O2}^{Anam}}{K_{O2}^{Anam} + S_{O2}}}{VSS_{Total}} \right) \end{cases}$$

$$\begin{cases} y_1 = \left(\dfrac{\beta_1 \cdot x_2 \cdot \frac{x_1}{K_1 + x_1} + \beta_2 \cdot x_5 \cdot \frac{x_1}{0.5 + x_1} + \beta_3 \cdot x_3 \cdot \frac{K_2}{K_2 + x_1}}{x_4} \right) \\ y_2 = \left(\dfrac{\beta_4 \cdot x_2 \cdot \frac{x_1}{K_1 + x_1} + \beta_5 \cdot x_5 \cdot \frac{x_1}{0.5 + x_1} + \beta_6 \cdot x_3 \cdot \frac{K_2}{K_2 + x_1}}{x_4} \right) \\ y_3 = \left(\dfrac{\beta_7 \cdot x_2 \cdot \frac{x_1}{K_1 + x_1} + \beta_8 \cdot x_5 \cdot \frac{x_1}{0.5 + x_1} + \beta_9 \cdot x_3 \cdot \frac{K_2}{K_2 + x_1}}{x_4} \right) \end{cases}$$

$$\begin{cases} y_1 = \dfrac{\beta_1 \cdot x_2 \cdot x_1}{x_4 \cdot (K_1 + x_1)} + \dfrac{\beta_2 \cdot x_5 \cdot x_1}{x_4 \cdot (0.5 + x_1)} + \dfrac{\beta_3 \cdot x_3 \cdot K_2}{x_4 \cdot (K_2 + x_1)} \\ y_2 = \dfrac{\beta_4 \cdot x_2 \cdot x_1}{x_4 \cdot (K_1 + x_1)} + \dfrac{\beta_5 \cdot x_5 \cdot x_1}{x_4 \cdot (0.5 + x_1)} + \dfrac{\beta_6 \cdot x_3 \cdot K_2}{x_4 \cdot (K_2 + x_1)} \\ y_3 = \dfrac{\beta_7 \cdot x_2 \cdot x_1}{x_4 \cdot (K_1 + x_1)} + \dfrac{\beta_8 \cdot x_5 \cdot x_1}{x_4 \cdot (0.5 + x_1)} + \dfrac{\beta_9 \cdot x_3 \cdot K_2}{x_4 \cdot (K_2 + x_1)} \end{cases}$$

Let

$$\vec{f}_{(k\times1)}=\begin{bmatrix}\dfrac{x_{21}\cdot x_{11}}{x_{41}\cdot(K_1+x_{11})}\\ \dfrac{x_{22}\cdot x_{12}}{x_{42}\cdot(K_1+x_{12})}\\ \vdots\\ \dfrac{x_{2k}\cdot x_{1k}}{x_{4k}\cdot(K_1+x_{1k})}\end{bmatrix}$$

$$\vec{g}_{(k\times1)}=\begin{bmatrix}\dfrac{x_{51}\cdot x_{11}}{x_{41}\cdot(0.5+x_{11})}\\ \dfrac{x_{52}\cdot x_{12}}{x_{42}\cdot(0.5+x_{12})}\\ \vdots\\ \dfrac{x_{5k}\cdot x_{1k}}{x_{4k}\cdot(0.5+x_{1k})}\end{bmatrix}$$

$$\vec{h}_{(k\times1)}=\begin{bmatrix}\dfrac{x_{31}\cdot K_2}{x_{41}\cdot(K_2+x_{11})}\\ \dfrac{x_{32}\cdot K_2}{x_{42}\cdot(K_2+x_{12})}\\ \vdots\\ \dfrac{x_{3k}\cdot K_2}{x_{4k}\cdot(K_2+x_{1k})}\end{bmatrix}$$

Thus, the literature formulas could be further simplified as:

$$\begin{cases}y_1=\beta_1\cdot f+\beta_2\cdot g+\beta_3\cdot h\\ y_2=\beta_4\cdot f+\beta_5\cdot g+\beta_6\cdot h\\ y_3=\beta_7\cdot f+\beta_8\cdot g+\beta_9\cdot h\end{cases}$$

Then, let:

$$\vec{Y}_{(n\times1)}=\begin{bmatrix}\overrightarrow{y_1}_{(n_1\times1)}\\ \overrightarrow{y_2}_{(n_2\times1)}\\ \overrightarrow{y_3}_{(n_3\times1)}\end{bmatrix}$$

Define

$$\vec{M}_{(k\times3)}=\begin{bmatrix}\vec{f}_{(k\times1)} & \vec{g}_{(k\times1)} & \vec{h}_{(k\times1)}\end{bmatrix}$$

and zero matrix

$$\vec{0}_{k3_{(k\times3)}} = \begin{bmatrix} 0 & 0 & 0 \\ 0 & 0 & 0 \\ \vdots & \vdots & \vdots \\ 0 & 0 & 0 \end{bmatrix}$$

Therefore, define

$$\vec{X}_{(3k\times9)} = \begin{bmatrix} \vec{M}_{(k\times3)} & \vec{0}_{k3_{(k\times3)}} & \vec{0}_{k3_{(k\times3)}} \\ \vec{0}_{k3_{(k\times3)}} & \vec{M}_{(k\times3)} & \vec{0}_{k3_{(k\times3)}} \\ \vec{0}_{k3_{(k\times3)}} & \vec{0}_{k3_{(k\times3)}} & \vec{M}_{(k\times3)} \end{bmatrix}$$

$$\vec{X}_{(3k\times9)} = \begin{bmatrix} \left[\vec{f}_{(k\times1)} \quad \vec{g}_{(k\times1)} \quad \vec{h}_{(k\times1)}\right]_{(k\times3)} & \vec{0}_{k3_{(k\times3)}} & \vec{0}_{k3_{(k\times3)}} \\ \vec{0}_{k3_{(k\times3)}} & \left[\vec{f}_{(k\times1)} \quad \vec{g}_{(k\times1)} \quad \vec{h}_{(k\times1)}\right]_{(k\times3)} & \vec{0}_{k3_{(k\times3)}} \\ \vec{0}_{k3_{(k\times3)}} & \vec{0}_{k3_{(k\times3)}} & \left[\vec{f}_{(k\times1)} \quad \vec{g}_{(k\times1)} \quad \vec{h}_{(k\times1)}\right]_{(k\times3)} \end{bmatrix}$$

Finally, experiment data can be listed as:

75rpm							
X1	X2	X3	X4	X5	Y1	Y2	Y3
X1 DO (mg O2/L)	X2 AOB (gCOD/L)	X3 Anam (gCOD/L)	X4 VSS total (gVSS/L)	X5 NOB (gCOD/L)	Y1 dSNH4/dt-VSS (gN/gVSS-hr)	Y2 dSNO2/dt-VSS (gN/gVSS-hr)	Y3 dSNO3/dt-VSS (gN/gVSS-hr)
0	0.169	0.554	1.781	0.009	-0.034	-0.036	0.009
0	0.184	0.650	1.934	0.009	-0.033	-0.034	0.010
0	0.182	0.527	1.631	0.009	-0.029	-0.036	0.009
0	0.180	0.517	1.822	0.009	-0.030	-0.034	0.008
0	0.180	0.603	1.972	0.009	-0.029	-0.031	0.009
0.780	0.169	0.554	1.781	0.009	-0.066	-0.006	0.009
1.209	0.184	0.650	1.934	0.009	-0.092	0.004	0.009
2.522	0.182	0.527	1.917	0.009	-0.063	0.037	0.004
4.033	0.180	0.517	1.822	0.009	-0.073	0.062	0.004
5.837	0.180	0.603	1.972	0.009	-0.066	0.060	0.003

150rpm							
X1	X2	X3	X4	X5	Y1	Y2	Y3
X1 DO (mg O2/L)	X2 AOB (gCOD/L)	X3 Anam (gCOD/L)	X4 VSS total (gVSS/L)	X5 NOB (gCOD/L)	Y1 dSNH4/dt-VSS (gN/gVSS-hr)	Y2 dSNO2/dt-VSS (gN/gVSS-hr)	Y3 dSNO3/dt-VSS (gN/gVSS-hr)
0	0.093	0.278	0.707	0.021	-0.044	-0.042	0.011
0	0.114	0.323	0.865	0.021	-0.037	-0.047	0.011
0	0.191	0.373	1.448	0.021	-0.018	-0.034	0.008
0	0.222	0.435	1.683	0.021	-0.023	-0.033	0.008
0	0.196	0.442	1.485	0.021	-0.029	-0.036	0.009
0	0.183	0.384	1.528	0.021	-0.027	-0.031	0.007
0	0.128	0.243	1.303	0.021	-0.027	-0.027	0.005
0	0.135	0.284	1.027	0.021	-0.034	-0.031	0.008
0	0.150	0.271	0.836	0.021	-0.035	-0.036	0.009
0.255	0.093	0.278	0.707	0.021	-0.069	-0.015	0.010
0.459	0.114	0.323	0.865	0.021	-0.053	-0.004	0.009
0.758	0.191	0.373	1.448	0.021	-0.056	0.016	0.009
1.210	0.222	0.435	1.683	0.021	-0.067	0.026	0.012
2.519	0.196	0.442	1.485	0.021	-0.080	0.069	0.008
4.032	0.183	0.384	1.528	0.021	-0.090	0.071	0.007
4.179	0.128	0.243	1.303	0.021	-0.072	0.061	0.005
6.363	0.135	0.284	1.027	0.021	-0.097	0.079	0.007
6.418	0.150	0.271	0.836	0.021	-0.145	0.085	0.008

Therefore, k, n1, n2, n3, and n have values as:

	75rpm	150rpm
k	10	18
n_1	10	18
n_2	10	18
n_3	10	18
n	30	54

Therefore, the dimension of $\vec{Y}$ is $n = n_1 + n_2 + n_3 = 3k$.

Finally, the literature formula can be simplified as:

$$\vec{Y}_{(n\times 1)} = \vec{X}_{(n\times 9)} \times \vec{\beta}_{(9\times 1)} + \vec{r}_{(n\times 1)}$$

where, $\vec{r}$ is the residual vector.

8.5.3 K1 K2 Estimation (Assuming α = 0.05)

Based on simplified model:

$$y_{11} = [f_{11} \quad g_{11} \quad h_{11}] \times \begin{bmatrix}\beta_1\\ \beta_2\\ \beta_3\end{bmatrix} + \vec{0}_{k3} \times \begin{bmatrix}\beta_4\\ \beta_5\\ \beta_6\end{bmatrix} + \vec{0}_{k3} \times \begin{bmatrix}\beta_7\\ \beta_8\\ \beta_9\end{bmatrix}$$

$$y_{21} = \vec{0}_{k3} \times \begin{bmatrix}\beta_1\\ \beta_2\\ \beta_3\end{bmatrix} + [f_{11} \quad g_{11} \quad h_{11}] \times \begin{bmatrix}\beta_4\\ \beta_5\\ \beta_6\end{bmatrix} + \vec{0}_{k3} \times \begin{bmatrix}\beta_7\\ \beta_8\\ \beta_9\end{bmatrix}$$

$$y_{31} = \vec{0}_{k3} \times \begin{bmatrix}\beta_1\\ \beta_2\\ \beta_3\end{bmatrix} + \vec{0}_{k3} \times \begin{bmatrix}\beta_4\\ \beta_5\\ \beta_6\end{bmatrix} + [f_{11} \quad g_{11} \quad h_{11}] \times \begin{bmatrix}\beta_7\\ \beta_8\\ \beta_9\end{bmatrix}$$

K1 and K2 can be expressed with the example of y11 after equation translation:

$$y_{11} = [f_{11} \quad g_{11} \quad h_{11}] \times \begin{bmatrix}\beta_1\\ \beta_2\\ \beta_3\end{bmatrix}$$

$$y_{11} = \frac{\beta_1 \cdot x_{21} \cdot x_{11}}{x_{41} \cdot (K_1 + x_{11})} + \frac{\beta_2 \cdot x_{51} \cdot x_{11}}{x_{41} \cdot (0.5 + x_{11})} + \frac{\beta_3 \cdot x_{31} \cdot K_2}{x_{41} \cdot (K_2 + x_{11})}$$

$$y_{11} - \frac{\beta_2 \cdot x_{51} \cdot x_{11}}{x_{41} \cdot (0.5 + x_{11})} = \frac{\beta_1 \cdot x_{21} \cdot x_{11}}{x_{41} \cdot (K_1 + x_{11})} + \frac{\beta_3 \cdot x_{31} \cdot K_2}{x_{41} \cdot (K_2 + x_{11})}$$

$$y_{11} - \frac{\beta_2 \cdot x_{51} \cdot x_{11}}{x_{41} \cdot (0.5 + x_{11})} = \frac{\beta_1 \cdot x_{21} \cdot x_{11}}{x_{41} \cdot (K_1 + x_{11})} + \frac{\beta_3 \cdot x_{31}}{x_{41}} \cdot \frac{(K_2 + x_{11}) - x_{11}}{(K_2 + x_{11})}$$

$$y_{11} - \frac{\beta_2 \cdot x_{51} \cdot x_{11}}{x_{41} \cdot (0.5 + x_{11})} = \frac{\beta_1 \cdot x_{21} \cdot x_{11}}{x_{41} \cdot (K_1 + x_{11})} + \frac{\beta_3 \cdot x_{31}}{x_{41}} \cdot \left(1 - \frac{x_{11}}{K_2 + x_{11}}\right)$$

$$y_{11} - \frac{\beta_2 \cdot x_{51} \cdot x_{11}}{x_{41} \cdot (0.5 + x_{11})} = \frac{\beta_1 \cdot x_{21} \cdot x_{11}}{x_{41} \cdot (K_1 + x_{11})} + \frac{\beta_3 \cdot x_{31}}{x_{41}} - \frac{\beta_3 \cdot x_{31} \cdot x_{11}}{x_{41}} \cdot \frac{1}{K_2 + x_{11}}$$

$$y_{11} - \frac{\beta_2 \cdot x_{51} \cdot x_{11}}{x_{41} \cdot (0.5 + x_{11})} - \frac{\beta_3 \cdot x_{31}}{x_{41}} = \frac{\beta_1 \cdot x_{21} \cdot x_{11}}{x_{41}} \cdot \frac{1}{K_1 + x_{11}} - \frac{\beta_3 \cdot x_{31} \cdot x_{11}}{x_{41}} \cdot \frac{1}{K_2 + x_{11}}$$

Let

$$U_{11} = y_{11} - \frac{\beta_2 \cdot x_{51} \cdot x_{11}}{x_{41} \cdot (0.5 + x_{11})} - \frac{\beta_3 \cdot x_{31}}{x_{41}}$$

$$V_{11} = \frac{\beta_1 \cdot x_{21} \cdot x_{11}}{x_{41}}$$

$$Z_{11} = \frac{\beta_3 \cdot x_{31} \cdot x_{11}}{x_{41}}$$

Therefore,

$$U_{11} = V_{11} \cdot \frac{1}{K_1 + x_{11}} - Z_{11} \cdot \frac{1}{K_2 + x_{11}}$$

Similarly,

$$U_{21} = V_{21} \cdot \frac{1}{K_1 + x_{11}} - Z_{21} \cdot \frac{1}{K_2 + x_{11}}$$

$$U_{31} = V_{31} \cdot \frac{1}{K_1 + x_{11}} - Z_{31} \cdot \frac{1}{K_2 + x_{11}}$$

Therefore, the residuals:

$$r_{11} = U_{11} - V_{11} \cdot \frac{1}{K_1 + x_{11}} + Z_{11} \cdot \frac{1}{K_2 + x_{11}}$$

$$r_{21} = U_{21} - V_{21} \cdot \frac{1}{K_1 + x_{11}} + Z_{21} \cdot \frac{1}{K_2 + x_{11}}$$

$$r_{31} = U_{31} - V_{31} \cdot \frac{1}{K_1 + x_{11}} + Z_{31} \cdot \frac{1}{K_2 + x_{11}}$$

Then, let $1 \leq i \leq k$, and

$$U_{1i} = y_{1\mathrm{i}} - \beta_2 \frac{x_{5\mathrm{i}} x_{1\mathrm{i}}}{x_{4\mathrm{i}}(0.5 + x_{1\mathrm{i}})} - \beta_3 \frac{x_{3\mathrm{i}}}{x_{4\mathrm{i}}} \qquad V_{1i} = \beta_1 \frac{x_{2\mathrm{i}} x_{1\mathrm{i}}}{x_{4\mathrm{i}}} \qquad Z_{1i} = \beta_3 \frac{x_{3\mathrm{i}} x_{1\mathrm{i}}}{x_{4\mathrm{i}}}$$

$$U_{2i} = y_{2\mathrm{i}} - \beta_5 \frac{x_{5\mathrm{i}} x_{1\mathrm{i}}}{x_{4\mathrm{i}}(0.5 + x_{1\mathrm{i}})} - \beta_6 \frac{x_{3\mathrm{i}}}{x_{4\mathrm{i}}} \qquad V_{2i} = \beta_4 \frac{x_{2\mathrm{i}} x_{1\mathrm{i}}}{x_{4\mathrm{i}}} \qquad Z_{2i} = \beta_6 \frac{x_{3\mathrm{i}} x_{1\mathrm{i}}}{x_{4\mathrm{i}}}$$

$$U_{3i} = y_{3\mathrm{i}} - \beta_8 \frac{x_{5\mathrm{i}} x_{1\mathrm{i}}}{x_{4\mathrm{i}}(0.5 + x_{1\mathrm{i}})} - \beta_9 \frac{x_{3\mathrm{i}}}{x_{4\mathrm{i}}} \qquad V_{3i} = \beta_7 \frac{x_{2\mathrm{i}} x_{1\mathrm{i}}}{x_{4\mathrm{i}}} \qquad Z_{3i} = \beta_9 \frac{x_{3\mathrm{i}} x_{1\mathrm{i}}}{x_{4\mathrm{i}}}$$

Then, the residual sum of square can be expressed as:

$$Q(K_1, K_2) = \sum_{j=1}^{3} \sum_{i=1}^{k} \left(U_{ji} - V_{ji} \frac{1}{K_1 + x_{1i}} + Z_{ji} \frac{1}{K_2 + x_{1i}} \right)^2$$

Therefore, the estimation of K1 and K2 can be formulated as:

$$\vec{\widehat{K}} = \begin{bmatrix} \widehat{K}_1 \\ \widehat{K}_2 \end{bmatrix} = argmin\, Q(K_1, K_2)$$

Now, the Newton's Method in 2 dimension was used to quickly find $\widehat{K}_1$ and $\widehat{K}_2$ with BioWin default values as initial guesses:

$$\begin{bmatrix} K_1^{(n+1)} \\ K_2^{(n+1)} \end{bmatrix} = \begin{bmatrix} K_1^{(n)} \\ K_2^{(n)} \end{bmatrix} - \vec{H}^{-1} \times \vec{S}$$

Where,

$$\vec{H} = \begin{bmatrix} \frac{\partial^2 Q}{\partial K_1^2} & \frac{\partial^2 Q}{\partial K_1 \partial K_2} \\ \frac{\partial^2 Q}{\partial K_1^2} & \frac{\partial^2 Q}{\partial K_2^2} \end{bmatrix} \qquad \vec{S} = \begin{bmatrix} \frac{\partial Q}{\partial K_1} \\ \frac{\partial Q}{\partial K_2} \end{bmatrix}$$

Calculate in loops until stop criteria was met:

$$\left|K_1^{(Next)} - K_1^{(Current)}\right| + \left|K_2^{(Next)} - K_2^{(Current)}\right| < 1 \times 10^{-5}$$

With the data provided, the estimated K1 and K2 are:

	$\widehat{K}_1$ (mg O2/L)	$\widehat{K}_2$ (mg O2/L)
75rpm	0.5424	0.5475
150rpm	0.6750	0.1306

8.5.4 Standard Deviation Estimation

From previous residual equations, U_{ji} is a function with 2 variables (i.e.V_{ji}, Z_{ji}) and 2 coefficients (i.e.K_1, K_2):

$$U_{ji} = \mathcal{F}\left(V_{ji}, Z_{ji}; K_1, K_2\right) + r_{ji} = V_{ji}\frac{1}{K_1 + x_{1i}} - Z_{ji}\frac{1}{K_2 + x_{1i}} + r_{ji}$$

where, $i = 1, 2, 3, \dots, n$ and $j = 1, 2, 3$.

r_{ji} was expected as an independent and identically distributed random variable where it had a normal distribution with a mean of 0 and a variance of σ^2, i.e. r_{ji} iid $\sim N(0, \sigma^2)$.

Although $\mathcal{F}\left(V_{ji}, Z_{ji}; K_1, K_2\right)$ is a non-linear model, the model could be approximated by a linear function, i.e. the Taylor series expansion at the place where $K_1 = K_2 = 0$:

$$\mathcal{F}\left(V_{ji}, Z_{ji}; K_1, K_2\right) \approx \mathcal{F}\left(V_{ji}, Z_{ji}; 0, 0\right) + \frac{\partial \mathcal{F}\left(V_{ji}, Z_{ji}; 0, 0\right)}{\partial K_1}K_1 + \frac{\partial \mathcal{F}\left(V_{ji}, Z_{ji}; 0, 0\right)}{\partial K_2}K_2$$

$$F_{jil} = \frac{\partial \mathcal{F}\left(V_{ji}, Z_{ji}; 0, 0\right)}{\partial K_l}$$

where, , $i = 1, 2, 3, \dots, n$; $j = 1, 2, 3$; $l = 1, 2$.

$$\vec{F}_{(n\times 2)} = \left[F_{jil}\right]$$

Then, $\vec{\widehat{K}}$ could be estimated as:

$$\vec{\hat{K}} \approx \left(\vec{F}^T \times \vec{F}\right)^{-1} \times \vec{F}^T \times \vec{U}$$

Then, $\vec{\hat{K}}$ was expected to have a normal distribution with a mean of $\vec{K}$ and a variance of $\left(\vec{F}^T \times \vec{F}\right)^{-1} \cdot \sigma^2$,i.e.:

$$\vec{\hat{K}} \sim N\left(\vec{K}, \left(\vec{F}^T \times \vec{F}\right)^{-1} \cdot \sigma^2\right)$$

$$SS_E = \left(\vec{U}_{(n\times 1)} - \vec{F}_{(n\times 2)} \times \vec{\hat{K}}_{(2\times 1)}\right)^T \times \left(\vec{U} - \vec{F} \times \vec{\hat{K}}\right)$$

$$\hat{\sigma}^2 = \frac{SS_E}{n-2}$$

Then, $\frac{(n-2)\hat{\sigma}^2}{\sigma^2}$ was distributed as chi-square with n-2 degrees of freedom, i.e. $\frac{(n-2)\hat{\sigma}^2}{\sigma^2} \sim \chi^2_{n-2}$.

Because the least squares estimator $\vec{\hat{K}}$ was a linear combination of the observations, it followed that $\vec{\hat{K}}$ was normally distributed with a mean vector $\vec{K}$ and a covariance matrix $\left(\vec{F}^T \times \vec{F}\right)_{ll}^{-1}\sigma^2$. Then each of the statistics:

$$\frac{\frac{\hat{K}_l - K_l}{\left(\vec{F}^T \times \vec{F}\right)_{ll}^{-1}\sigma^2}}{\sqrt{\frac{\hat{\sigma}^2}{\sigma^2}}} = \frac{\hat{K}_l - K_l}{\left(\vec{F}^T \times \vec{F}\right)_{ll}^{-1}\hat{\sigma}^2} \qquad l = 1, 2$$

was distributed as *student – t* distribution with *n-p* degrees of freedom, i.e. $\frac{\hat{K}_l - K_l}{\left(\vec{F}^T \times \vec{F}\right)_{ll}^{-1}\hat{\sigma}^2} \sim t_{n-p}$.

$\hat{K}$ which was calculated in this way had some bias because Taylor expansion omitted some higher order part. However, it could still give us a strong belief on the standard deviation of K_1 *and* K_2. In conclusion,

$$se\left(\hat{K}_l\right) = \sqrt{\left(\vec{F}^T \times \vec{F}\right)_{ll}^{-1}\hat{\sigma}^2} \qquad l = 1, 2$$

Therefore, a 100(1-α)% = 95% confidence interval for the regression coefficients $K_l, l = 1, 2$, is

$$\hat{K}_l - t_{\alpha/2,n-p}\, se\left(\hat{K}_l\right) \le K_l \le \hat{K}_l + t_{\alpha/2,n-p}\, se\left(\hat{K}_l\right)$$

As a result, variance covariance matrices for both 75rpm and 150rpm were calculated using R (a programming language):

Variance Covariance Matrix ($\overrightarrow{Cov}_{75rpm}$ and $\overrightarrow{Cov}_{150rpm}$):

$$\overrightarrow{Cov}_{75rpm} = \begin{bmatrix} 0.3141 & -0.008608 \\ -0.008608 & 0.1630 \end{bmatrix}$$

$$\overrightarrow{Cov}_{150rpm} = \begin{bmatrix} 0.1153 & -0.0009630 \\ -0.0009630 & 0.008041 \end{bmatrix}$$

Therefore, the variances were:

	$\widehat{K}_1$ Variance	$\widehat{K}_2$ Variance
75rpm	0.314	0.163
150rpm	0.115	0.00804

8.5.5 K_1 and K_2 Two-Sample t-Tests

First, the equality of the variances of two mixing intensities for one K were tested. The test statistic for:

$$\begin{cases} H_0: \sigma_1^2 = \sigma_2^2 \\ H_1: \sigma_1^2 \neq \sigma_2^2 \end{cases}$$

is the ratio of the sample variances

$$F_0 = \frac{se_1^2}{se_2^2}$$

	$\widehat{K}_1$ F-test p-value	$\widehat{K}_2$ F-test p-value
75rpm vs. 150rpm	$2.72 > \alpha = 0.05$	$20.3 > \alpha = 0.05$

Therefore, there was not sufficient evidence to reject $H_0: \sigma_1^2 = \sigma_2^2$. As a result, both $\widehat{K}_1$ and $\widehat{K}_2$ had equal variances under 75rpm and 150rpm.

The equality of the K values under two mixing intensities were tested. The test statistic for:

$$\begin{cases} H_0: K_l|_{75rpm} - K_l|_{150rpm} = 0 \\ H_1: K_l|_{75rpm} - K_l|_{150rpm} \neq 0 \end{cases} \qquad l = 1, 2$$

was:

$$t_0 = \frac{\widehat{K}_l\big|_{75rpm} - \widehat{K}_l\big|_{150rpm}}{S_p\sqrt{\frac{1}{df_l|_{75rpm}} + \frac{1}{df_l|_{150rpm}}}} \qquad l = 1, 2$$

where S_p^2 was an estimate of the common variance computed from:

$$S_p^2 = \frac{\left(df_{l_{75rpm}} - 1\right) se\left(\widehat{K}_l\right)^2_{75rpm} + \left(df_{l_{150rpm}} - 1\right) se\left(\widehat{K}_l\right)^2_{150rpm}}{df_{l_{75rpm}} + df_{l_{150rpm}} - 2} \qquad l = 1, 2$$

	$df_{l_{75rpm}}$	$df_{l_{150rpm}}$	$se\left(\widehat{K}_l\right)^2_{75rpm}$	$se\left(\widehat{K}_l\right)^2_{150rpm}$	S_p	t-test p-value
K_1	28	52	0.3141	0.1153	0.429	$0.19 < \alpha = 0.05$
K_2	28	52	0.1630	0.008041	0.248	$3.9 \times 10^{-10} < \alpha = 0.05$

Since the p-values for K1 was greater than 0.05, there was no evidence against H_0. Therefore, $K_2|_{75rpm} = K_2|_{150rpm}$.

Since the p-values for K2 was smaller than 0.05, there was evidence against H_0. Therefore, $K_2|_{75rpm} \neq K_2|_{150rpm}$.